Relationship between 20th Century Dune Migration and Wetland Formation at Cape Cod National Seashore, Massachusetts

THESIS · MAY 2006

1 AUTHOR:

Jay Sagin
Nazarbayev University
27 PUBLICATIONS **54** CITATIONS

SEE PROFILE

ABSTRACT

THESIS: Relationship between 20th Century Dune Migration and Wetland Formation at Cape Cod National Seashore, Massachusetts

STUDENT: Zhanay Sagintayev

DEGREE: Master of Science

COLLEGE: Sciences and Humanities

DATE: May 2006

PAGES: 124

Outer Cape Cod (Massachusetts) is dominated by active and stabilizing parabolic and transverse dunes interspersed with numerous inter-dune wetlands. Dune migration has been significantly affected by human activities; conversely, current dune movements are affecting local populations. The objective of the reported research was to assess, using remote sensing and geographic information systems (GIS) technologies, migration of the Cape Cod dunes and the effect of dune movement on distribution of associated wetlands. Aerial photographs from 1938 through 2003 were analyzed to track individual dune movements and subsequent wetland propagation and expansion. Absolute dune movement rates during this period were computed, with a plot of dune movement as a cumulative function. One sub-problem of this study was to quantify 'white' areas of active moving sand and 'dark' areas of vegetation, in order to quantify changes in vegetative cover with wetland propagation and, conversely, vegetative disappearance with dune movement. Attempts were made to correlate the Palmer Drought Severity Index (PDSI) with dune migration. Based on review of aerial photographs, parabolic dunes have migrated 150 to 250 m since 1938, with 60% of the movement occurring between 1938 and 1977. The relation between absolute parabolic dune migration and corresponding PDSI is approximately logarithmic. Maximum dune migration is associated with PDSI values lower than –2 and reflects moderate drought conditions. Wetlands consistently trailed the dunes, and the distance of wetland movement was related to dune movement distances. Wetland migration was particularly marked from the 1950s to the 1980s. Based on review of georeferenced aerial photographs, it is concluded that marked stabilization of Cape Cod dunes occurred in the 1980s and 1990s, with renewed movement in the 21st Century. This study provides a practical application for assessment of dune migration and vegetative transformations over time using remote sensing and GIS technologies.

TABLE OF CONTENTS

LIST OF TABLES

LIST OF FIGURES

CHAPTER 1: INTRODUCTION

1.1 Statement of the Problem

Applications of interdisciplinary research in environmental and geological sciences and related fields often require integration of a number of spatial data sets to enable a better understanding of the relationships between these datasets. With the advent of geographic information systems (GIS) and remote sensing technologies and their massive potential for data integration, visualization, and modeling, a researcher's ability to address and analyze spatial data sets has dramatically improved.

Cape Cod National Seashore (CCNS) in Massachusetts, USA, comprises 177 square km of shoreline and upland landscape features, including a 64-km-long stretch of pristine beach. A variety of historic and practical structures occur within the boundary of the seashore including lighthouses, a lifesaving station, and numerous Cape Cod-style houses. The seashore offers six swimming beaches, 11 self-guided nature trails, and a variety of picnic areas and scenic overlooks.

CCNS was established after the area had been settled for more than 300 years. In the Provincetown area, visitors can see where the Pilgrims landed in 1620 before sailing across the bay to Plymouth. The manner and timing of the National Seashore's creation in1961 has resulted in great challenges for park managers. There is an ongoing process of respecting historical jurisdiction and practices in ways that preserve the mandate of the National Seashore (NPS, 2006).

In the past 30 years, the CCNS permanent population has increased from 70,000 to 190,000, a figure that nearly triples during the peak summer season (Finch, 1997). Since the National Seashore is neither wilderness nor exclusively recreational, the park must be managed as a responsible combination of the two, optimizing both needs within a context of increasing popularity (NPS, 2006).

Dunes and associate ecosystems (e.g., wetlands) are shaped by nature over long periods, and the Cape Cod area is no exception. The dunes migrate partly as a function of local climatic conditions (e.g. drought versus wet) and consequent presence of vegetative types. In addition, human activities affect dunes including those of the CCNS in a number of ways; for example, livestock grazing may remove certain vegetative types thus causing dunes to expand and/or migrate. Population pressures may cause excessive water use with consequent lowering of water tables.

The tasks accomplished in the reported study were: a) development of co-registered digital mosaics of aerial photograph dune movements over the Cape Cod peninsula from 1938 to 2005; b) development of methods to identify wetland areas and their changes with potential dune movements; and c) analyses of dune and wetland movements on the Cape Cod peninsula. These tasks were required by the U.S. National Park Service (NPS) which serve the CCNS (Fig. 1.1). NPS is gathering information to meet its performance management goals and provide a knowledge base that is needed to address its stewardship responsibilities.

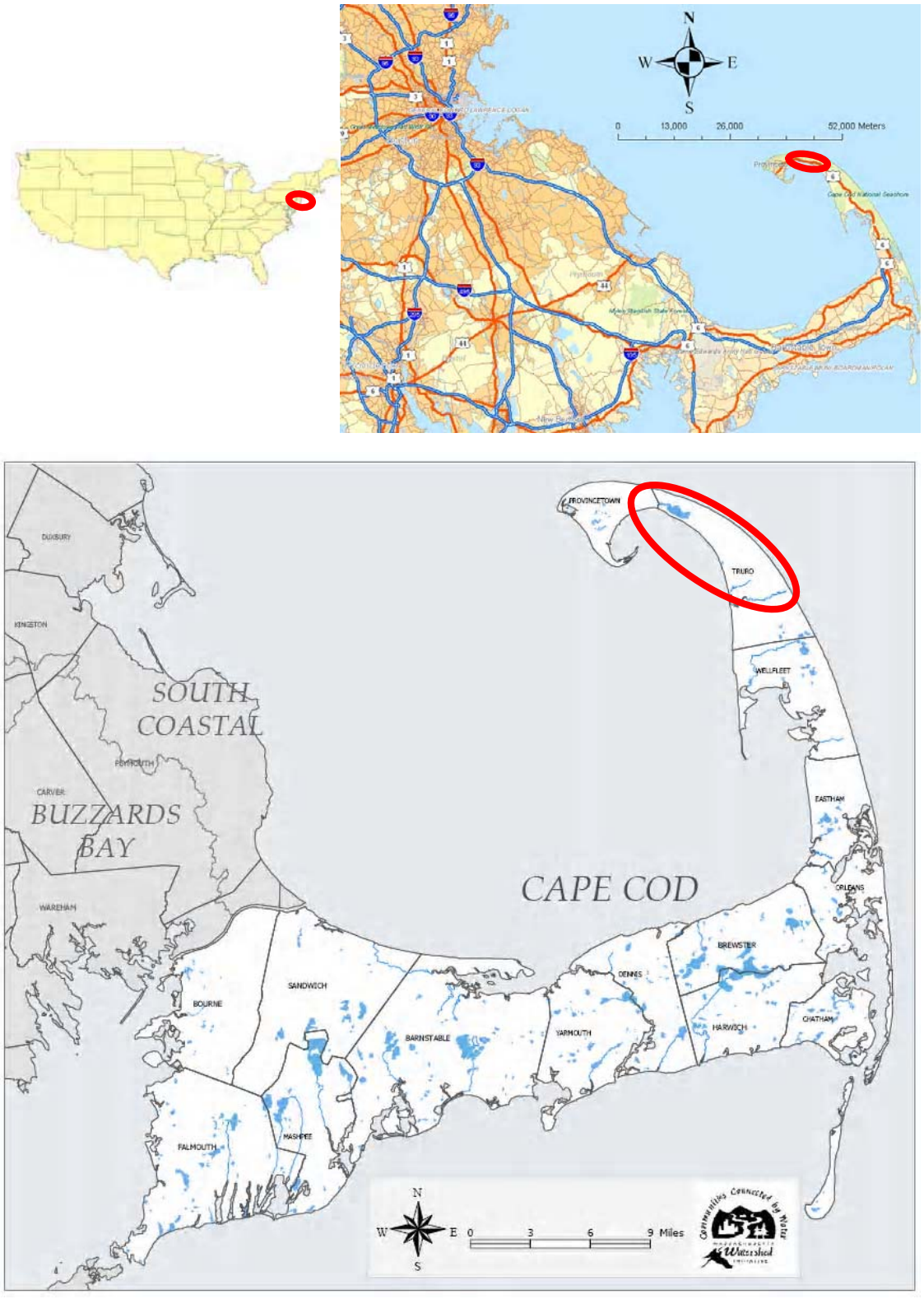

Figure 1.1. CCNS location. Study area in red oval.

1.2. Geography and Geology of Cape Cod and History of Settlement

At the northern tip of Cape Cod, spanning approximately 1,800 hectares within the CCNS, latitude 41°45'0"N - 42°45'0"N, longitude 70°0'0"W- 70°10'0"W, lies a vast system of dunes and interdunal wetlands known as the Provincelands (Fig. 1.1).

The geologic history of Cape Cod mostly involves the advance and retreat of the last continental ice sheet (named the Laurentide after the Laurentian region of Canada where it first formed) and the rise in sea level that followed the retreat of the ice sheet. On Cape Cod, these events occurred within the last 25,000 years dated using radiocarbon techniques (Rockmore, 1979).

The ice sheet was characterized by lobes that occupied large basins in the bedrock surface. These lobes were responsible for the location and overall shape of Cape Cod and the islands. Thus, the western side of Cape Cod was formed by the Buzzards Bay lobe, the middle part by the Cape Cod Bay lobe, and the lower or outer Cape by the South Channel lobe, which occupies a deep basin to the east of the Cape. During the maximum ice advance the landscape, where Cape Cod was soon to exist, glacial ice was ubiquitous. Within a few thousand years or possibly less, the ice sheet started to retreat rapidly and 18,000 years ago it had retreated away from Cape Cod and into the Gulf of Maine, which lies to the east and to the north of the Cape. Thus the retreat of the ice from the islands to a position north of Cape Cod may have taken only a few thousand years. By roughly 15,000 years ago the ice had retreated from the Gulf of Maine and all of southern New England (Strahler, 1988). This part of the Cape Cod peninsula began forming 18,000

years ago (Fig. 1.2) as longshore currents transported eroded materials from Atlantic-side beaches in a northward direction. Concurrently, wind carried sand grains inland and the landform gradually assumed its characteristic shape (USGS, 2006).

Cape Cod resembles a flexed arm of sand thrust out into the Atlantic Ocean. It owes its origin to glaciers, which were active in the area as recently as 14,000 years ago. Since that time, waves and near-shore currents have extensively reshaped the sedimentary deposits left by these glaciers into a variety of coastal environments, for example, sandy beaches flanked by towering sea cliffs and bluffs and discontinuous chains of barrier islands, many with elegantly curved sand spits. The 40-mile-long eastern coastline of Cape Cod, despite its proximity to Boston, possesses few shore-protection structures; it is the longest pristine shoreline of sand in New England (Pinet, 1992).

About 15,300 years ago a huge ice sheet, which flowed southward from Canada, covered all of New England. As the ice mass crept across the continental shelf one of its lobes, the Cape Cod Bay Lobe, deposited sediment at its margin and formed a morainal ridge, the terminal moraine. This ridge can now be traced across Martha's Vineyard and Nantucket, the two principal islands south of the Cape. In addition to the terminal moraine, recessional moraines also indicate the presence of the former ice sheet in southeastern Massachusetts. As the ice sheet retreated northward, meltwater trapped by the recessional moraine formed Glacial Lake Cape Cod (Uchupi et al., 2001).

Figure 1.2. Glaciations 18,000 years B.P. (Source: USGS, 2006).

About 6,000 years ago the rising sea submerged Georges Bank, exposing the Cape to wave attack from the southeast, resulting in the northerly transport of sand that eventually formed the curved spit system of the Provincelands surrounding Provincetown. The appearance of the spit sheltered the northern shoreline and resulted in a northward transport direction of currents on the bayside whereas further south, littoral transport was directed southward along Cape Cod Bay (Finch, 2003).

When the ice sheet disappeared, the landforms of the Cape looked quite different than they do today. As the ice melted, sea level rose and flooded the area. Paleogeographic reconstructions of the shoreline indicate it was quite irregular at that time, a series of headlands and embayments composed of unconsolidated glacial sediments (glacial drift). This original coastline was located as much as three miles seaward of the

present shoreline. Since then, sediment redistribution by waves and near-shore currents has changed the morphology of the landforms. Landscapes change quickly in Cape Cod, and the retreat of the ice sheet is no exception, taking less than 3,000 years (O'Brien , 1990).

Many spits shelter a quiet body of water termed a lagoon. Associated with lagoons are salt marshes and sand or mud flats. The spits also form the foundation for coastal sand dunes, the best examples of which occur in the Provincetown and Truro area and on Sandy Neck. The combination of spit, lagoon, salt marsh, and sand dune make up what is called a barrier island. "Barrier Island" is a generic term that also includes barriers tied to headlands. The growth and development of these features as well as the lagoon are closely related to the growth of the protecting spit (Oldale, 1992).

Once formed, spits and barrier islands do not remain unchanged for long. The forces of waves and wind continue to transport and redeposit the beach and dune deposits. The eroded material carried by the waves and currents is washed into the lagoon during northeast storms and hurricanes to form a new foundation for the dunes. In this manner, the barrier islands migrate landward. Without this landward migration, in response to the rising sea level, the spits and barrier islands would flood. Strong onshore winds also transport sand inland where it is deposited to form dunes. On young spits, the dunes are usually small, but on mature barrier islands such as Sandy Neck, Monomoy Island, and Provincetown, the dunes reach heights of 40 to 100 feet (Strahler, 1988).

The dunes themselves are attacked by the wind and, where unprotected by vegetation, continuously change shape. For example, the parabolic dunes in Provincetown and Truro were formed when the prevailing west wind blows out the middle of an existing

dune. In the past, the dunes were covered by mature forest and were stable. A remnant of this cover, the beech (*Fagus grandifolia*) forest, can be seen in Provincetown. Unfortunately, sand transported from adjacent unstable dune areas is slowly burying the forest. Elsewhere, evidence of past forest cover includes forest floor layers exposed by the wind in unstable dunes. On Sandy Neck flint chips, charcoal, and hearth stones from Indian encampments are associated with some of the exposed forest floor layers (Oldale, 1992).

Moraines are ridges of drift formed by moving ice. Most moraines are formed when the ice front remains more or less in the same place because advance of the glacier is balanced by melting along the ice front (Fig 1.3). When glacial debris falls free of the ice, it accumulates along the ice front much like material at the end of a conveyor belt. The advancing ice thrust sheets of drift upward and forward to form a large ridge beyond the ice front (Rockmore, 1979).

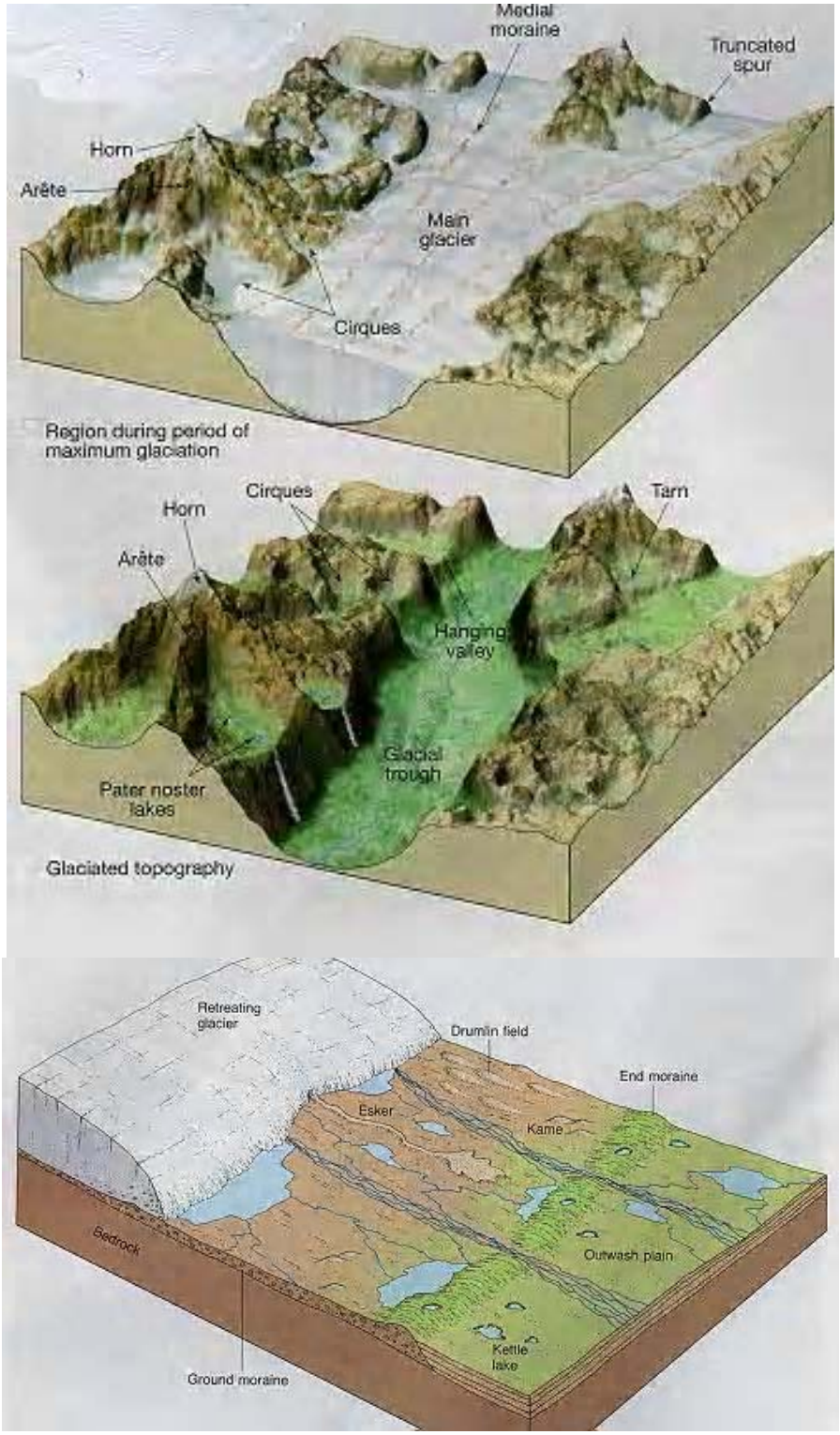

Figure 1.3. Moraine formation after ice movement. (Source: USGS, 2006).

The Buzzards Bay and Sandwich moraines were formed in a different manner (Figs.1.4 and 1.5); they were formed when an advancing ice front overrode sediments it had previously deposited or sediments that were older than the previous glaciations (Strahler, 1988).

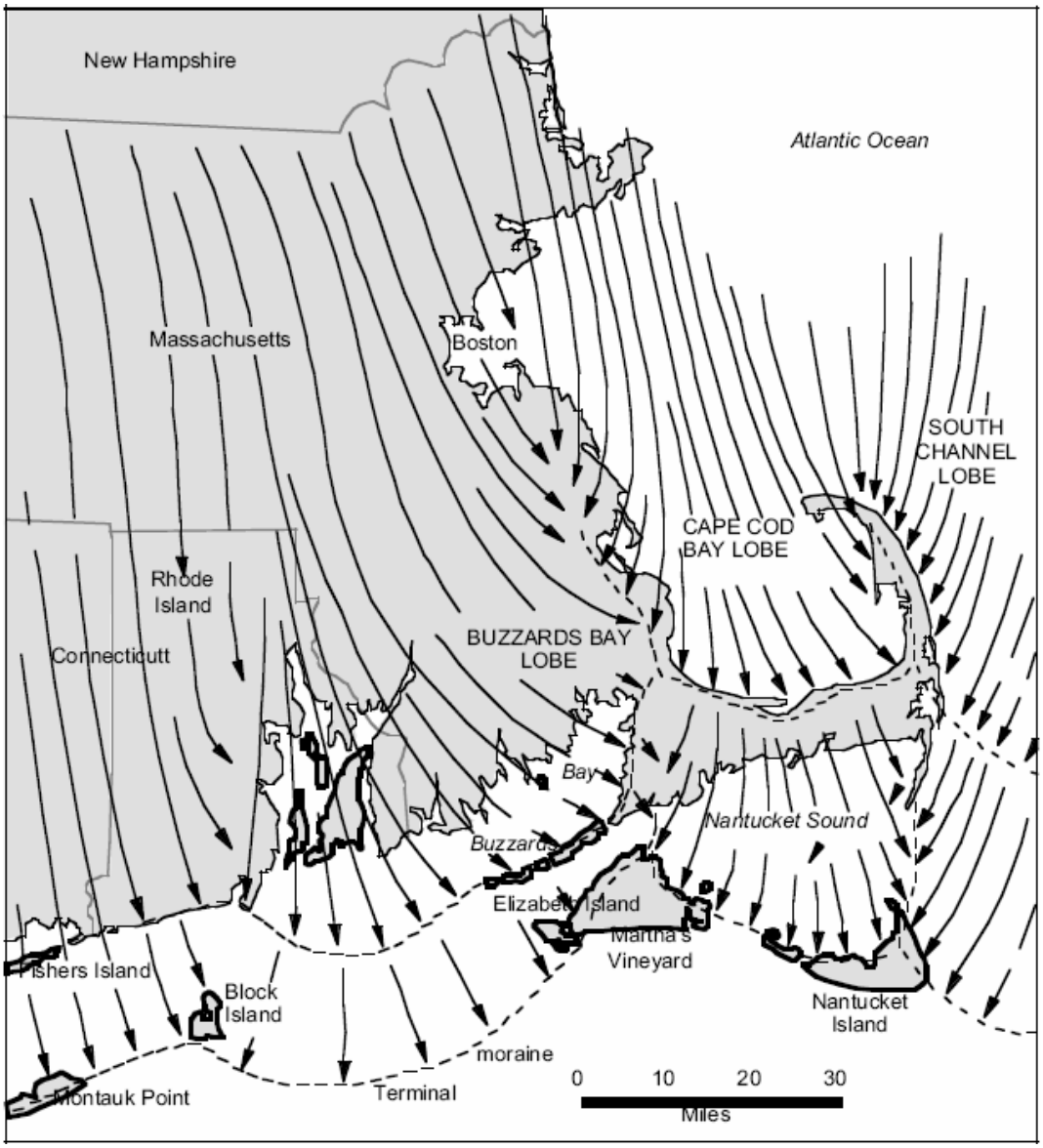

Figure 1.4. Southern New England showing the directions of flow of ice of the Wisconsin Stage (by arrows) and the two portions of ice standstill (dashed lines). (Source: Strahler, 1988).

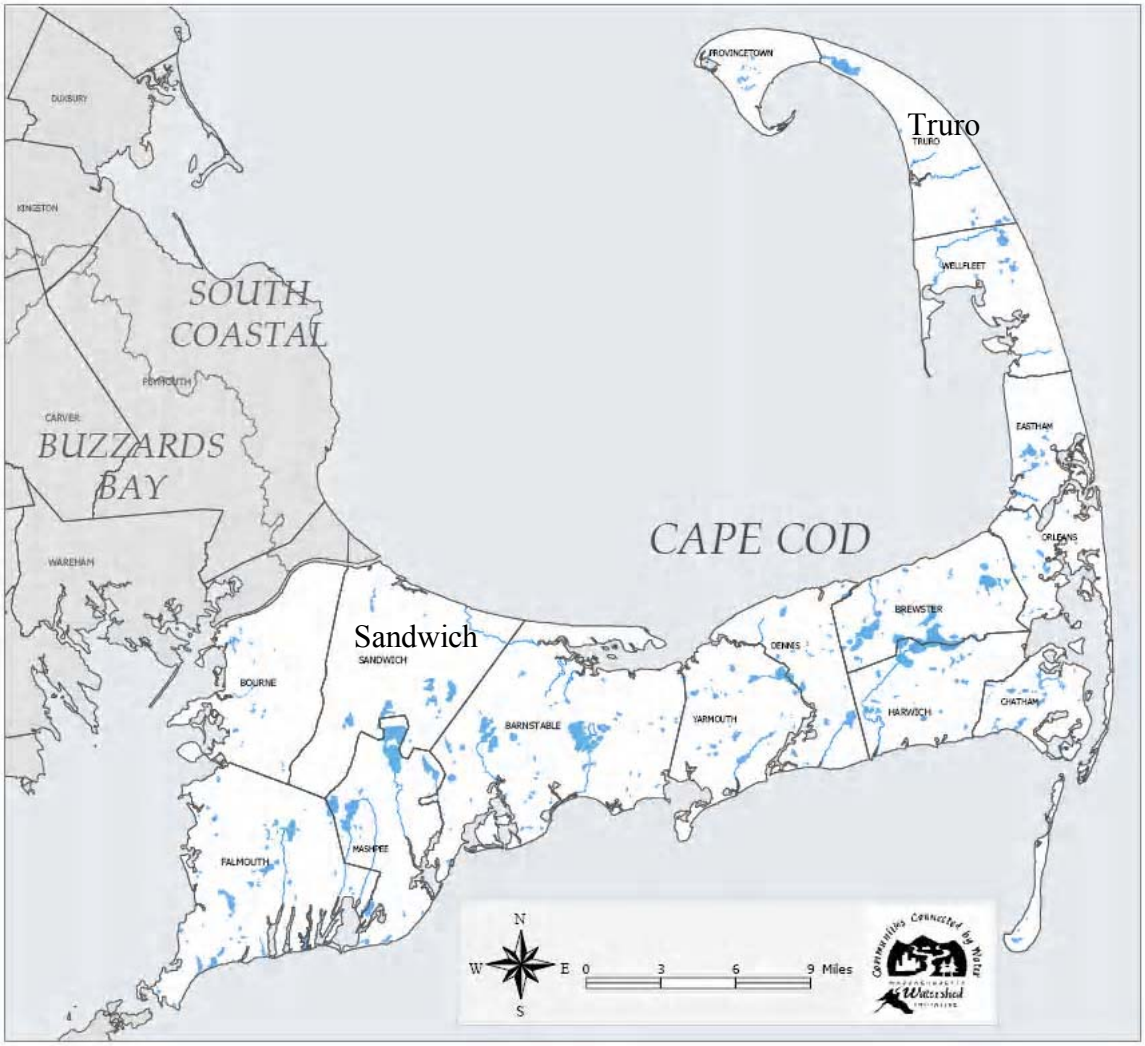

Figure 1.5. Buzzards Bay and Sandwich locations on Cape Cod. (Source: Massachusetts Government Publications, 2005).

Outwash plains make up most of the Cape Cod landscape. Such plains are composed up of sand and gravel deposited by meltwater streams that flowed across the plain in a braided pattern. This resulted in a broad flat depositional surface that sloped gently away from the ice front. This slope is called an ice-contact head of outwash. Outwash deposits also form a highly irregular and unorganized morphology called kame

and kettle terrain. A kame is a knoll or hill composed of outwash deposits, which originally filled a hole in the ice. When the ice melted, the deposits collapsed to form a hill. A kettle is just the opposite of a kame. The outwash is deposited around and over an ice block. When the ice block melts away, the outwash collapses to form a hole (Strahler, 1988).

Kettle holes mark the site of ice blocks that were left behind by the retreating glacier and buried by the outwash deposits. The buried ice was well insulated from the warmer post-glacial temperatures and may have persisted for several thousand years. Kettle holes that are deep enough to expose the water table contain ponds or lakes (Fig. 1.6). Similar to the ocean shore, waves have eroded sections along the shore to form cliffs and the eroded sand and gravel have been carried along the shore and deposited across the shoreline. These low ridges composed of beach sand are called bay mouth bars (Uchupi et al., 2001). In many kettle ponds, these processes have smoothed the shoreline so that the ponds are almost circular. Basal organic sediments in kettle ponds have been carbon-dated; the oldest are approximately 12 thousand years old. These early dates appear to occur in kettles that are underlain by fine sediments, which prevented or impeded the percolation of rain and snow melt. Other kettle pond basal sediments are much younger and appear to indicate the time when the rising water table, caused by the rising sea level, first intersected the floor of the kettle hole (Uchupi et al., 2001).

Figure 1.6. Kettle hole in Cape Cod (CCNS, 2006).

Most, if not all, of the outwash plains were formed as deltas in glacial lakes. The outwash plains on the upper Cape were formed in glacial lakes that occupied Nantucket Sound and Vineyard Sound, and those on the lower Cape were formed in a lake that occupied Cape Cod Bay (Fig. 1.5). This is the best known of all the glacial lakes because outwash deltas graded to the lake occur all around Cape Cod Bay from Duxbury to Truro. Stratified muds, silts, and deltaic sands accumulated in this glacial lake, which covered an area amounting to about 400 square miles. A river outlet cutting into the recessional moraine drained water out of the lake, presumably in the area of Eastham and the Town Cove section of Nauset Beach. The South Channel lobe was situated just to the east, and its meltwater carried huge quantities of sediment from the glacier. This sediment formed the gently sloping (towards the west) outwash plains that are several miles long and now comprise much of the Outer Cape (Rockmore, 1979).

The lake was given the name Glacial Lake Cape Cod. The earliest levels of the lake ranged between roughly 80 and 50 feet above present sea level, and during these stages the lake drained across the Sandwich moraine and into the lowland that was to become Buzzards Bay. As the Cape Cod Bay lobe retreated northward, lower outlets were occupied and eventually the lake drained completely. The initial outlet across the Sandwich moraine was continuously lowered by erosion as the water escaped, and when the outlet was eroded to an elevation of about 30 feet, the outlet was closed (Finch, 2003).

Many other features on Cape Cod owe their existence, at least in part, to glaciations. The most common feature may be the large to very large boulders scattered about the glacial surface, usually in the moraines or ice contact terrains. These glacial boulders are too large to have been carried by running water and thus must have been deposited directly by the ice. Doane Rock in Eastham is the largest glacial boulder known on Cape Cod, and pits dug at the base show as much rock below the surface as above (Fig.1.7) (Thoreau, 1989).

Figure 1.7. Doane Rock in Eastham is a glacial boulder. (Source: CCNS, 2006).

Perhaps the most intriguing features related to glaciations are the valleys eroded in the outwash plains. The valleys are relict because most do not contain rivers or streams. They are dry except where their lower reaches have been inundated by the rise in sea level. The origin of these valleys is complex. They most likely were formed by a process called spring sapping. This occurs when the water issuing from a spring carries away loose sand and gravel and causes the spring to migrate headward, carving a long straight valley (Uchupi et al., 2001).

In the case of the outwash plain valleys on Cape Cod, some special conditions were required for valley formation. Presently there are few springs on Cape Cod because in almost all places the outwash deposits are very permeable and the upper part of the outwash plain deposits is dry. In order for spring sapping to occur, a higher than present water table is required. This could be accomplished by the presence of glacial lakes with altitudes well above present sea level being dammed by the outwash plains. The best example would be Glacial Lake Cape Cod that was dammed by the outwash plains and the Sandwich moraine on upper Cape Cod (Figs. 1.4 and 1.5). The high lake levels would cause a rise in the water table that would, in turn, cause springs to form on the outwash plains. There is evidence for a glacial lake to the east of the lower Cape outwash plains in the form of silt and clay beds exposed in the cliff below Highland Light in Truro. Nothing more is known of this lake, but it may have provided a higher than present water table to allow spring sapping to form the valleys in the lower Cape outwash plains (Rockmore, 1979).

The Pamet Valley in Truro is wider and deeper than all other valleys on Cape Cod. The original floor of the valley, made up of glacial outwash, is well below sea level and

overlain mostly by salt marsh deposits. The Pamet Valley may have started out like all other spring sapping valleys; however, the extreme width and depth of the valley requires further explanation. It is likely that headward erosion by spring sapping cut completely across the Wellfleet outwash plain, reaching the outwash dam holding in a glacial lake to the east of the lower Cape. A breach caused the lake to drain catastrophically. This great flood carried away vast amounts of outwash to widen and deepen the original spring sapping valley (Finch, 2003).

Because of its exposed location, Cape Cod was visited by many early explorers. Although clear-cut evidence is lacking, the Vikings may have sighted this land about 1,000 years ago. It was visited by Samuel de Champlain in 1605 who described the region. Bartholomew Gosnold, a lesser known explorer, settled for a short time on the Elizabeth Islands to the southwest of Woods Hole and gave Cape Cod its name in 1602. The pilgrims first landed in America on the tip of lower Cape Cod after they were turned back from their more southerly destination by shoals between Cape Cod and Nantucket Island. On Cape Cod potable water and food were found. The Pilgrims, however, decided that this land was too sandy to support them, and they sailed across Cape Cod Bay to establish Plymouth (Finch, 2003).

Although once covered by mature forest, European settlers engaged in clear-cutting and grazing practices that by the early 1800s had eliminated much of this vegetative community and destabilized the land surface. The legacy of these activities is a sparsely vegetated landscape of shifting dunes and interdunal depressions. The latter are formed by the scouring action of wind, which can lower ground elevations to the point that they intersect the groundwater table for part of the year. These

seasonally flooded wetlands, also known as dune slacks, develop distinctive hydrophilic plant communities and are virtual oases of biodiversity in an otherwise desert-like environment (Fig. 1.8) (Foster, 1998).

Figure 1.8. Dune slacks in Cape Cod.

Hydrology and water quality are of critical importance to the structure and function of dune slacks (van der Laan, 1979; Seliskar, 1988, 1990; Mitsch and Gosselink, 1993; Chadde et al., 1998). Hence, CCNS's dune slacks may be at risk since the rapid growth of towns adjacent to the seashore has been accompanied by increased demands for freshwater, which can lower the groundwater table (Martin, 1993). Urban development

also carries with it the potential for groundwater contamination from a wide variety of pollutants (Winkler, 1994). Other threats include infestations of exotic plants such as *Phragmites australis* and *Lythrum salicaria*. On a broader scale, atmospheric deposition, troposphere ozone depletion, sea level rise, and global warming may affect the condition of these wetlands. Unfortunately, relatively little is known about dune slacks within CCNS and, more importantly, how they are influenced by changes in the regional and global environment. A rigorous assessment of CCNS's dune slack habitat is needed to provide a basis for understanding, evaluating, and effectively managing this resource.

Sand dunes cover the northern part of Cape Cod. Dunes are shaped by the prevailing winds and migrate constantly. On the Provincetown spit there are parabolic, or U shaped dunes, with the open end facing the wind. These are formed when the wind blows away the sand in the middle of the dune, exposing the underlying beach deposits. The eroded sand is transported by the wind and deposited along the advancing leeward face of the dunes (USGS, 2006). The parabolic dune orientation is driven by strong winds from the northwest predominantly in the winter, but is occasionally important in summer (Allen et al., 2001).

Active coastal dunes are dynamic landforms whose shape and location are ever-changing. Youthful, unvegetated dunes are on the move as the sand, exposed to the prevailing wind, is picked up, transported, and redeposited repeatedly. When the dunes become vegetated, they stabilize and tend to remain unchanged for some time. If the dunes lose the protective vegetation, they will move again. This can be seen along US Route 6 in Provincetown, where once stable dunes are advancing on the forest and highway and are filling Pilgrim Lake (CCNS, 2006).

1.3. Geologic Hazards at Cape Cod

The forces of marine erosion will continue to attack Cape Cod and new lands built by waves, currents, and winds will not balance the loss of land to the sea. Current dune movement is approximately 9 feet per year, and the cliffed oceanside of lower Cape Cod loses about 5 acres per year to marine erosion (Oldale, 1992). New land constructed from this eroded material averages about 1 acre per year. Thus for each acre lost, less than half an acre is gained. Estimates for other parts of the Cape vary greatly from this figure (Oldale, 1992). The shore erosion is threatening the lighthouse (Fig. 1.9), as the sea wall of boulders was built in a futile effort to protect the lighthouse from wave attack.

Figure 1.9. Cape Cod lighthouse. (Source: CCNS, 2006).

Unfortunately, the sea wall was poorly placed and actually increased the rate of erosion. The situation might be like that of Billingsgate Island that, in the middle 1800s, was about a mile long and about a half mile wide and included about 30 homes, a school house, and a lighthouse. Today, Billingsgate Island is a shoal that is exposed above sea

level only during the lowest tides (Figs. 1.10 and 1.11). The island was described by the Pilgrims in 1620 as "an island of 60 acres southwest of Wellfleet" (Clark, 1992), and due south of Jeremy Point. The island no longer exists - a victim of the ever-changing boundaries of the Cape. Since the area was an excellent location for fishermen, a fourteen-foot lighthouse on a granite foundation was built at the island in 1822. In 1858, a new lighthouse was built, similar in design to the previous structure. Over this period, the island was clearly disappearing due to erosion (Clark, 1992). In 1888, the lighthouse was so threatened from the sea that 1000 feet of bulkheads and jetties were built around the lighthouse. By 1915 Billingsgate Island was destroyed by storm, and the only remaining occupants of the island were the keeper and a watchman who guarded the Wellfleet oyster bed. The island itself completely vanished by 1942. Only a shoal marked by a beacon remains today. Interestingly, the 1992-93 AAA Connecticut-Massachusetts-Rhode Island map, which this author used for local travels, still shows Billingsgate Island less than a mile south of the tip of Jeremy Point (Clifford, 1994). The fate of Billingsgate Island may be a precursor for Cape Cod as the sea continues to erode the fragile land (USGS, 2006).

Figure 1.10. Billingsgate Island. (Source: New England Lighthouses, 2005).

Figure 1.11. Billingsgate Island lighthouse in 1893. (Source: National Museum of American history, 2006).

Cape Cod is affected by hurricanes on average every 5.62 years, and the average years between direct hurricane hits is 33.75 years (NOAA, 2006). CCNS was last affected when the 2004 Aug 31st thunder storm Hermine hit from the SW with 40mph winds. Previous hurricanes occurred in 1879; 1916 (85 mph); 1944 (80 mph winds from the SSW); 1954 (90 mph winds); 1961 (120 mph); and 1991 hurricane Bob (97 mph winds, and the area had sustained winds of 70 mph and 5 associated tornadoes) (Figs. 1.12)

Slope failure events, when a landslide event occurs, is another geologic hazard of the area. Landslides include a wide range of phenomena involving downslope ground movement such as deep slope failure, shallow debris flows, and avalanches (Fig. 1.12).

Figure 1.12. Evidence of natural hazards on Cape Cod. (Source: CCNS, 2006).

Gravity acting on a slope is the primary cause of landslides, but there are other important and dynamic factors that serve as triggers. Saturation of slopes by precipitation (rain or snowmelt) weakens soil by reducing cohesion and increasing the pressure in pore spaces, pushing grains away from each other. Erosion and undercutting of slopes by streams, rivers, glaciers, or waves increase slope angles and decrease slope stability. Perhaps most significant from a management perspective, the overweighting and/or undercutting of slopes for facilities, roads, trails, mines, and other manmade structures change the natural slope equilibrium and cause slopes to fail (Keller, 2004).

In the past landslides were often viewed as extreme or unusual events that had to be cleaned up and/or stabilized. More recently, it has been recognized that landslides, like other geologic processes, are natural and play a fundamental role in shaping ecosystems. Nevertheless, human activities may accelerate landsliding processes by altering the land surface for agriculture, grazing, development, or other uses (Keller, 2004).

Erosion of the glacial deposits produced imposing marine cliffs, many of which are currently retreating at alarming rates. Although scarp retreat of the eastern shoreline averages 0.67 m/yr, specific coastal sites are losing land to the sea at higher rates. For example, the cliffs below Wellfleet-by-the-Sea are retreating approximately 1.0 m/yr (Pinet, 1992). Because most of this erosion occurs during storm events, cliff retreat is not constant over time.

1.4. Application of Remote Sensing and GIS Technologies

Remote sensing is the non-contact image recording of different objects from aircraft or spacecraft. Remote sensing technology has been widely used for map processing and applied research of different regions across the earth. This technology was useful during the Second World War and the Cold War for spying by governments. It is still being intensively used for military purposes. At the same time, remote sensing provides many applications for non-military purposes, including natural resource management.

Remote sensing information may be useful for modeling and earth resource analysis perspectives, including monitoring the global carbon cycle, biology and biochemistry of ecosystems, aspects of the global water and energy cycles, climate variability and prediction, atmospheric chemistry, and monitoring land-use change and natural hazards (Sadler, 2004). The American Society for Photogrammetry and Remote Sensing (ASPRS) adopted the definition of remote sensing as the art, science, and technology of obtaining reliable information about physical objects and the environment, through the process of recording, measuring and interpreting imagery and digital representations of energy patterns derived from noncontact sensor systems (ASPRS, 2006).

Remote sensing can provide information about the chemical composition of rocks and minerals on the Earth's surface that are not completely covered by dense vegetation. Emphasis is placed on understanding unique absorption bands associated with specific

types of rocks and minerals using imaging spectroscopy techniques (Jensen, 2000). Remote sensing can be used to extract geologic information including lithology, structure, drainage patterns, geomorphology, landforms, and patterns and processes, including eolian, igneous, tectonic, karstic, fluvial, shoreline, and glacial.

Soil is defined as unconsolidated material at the surface of the Earth. Soil is the weathered material between the atmosphere at the Earth's surface and the bedrock below the surface to a maximum depth of approximately 200 cm (USDA, 2006). Soil is a mixture of inorganic mineral particles and organic matter of varying size and composition. The particles make up about 50 percent of the soil's volume.

Radiant energy from soil can be recorded by a remote sensing system over exposed soil and is a function of electromagnetic energy from several sources. Spectral reflectance characteristics of soils are a function of several important characteristics, such as soil texture (percentage of sand, silt, and clay), soil moisture content (e.g. dry, moist, saturated), organic matter content, iron-oxide content, and surface roughness (NASA, 2006). *In situ* spectroradiometer reflectance curves can be used for dry silt and sand soils. Radiant energy may be reflected from the surface of the dry soil, or it penetrates soil particles, where it may be absorbed or scattered. Total reflectance from dry soil is a function of spectral reflectance and internal volume reflectance. As soil moisture increases, each soil particle may be encapsulated with a thin membrane of capillary water. The interstitial spaces may also fill with water. The greater the amount of water in the soil, the greater the absorption of incident energy and the lower the soil reflectance. Higher moisture contents in sandy soil and clayey soil result in decreased reflectance throughout the visible and near-infrared region, especially in the water-absorption bands at 1.4, 1.9,

and 2.7 μm (Huete, 1988). Generally, the greater the amount of organic content in a soil, the greater the absorption of incident energy and the lower the spectral reflectance. Iron oxide in a sandy loam soil causes an increase in reflectance in the red portion of the spectrum (0.6 - 0.7 μm) and a decrease in the near-infrared (0.85 - 0.90 μm) reflectance.

Rocks are assemblages of minerals that have interlocking grains or are bound together by various types of cement (usually silica or calcium carbonate). When there is minimal vegetation and soil present and the rock material is visible directly by the remote sensing system, it may be possible to differentiate between several rock types and obtain information about their characteristics using remote sensing techniques (Anderson, 1976).

There are a number of processes that determine how a mineral will absorb or scatter the incident energy. Also, the processes absorb and scatter light differently depending on the wavelength of light being investigated. The variety of absorption processes (e.g., electronic and vibrational) and their wavelength dependence allow the investigator to derive information about the chemistry of a mineral from its reflected or emitted energy. The ideal sensor to use is the imaging spectrometer in remote sensing because it can record much of the absorption information, much like using an *in situ* spectroradiometer (Atkinson, 2000).

Geologists often use remote sensing in conjunction with *in situ* observation to identify the lithology of a rock type, i.e., its origin. The type of rock determines how much differential stress (or compression) it can withstand. When a rock is subjected to compression, it may experience: 1) elastic deformation in which case it may return to its original shape and size after the stress is removed; 2) plastic deformation of rock, called folding, which is irreversible (i.e., the compressional stress is beyond the elastic limit);

and/or 3) fracturing, where the plastic limit is exceeded and the rock breaks into pieces. This may result in faulting (Keller, 2004). Folding takes place when horizontally bedded materials are compressed. The compression results in wavelike undulations imposed on the strata. There are four basic types of folds: 1) monoclines (a single fold on horizontally bedded material, like a rounded ramp); 2) anticlines (archlike convex upfold domes - oldest rocks in the center); 3) synclines (troughlike concave downfold - youngest rocks in the center); and 4) overturned (where the folds are on top of one another). Such landforms can be detected using remote sensing technologies. The U.S. Geological Survey (USGS) developed *Land-Use/Land Cover System for Use with Remote Sensor Data* (USGS, 2006).

Earth landscapes exhibit varying stream densities and patterns that can be identified using remote sensing data. The permeability of a soil or rock (i.e., how easily water passes through the material) is closely related to drainage density. Permeability is inversely proportional to runoff. Where permeability is low and runoff is high, many gullies typically form. Conversely, when permeability is high and runoff is low, much of the water infiltrates into the ground and a larger surface area is required to provide sufficient runoff for the creation and maintenance of a channel (tributary). Weak impermeable clays and shales produce the highest drainage density (Keller, 2004).

Drainage patterns developed through time on a landscape provide clues about bedrock lithology (e.g., igneous, sedimentary, metamorphic), topography (slope, aspect), the texture of the soil and/or bedrock materials, the permeability of the soil (how well water percolates through it), and the type of landform present (e.g,. alluvial, eolian, glacial). While *in situ* observations are essential, physical scientists often use the synoptic

bird's-eye-view provided by remote sensing to appreciate regional drainage patterns, including dendritic, pinnate, trellis, rectangular, parallel, annular, dichotomic, braided, deranged, anastomotic, sinkhole (doline), radial (centrifugal) and centripetal patterns (Keller, 2004).

Remote sensing and GIS techniques are powerful tools to register land surface changes and to quantify dune migration (Martin, 2005). A worldwide inventory of dune types has been developed using images from space and aircraft. The inventory defines five basic types of dunes: crescentic, linear, star, dome, and parabolic (USGS, 2006).

U-shaped mounds of sand with convex noses trailed by elongated arms are parabolic dunes (Fig. 1.13). Sometimes these dunes are called U-shaped, blowout, or hairpin dunes. The elongated arms of parabolic dunes follow rather than lead because they have been fixed by vegetation, while the bulk of the sand in the dune migrates forward (USGS, 2006).

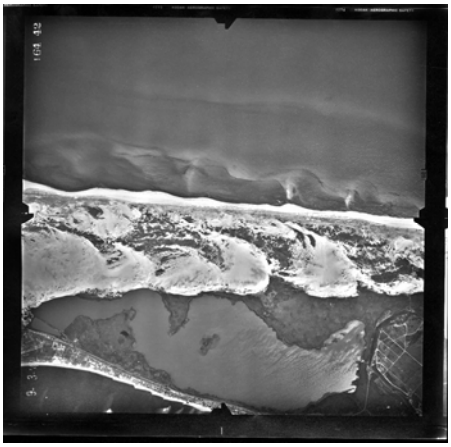

Figure 1.13. U-shaped, or parabolic, or blowout, or hairpin dunes. (Source: CCNS, 2006).

When strong winds erode a section of the vegetated sand (a blowout), a parabolic dune may form. Leeward motion occurs if sand from the blowout is deposited on the opposite slope of the parabolic dune (Figs. 1.14 and 1.15). Vegetation holds the "arms" of the dune in place as the leeward "nose" of the dune migrates forward toward the main dune field (PD, 2006).

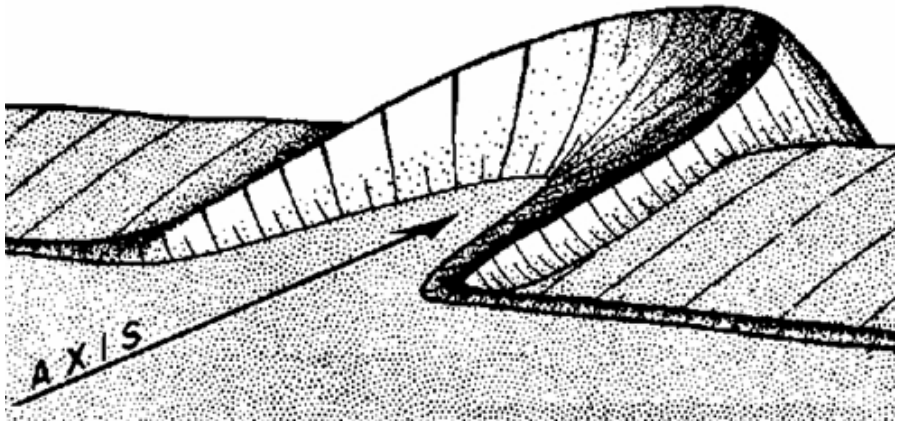

Figure 1.14. Parabolic dunes structure. (Source: PD, 2006).

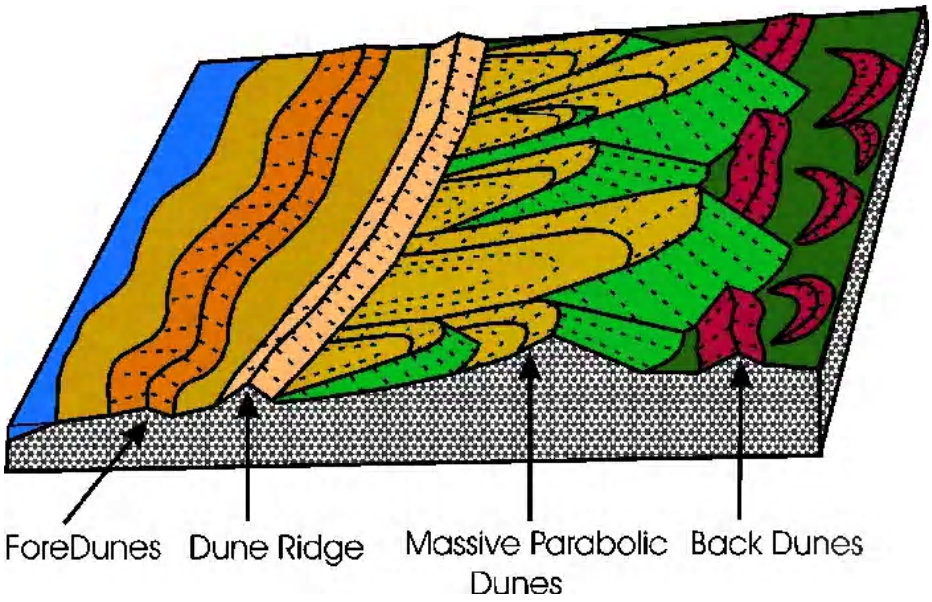

Figure 1.15. Parabolic dunes structure. (Source: PD, 2006).

Aerial photographs have been used to examine dune migration in the Great Sand Dunes National Park and Preserve (GSDNPP) in Colorado (Wiegand, 1977; Martin, 2005). The first area, located on the west periphery of the main dune mass near Sand Creek, showed that barchan dunes advanced up to 9 m/year toward the northeast and east from 1966 to 1975. The second area along the eastern periphery of the main dune mass showed two distinctive patterns of dune migration from 1936 to 1975. Transverse dunes trending northwest –southeast moved from 7 to 16 m/year, whereas those oriented N–S migrated 1 to 7 m/year (Wiegand, 1977). Parabolic dunes in the third area at the eastern periphery of the main dune mass advanced between 2 and 16 m/year from 1936 to 1975. Finally, the dunes located east of Medano Creek showed net migration from 3 to 6 m between 1936 and 1966, and dune migration slowed to 3–10 m/year between 1966 and 1975.

Hammond (1998) determined the extent, number, size, and the spatial distribution of wetlands for an area adjacent to Sand Creek using 12 sets of aerial photographs from 1936 to 1995. This analysis indicates that the number and area of the wetlands was greatest in the 1930s, decreasing in number from 114 wetlands in 1937 to 22 wetlands in 1979. In 1995, the number of wetlands increased to 51 in response to subirrigation of meadows and to groundwater discharge.

Synoptic land cover information was mapped at the GSDNPP based on an unsupervised classification of a Landsat image on June 23, 1990. This classification categorized the area as 41.3% sand deposits, 0.6% water, 49.5% treeless vegetation, 7.5% conifers, and 1% riparian/Cotton-wood (*Populus angustifolia*)/Aspen (*Populus tremuloides*) (Curdts et al., 1999). Janke (2002) evaluated changes in the dune mass

extent and in land cover for the GSDNPP using supervised classification of two Landsat images on 7 July 1984 and 18 August 1998 with subsequent field assessment in August 2001. This study concluded that semidesert scrub was the only class that increased by 5% (1457.3 ha) during this interval, at the expense of dune grass. The most dramatic changes occurred on the western side of the main mass, where dune grass was replaced by scrub and on the eastern side where dune grass and scrub expanded on the dunes. Janke (2002) concluded that the main dune mass is stable, although studies by Schlesinger et al. (1990) indicate that eolian transport may be enhanced on semiarid landscapes with the dominance of shrubs.

Some researchers and users may rely on remote sensing data interpretations without paying much attention to the uncertainties and errors of such data. One of the main research decisions using remotely sensed data is to determine what the desired suitable precision and accuracy level is and what kind of error is reasonable for the specific research or map (Woodcock, 2002). The important factor is the input data, quality, nature and source of such data, the kind of technology used to prepare data, including type of cameras, scanning equipment, what type of platforms (i.e. based on airplanes or spacecrafts), relevant environment conditions, seasons and time of day. Another consideration is what should be mapped, (e.g., size of area), which is connected directly to the mapping accuracy. To ensure overall accuracy metric analysis is applied, including the Kappa statistic (Woodcock, 2002). The Kappa statistic is used to measure the agreement between two sets of categorizations of a dataset. In terms of landscape analysis, this statistic estimates the accuracy of predictive models by measuring the agreement between the predictive model and a set of field-surveyed sample points in an error matrix. Schott

(1997) proposed to utilize the image chain approach for the uncertainties analyses, to review comprehensive perspectives for potential remote sensing uncertainties. Such an approach should help to avoid constricted or parochial tendencies, when a problem is narrowly reviewed i.e., only one part without analyzing entire procedures.

In advanced remote sensing, procedures should be presented as a detailed chain of interconnected steps. Each step has to be analyzed for its weaknesses. Improvements of the weakest link will improve the whole chain, thus ensuring better accuracy of data. The chain should consist of step-wise analyses such as: 1) what kind of recording equipment was used, including instruments such as cameras, scanners, lasers, linear arrays, and/or area arrays located on platforms such as aircraft or spacecraft; 2) which regions of the electromagnetic spectrum (ultraviolet, visible, infrared, or microwave) are addressed; 3) what type of algorithm can be employed to work with the acquired information by means of visual and digital image processing; and 4) what are the uncertainty and error examination mechanisms.

In order to study CCNS dune and wetland areas, datasets were generated that comprise a number of scientific disciplines. This includes data for locating dune regions, aerial photographs, geologic maps and digital elevation model (DEM) for watershed delineation and stream delineation. Thus, this approach involved 1) generation of digital mosaics of these datasets, and 2) assembly of the datasets into GIS formats.

CHAPTER 2: METHODS

Twelve dunes within the CCNS were chosen and named A through L (Fig. 2.1) and aerial photographs with maps from 1938 until 2005 were studied.

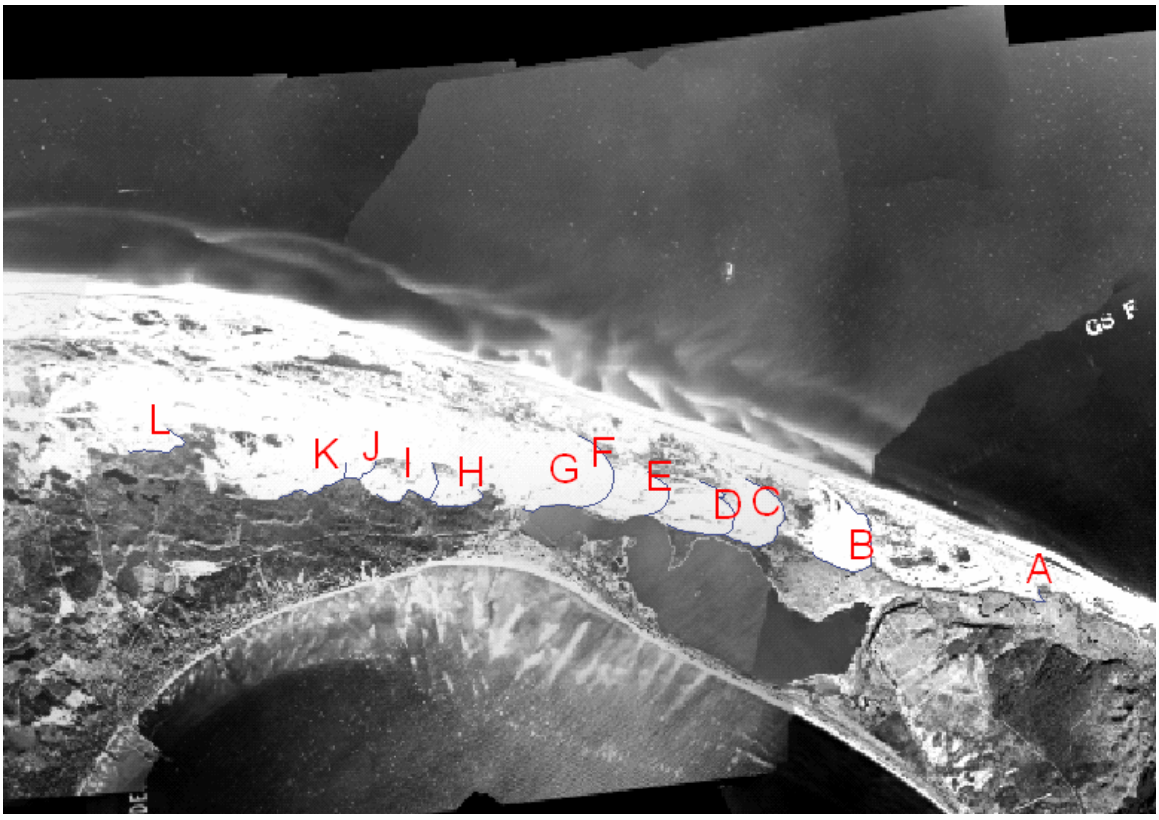

Figure 2.1. 1938 Cape Cod area with 12 selected dunes named A through L.

The study area of 12 dunes was selected in conjunction with the CCNS. The aerial photographs were obtained from the NPS archive. Aerial photographs were analyzed to track areas of individual dune movement and subsequent wetland propagation and expansion.

All aerial photographs were reviewed and photographs of the 12 dune region were selected. One of the 1967 aerial photographs is shown (Fig. 2.2). The aerial photographs with region of 12 dunes were georeferenced and digital maps created for the years 1938 through 2005.

Figure 2.2. 1967 Cape Cod aerial photograph.

A series of aerial photographs for 1938, 1947, 1960, 1969, 1977, 1986, 1987, 1994, 2001, 2003 and 2005 were collected, an example of 187 aerial photographs is shown (Fig. 2.3).

Cumulative distances of dune movement were analyzed; specifically, the areas of dunes B, C, and D were selected to create DEM, and aerial photographs from 1947 for this region were considered the most applicable for preparing the DEM. Catchments and drainage maps show changes of the wetland regions and their association with dune progress from these DEM images.

In this section, the main steps which were involved in the generation of the mosaics and DEM will be discussed.

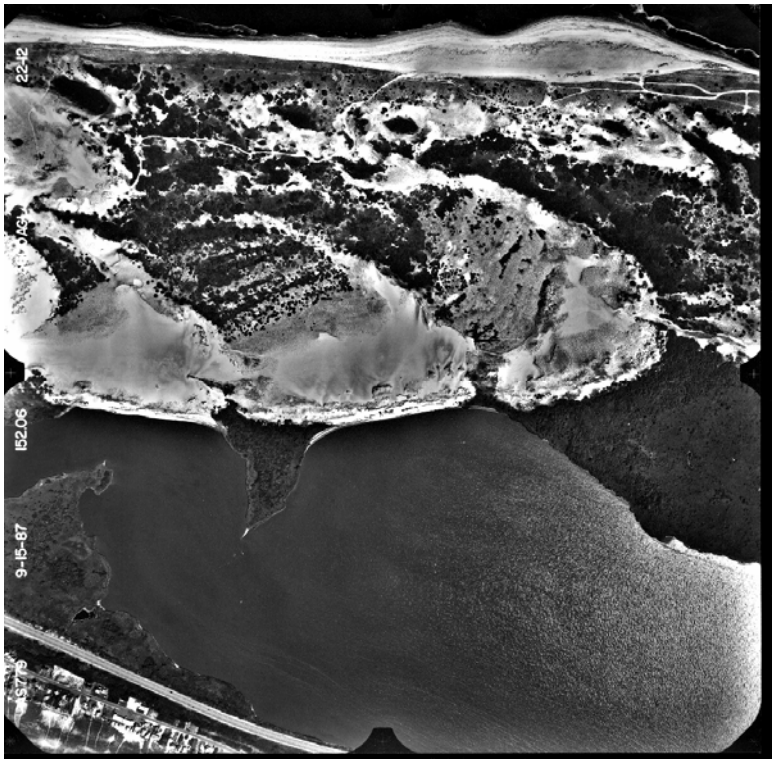

Figure 2.3. 1987 Cape Cod aerial photograph.

Aerial photographs from 1938 until 1987 were available in hard copy measuring 8'x 8', 9'x 9' or 10' x 10' inches. The aerial photographs from 1994 until 2005 were in digital version.

Remote sensing software ENVI, the remote sensing exploitation package (RSI, 2005); PCI Geomatics, Ortho Engine air photo models (PCI, 2005); ERDAS Image mapping and visualization software (Leica, 2005); and GIS, ArcGIS program (ESRI, 2005) are powerful tools to register land surface changes to quantify dune migration and were used in this research.

The absolute dune movement rates for the intervals 1938-1947, 1947-1960, 1960-1977, 1977-1986, 1986-1994, 1994-2001, and 2001-2003, with a plot of dune movement as a cumulative function were computed also.

2.1 Digital maps used and digital mosaics generated over the Cape Cod dunes area.

The digital data used for the study include:

(1) Rectified aerial photograph mosaic of Cape Cod, 2001;

(2) LIDAR aerial photographs of Cape Cod, 1998 and 2001;

(3) Aerial photographs for 1938, 1947, 1960, 1969, 1977, 1986, and 1987;

(4) Orthorectified georeferenced mosaic of aerial photographs for 1994, 2003, 2005;

(5) DEM generated from stereo pairs of aerial photographs acquired in 1947;

(6) Coverage of stream networks derived from DEM data, 1947 and 2001;

(7) Watershed boundaries derived from DEM data, 1947 and 2001;

(8) Dune boundaries and distances moved derived from mosaics of 1938 to 2003;

(9) Catchment areas and drainage networks extracted from the 1947 DEM and 2001 DEM images.

Details of the above mentioned digital data are follows:

(1) **Digital map of Cape Cod 2001** coverage, raster dataset - MrSID, was used as a base image to geo-reference all scanned aerial photos in TIFF format. The projected coordinate system is NAD_1983_StatePlane_Massachusetts_Mainland_FIPS_2001 (Fig. 2.4). MrSID is an acronym for ***M**ulti-resolution **S**eamless **I**mage **D**atabase*, a powerful wavelet-based image compressor, viewer and file format for massive raster images that enables instantaneous viewing and manipulation of images locally and over networks while maintaining maximum image quality. TIFF is an acronym for ***T**agged **I**mage **F**ile **F**ormat*, one of the most widely supported file formats for storing bit-mapped images on personal computers.

Figure 2.4. 2001 Cape Cod digital maps. (Source CCNS, 2005).

(2) **LIDAR images of Cape Cod for 1998 and 2000**. LIDAR is an acronym for ***LI**ght **D**etection **A**nd **R**anging*. It is a rapidly emerging technology for determining the shape of the ground surface plus natural and man-made features.

(3) **Mosaics of aerial photographs for 1938, 1947, 1960, 1969, 1977, 1986, 1987**. Scanned aerial photographs were referenced and jointly mapped (Fig. 2.5). Errors in location on this product are approximately 1 pixel size (1 m) on the average. The entire processing was performed using PCI, ENVI, or ERDAS - image processing software.

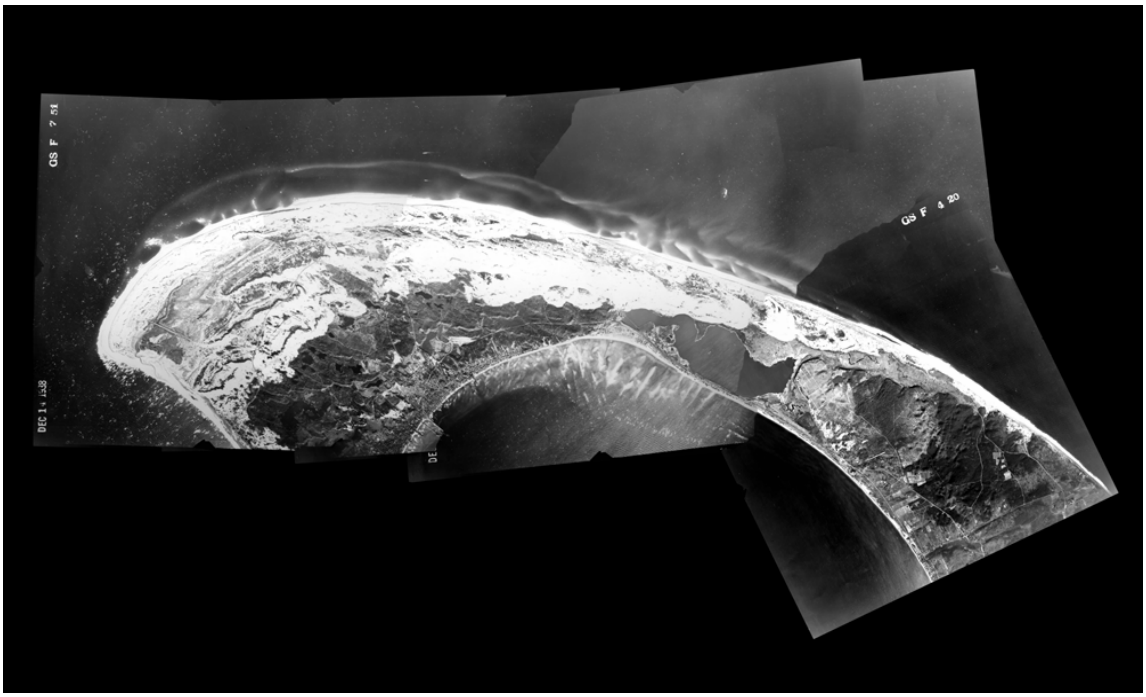

Figure 2.5. 1938 Cape Cod mosaics of aerial photographs.

(4) **Ortho rectified mosaic for 1994, 2003, and 2005** was provided by NPS CCNS. Ortho imagery is the next step beyond rectified imagery. In an orthorectified image, every point in the image appears as if it is being viewed from directly above.

(5) **DEM generated from stereo pairs of aerial photographs acquired in 1947** (Fig. 2.6). PCI geomatica software was used to generate a 30 m DEM.

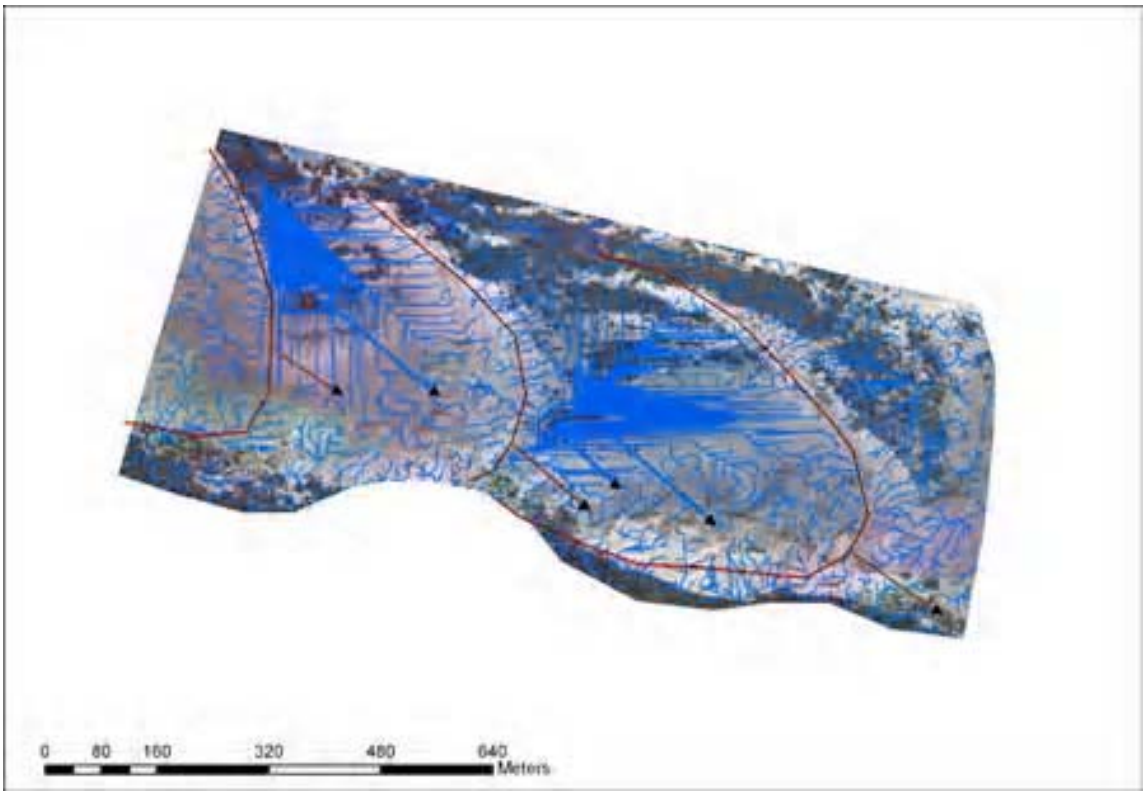

Figure 2.6. DEM generated from stereo pairs of aerial photographs acquired in 1947.

(6) **Coverage of stream networks derived from DEM data** (Fig. 2.7). DEM data was used to generate streams using ArcGIS software, an integrated collection of GIS software products for building a complete GIS (ESRI, 2005).

(7) **Watershed boundaries derived from DEM data** (Fig. 2.7). The DEM data were used to generate the Cape Cod watershed boundaries using ArcGIS. Watershed boundaries are presented in different colors.

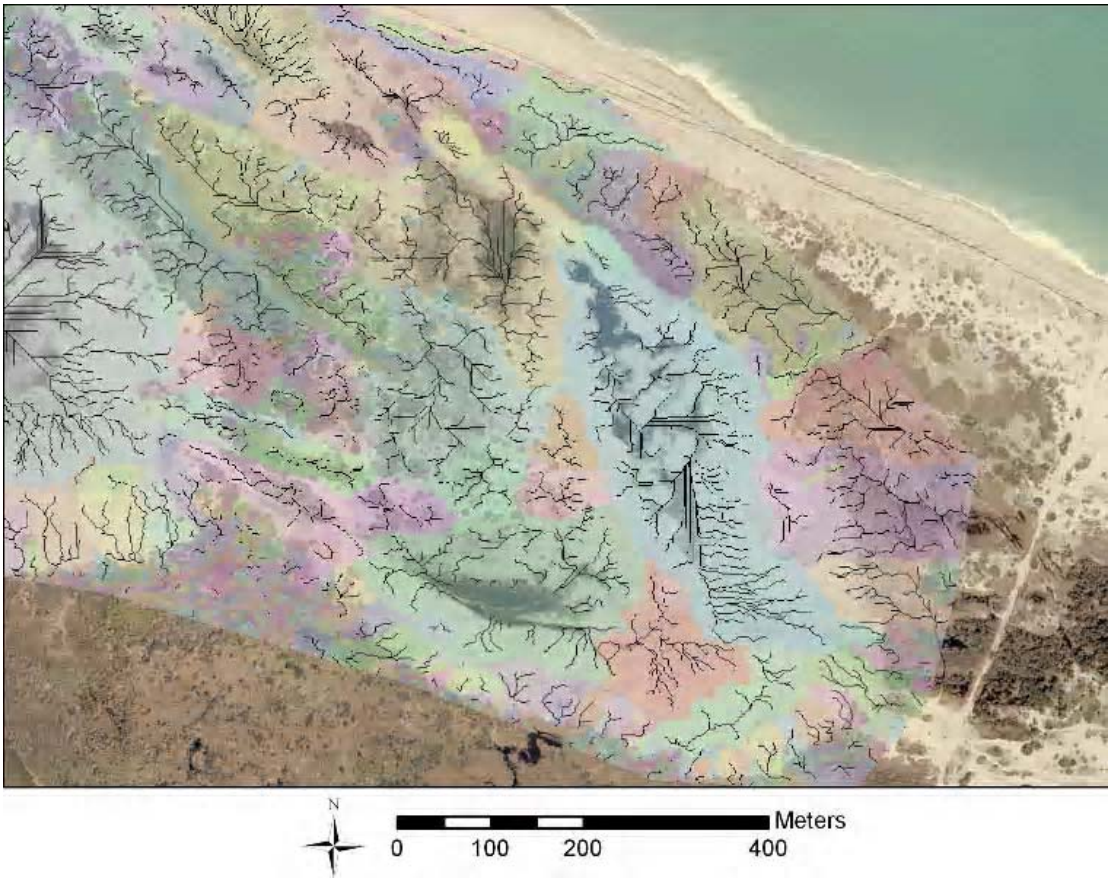

Figure 2.7. Stream network and watershed boundaries derived from DEM data, 2001.

(8) **Dune boundaries and moved distance derived from mosaics of 1938 to 2003.** The dune boundaries for the years 1938 to 2003 were drawn using ArcGIS tools, and distances moved were drawn and measured also in ArcGIS. Moreover, polygons were drawn which show the area of each dune covered from 1938 to 2003.

(9) **Catchment areas and drainage networks extracted from the 1947 DEM and 2000 DEM aerial photographs.** This image shows stream networks, catchment areas, wetlands and dune fronts (Fig. 2.8).

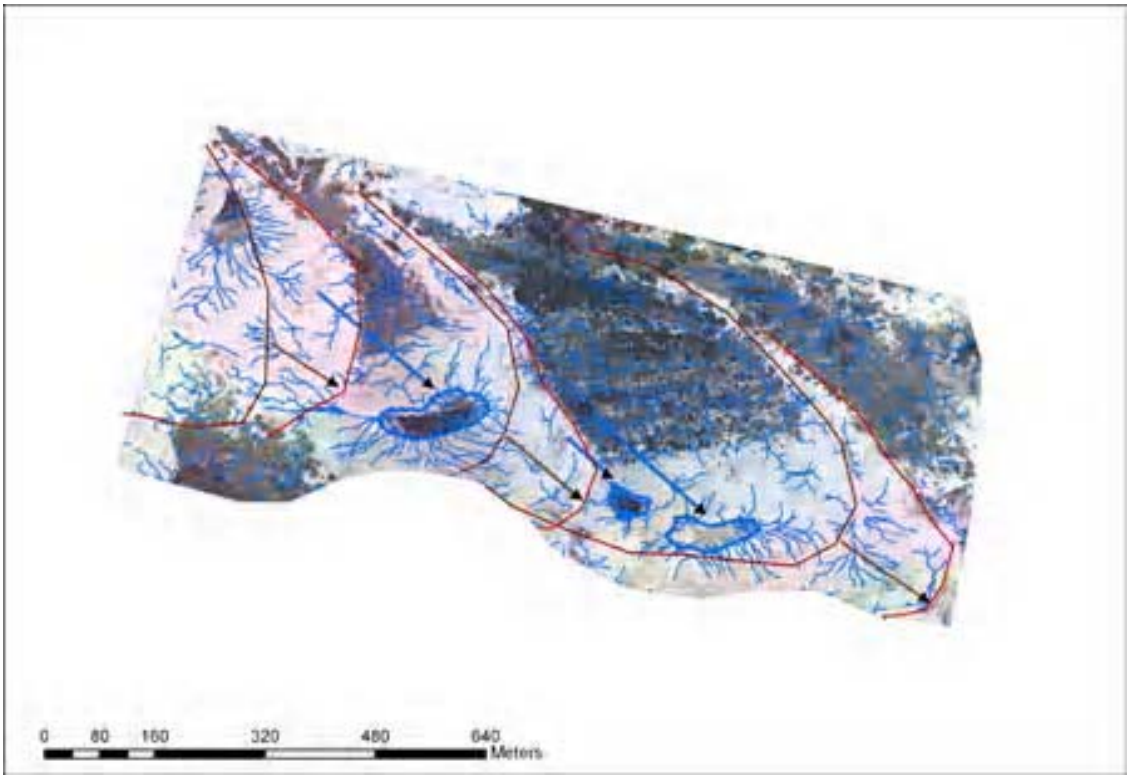

Figure 2.8. Catchment areas and drainage networks from the 2000 LIDAR aerial photographs.

2.2 Procedures used to generate products.

1) Aerial Photographs Mosaic.

For the generation of the georeferenced images, it was necessary to scan all aerial photographs which were not digitally represented. Such images include aerial photographs for 1938, 1947, 1960, 1977, 1986, and 1987. It is important to use a sophisticated scanner with specialized software for scanning; otherwise, it may be complicated to make useful georeferenced images for the analyses in DEM. The reasonable size of each scanned image in TIFF format (size 10'x10' inches) was about 0.5 Gigabytes, with 2400 dots per inch (dpi). The scanner ScanMaker9800XL Microtek TMA1600 was used with SilverFast Ai6 software, which is typically used for this type of aerial scanning. The scanner and software effectively scans both positive as well as negative photographs. The 1938, 1986, and 1987 photographs were in positive, and some including 1969 in negative versions.

The following steps were conducted separately for the 1938, 1947, 1960, 1969, 1977, 1986, and 1987 photographs:

a) Ground Control Points (GCPs) were collected in a standard coordinate system with the projected coordinate system: NAD_1983_StatePlane_Massachusetts_Mainland_FIPS_2001 and with the geographic coordinate system: GCS_North_American_1983.

b) Based on the collected GCPs digital aerial photographs were geo registered with tightening to the correlated geographic location.

c) Cut lines were created for each geographically referenced digital aerial photograph. Areas of interest were the dune regions. The dune areas were selected and the rest of the regions were eliminated.

d) Selected parts of geographically referenced digital aerial photographs were connected to each other by geographic location. The pixel spacing value is 1m.

e) The map mosaic was reviewed. The collars were removed. No color corrections were made, which is why variations in color exist between original aerial photographs and map mosaics.

f) The final map mosaic was compressed.

2) DEM for the dune areas of the Cape Cod peninsula.

The 1947 aerial photographs were chosen for DEM generation. For this research activity it was necessary to select the earliest aerial photographs to analyze dune and wetland changes to the present. The earliest aerial photographs available are from 1938; unfortunately, their quality was very poor for preparing wetland and dune DEM.

The following steps were conducted to create the 1947 DEM:

a) A new PCI project was created with projected coordinate system: NAD_1983_StatePlane_Massachusetts_Mainland_FIPS_2001; and geographic coordinate system: GCS_North_American_1983

b) Two 1947 neighboring aerial photographs were selected which cover the maximum of the same area in both aerial photographs (up to 50 %) (Fig 2.9).

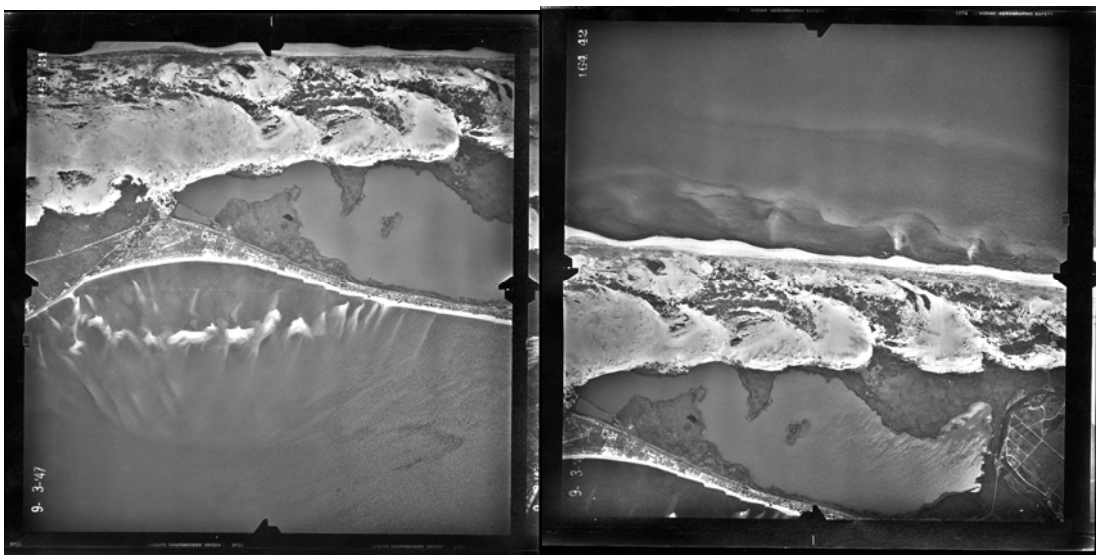

Figure 2.9. 1947 selected neighboring aerial photographs covering up to 50 % of the same areas in both photographs.

c) Four fixed points in each aerial photograph to which other GCPs can be related were selected; these four fixed points are called fiducial marks (Fig 2.10).

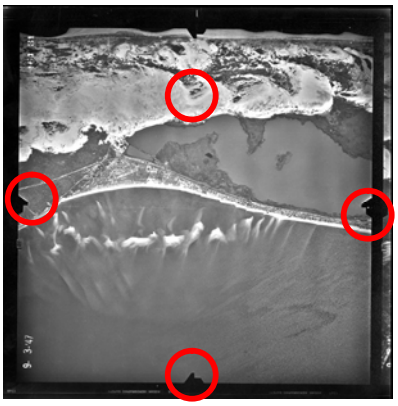

Figure 2.10. Fiducial marks at four sides of the aerial photograph, indicated by circles.

d) A digital map of CCNS 2001 coverage, raster dataset - MrSID, was imported into PCI to use as a base image to geo reference all aerial photographs.

e) GCPs were collected for each pair of scenes for all aerial photographs (about 20 edge points per aerial photograph). A map of Cape Cod 2001 coverage was used as the base map. Z elevations were supplied for each GCP.

f) Tie points were chosen which tie together interconnected neighboring aerial photographs. Tie points are those that are co-located on two images that have an overlapping geographic extent.

g) A new stereo image was created from the two interconnected neighboring aerial photographs, termed the Epipolar image.

h) A DEM was created from the Epipolar image.

i) A projected DEM was prepared based on x, and y locations of GCPs.

j) The DEM was filtered to fill areas where stereo solution failed, and to obtain the best edge matching of strips.

k) The corrected DEM was exported to GIS format.

3) Coverage of stream networks derived from DEM data.

Stream networks for Cape Cod were generated (Fig 2.11) from the DEM.

4) Watershed boundaries derived from DEM data.

Watershed boundaries were extracted from 1948 Cape Cod aerial photographs (Fig 2.11).

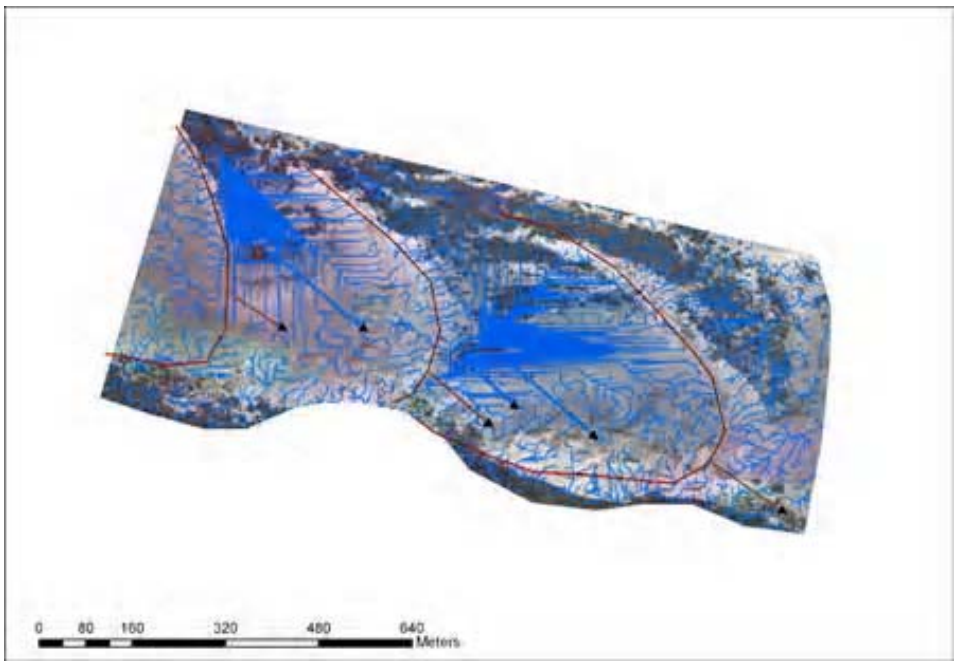

Figure 2.11. Coverage of a stream network and watershed boundaries from DEM data.

2.3 Information extracted from each dataset.

Identification of dune zones and wetlands is important in order to identify the location of catchments and dune areas. Rain water can potentially reside in fractured domains (e.g. lower regions, faults) within the crystalline basement. Intersection of the faults, fractures and shear zones within areas of the basement complex are potential areas

for surface and groundwater collection. The intersection of these discontinuities will enhance porosity and will create opportunities for water storage.

From the 12 working dunes (A through L) the areas of interest for preparing DEM were the regions around dunes D, E, and F (Fig. 2.12). The quality of 1947 aerial photographs was the most suitable for the DEM preparation. The stream networks were created for the D, E and F dune regions from the DEM. The stream network is useful to identify the wetland areas connected to dunes D, E, and F.

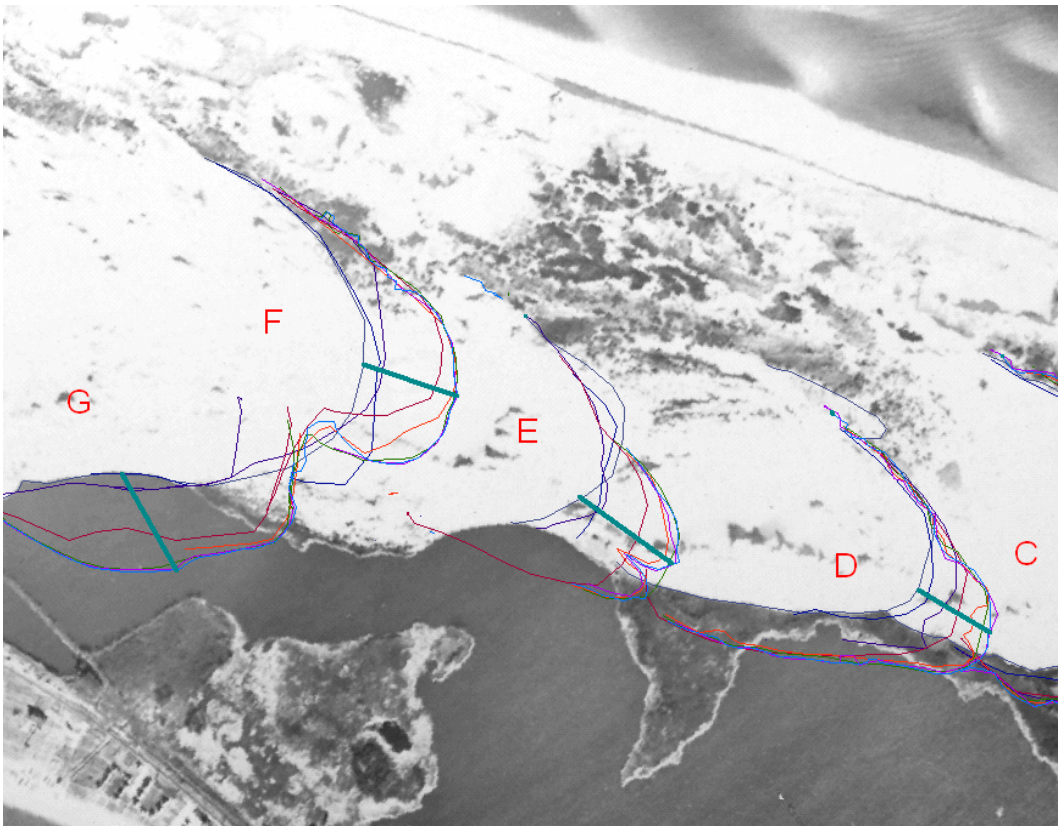

Figure 2.12. Area of dunes D, E and F from 1938 aerial photographs.

The delineation of the watersheds from the dataset was used to define watershed locations in the Cape Cod dune region. Normalized Difference Vegetation Index (NDVI) is a first-order representation of the intensity of vegetation. NDVI provides a method of estimating net primary production over varying biome types (Lenney et al., 1996), identifying eco regions (Ramsey et al., 1995), monitoring phenological patterns of the earth's vegetative surface, and assessing the length of the growing season and dry-down periods (Huete and Liu, 1994).

The application of this technique is more suited to areas where vegetation is considerable. In arid areas the use of the NDVI is complicated by the presence of a large proportion of exposed soil. The working hypothesis is that areas that receive higher amounts of precipitation will have a relatively higher index.

2.4 ArcGIS application for aerial mosaics from 1938 until 2003.

All datasets were loaded into the ArcGIS. Applications of interdisciplinary research in geological, hydrogeological sciences, and related fields often require integration of a number of spatial data sets to enable a better understanding of the relationships between datasets. Thus, the GIS - based data is an adequate platform for researchers to address and analyze the spatial data sets. Metadata was created using a standard GIS ESRI FGDC (Federal Geographic Data Committee) format which contains spatial as well as non-spatial information about a particular dataset. The metadata includes

such information as the purpose of the dataset, dates of acquisition, spatial reference, resolution and other relevant publication information.

Histograms were generated of the regions of interest for total accumulated dune movement from 1938 until 2003.

CHAPTER 3: RESULTS AND DISCUSSION

3.1. Dune movement, 1938-2003

The rate of parabolic dune migration at CCNS varied widely (Fig. 3.1). The greatest net movement was for dune J (222 meters) with drift rates of 3.4 m/year from 1936 until 2003 (Fig. 3.1, Tables 3.1 and 3.2). The next greatest movements were for dune C (192 meters) with drift rate 3.0 m/year; and dune H (186 meters) with drift rate 2.9 m/year. The lowest net movement was for dune D (138 meters) with a drift rate of 2.1 m/year.

Parabolic dunes have migrated 138 to 222 m since 1938, with 60% of the movement occurring between 1938 and 1970. Stabilization of dunes occurred in the 1980s and 1990s (Fig. 3.1, Tables 3.1 and 3.2), with renewed movement in the 21st Century.

Larger dunes may migrate faster because coalescent, wavy forms have ample sand supplies for wind entrainment and less vegetation to impede saltation. In addition less near-surface obstruction reduces turbulence favoring laminar flow and efficient downwind transport of sand and sustained grain flow near the dune crest, enhancing migration (Marin, 2005). Coalescent dune forms are highly curved segments in continuous dune ridges more or less perpendicular to the wind direction. These coalescent, wavy dune forms contrast with the straight or slightly curved segments of dunes.

Figure 3.1. Aerial photograph composite with dune fronts for 1938, 1947, 1960, 1977, 1986, 1994, 2001 and 2003.

Intervals	Net migration of parabolic dunes (m)											
	A	B	C	D	E	F	G	H	I	J	K	L
2001-03	0	nd*	nd*	3	2	1	4	nd*	nd*	2	3	2
1994-01	0	nd*	nd*	14	3	3	8	2	5	3	4	2
1986-94	0	nd*	nd*	20	6	3	26	nd*	nd*	nd*	nd*	nd*
1977-86	0	20	3	27	52	30	25	nd*	nd*	nd*	nd*	nd*
1977-94	0	nd*	nd*	nd*	nd*	nd*	nd*	56	27	53	15	24
1960-77	0	52	45	24	78	90	86	36	27	77	65	32
1947-60	0	60	96	31	5	7	30	67	73	62	69	73
1938-47	0	38	48	19	32	25	nd*	25	34	25	23	12
Total dune movement (m)	0	170	192	138	178	159	179	186	166	222	179	145

Table 3.1. Absolute net migration of parabolic dunes measured from 1938 until 2003 at CCNS in meters.
*nd=not determined.

Period	Migration rates for parabolic dunes (m/year)												
	A	B	C	D	E	F	G	H	I	J	K	L	Ave. rate
2001-03	0	nd*	nd*	3	2	1	4	nd*	nd*	2	3	2	2.4
1994-01	0	nd*	nd*	2	0.4	0.4	1.1	0.3	0.7	0.4	0.6	0.3	0.7
1986-94	0	nd*	nd*	2.5	0.8	0.4	3.3	nd*	nd*	nd*	nd*	nd*	1.7
1977-86	0	2.2	0.3	3.0	5.8	3.3	2.8	nd*	nd*	nd*	nd*	nd*	2.9
1977-94	0	nd*	nd*	nd*	nd*	nd*	nd*	8	3.9	7.6	2.1	3.4	6.3
1960-77	0	3.1	2.6	1.4	4.6	5.3	5.1	2.1	1.6	4.5	3.8	1.9	3.3
1947-60	0	4.6	7.4	2.4	0.4	0.5	2.3	5.2	5.6	4.8	5.3	5.6	4.0
1938-47	0	4.2	5.3	2.1	3.6	2.8		2.8	3.8	2.8	2.6	1.3	3.1
Average dune movement per year from 1938 until 2003 (m)	0	2.6	3.0	2.1	2.7	2.4	2.8	2.9	2.6	3.4	2.8	2.2	2.7

Table 3.2. Migration rates of parabolic dunes measured from 1938 until 2003 at CCNS in meters/year.
*nd=not determined.

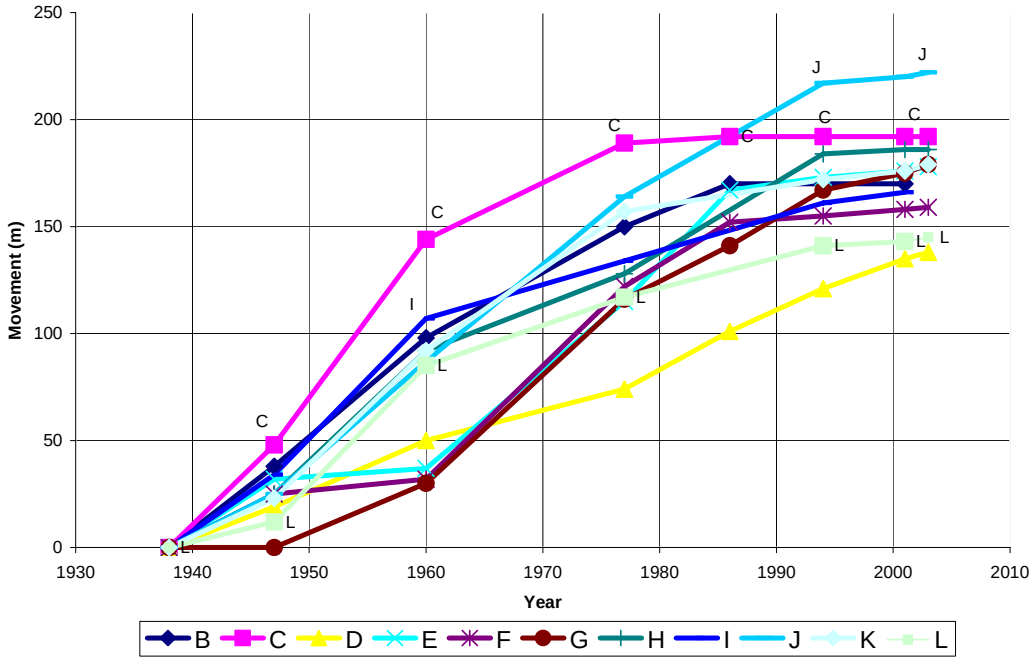

Figure 3.2. Cumulative parabolic dune movement from 1938 until 2003 at CCNS.

Dune/ Year	A	B	C	D	E	F	G	H	I	J	K	L
1938	0	0	0	0	0	0	0	0	0	0	0	0
1947	0	38	48	19	32	25	nd*	25	34	25	23	12
1960	0	98	144	50	37	32	30	92	107	87	92	85
1977	0	150	189	74	115	122	116	128	134	164	157	117
1986	0	170	192	101	167	152	141	nd*	nd*	nd*	nd*	nd*
1994	0	170	192	121	173	155	167	184	161	217	172	141
2001	0	170	192	135	176	158	175	186	166	220	176	143
2003	0	170	192	138	178	159	179	186	166	222	179	145

Table 3.3. Cumulative parabolic dune movement from 1938 until 2003 at CCNS. *nd=not determined.

The total area that the 12 dunes newly covered as a result of migration from 1938 until present is 664,375 m^2 (Fig. 3.3). All these 65 hectares of land were covered by vegetation until 1938 (Fig. 3.3) except dune G, which covered the Pilgrim Lake with an area of about 6 hectares (Fig. 3.3). An aerial photograph mosaic for 1938 shows these 65 hectares as a dark vegetated region (Fig. 3.4). This information can be used for the prediction for future changes of this region. The base information such as movement rate per year (3 meters/year) and covered area (about one hectare/year) can be used for the prediction analyses.

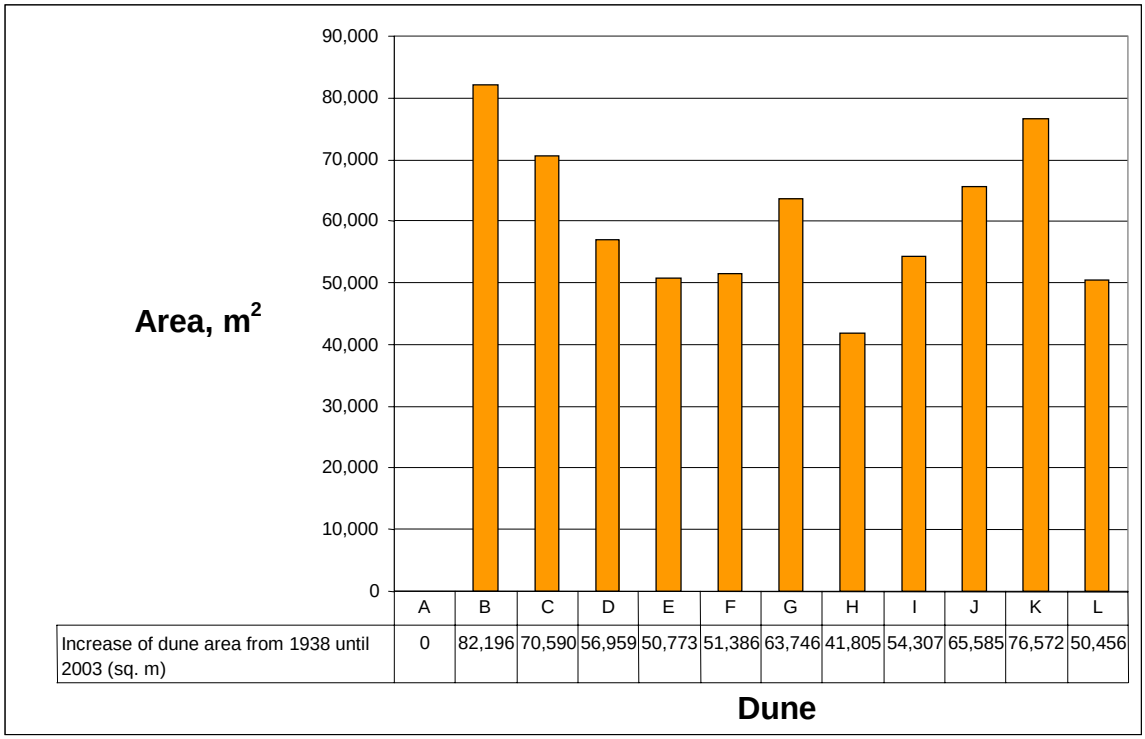

	A	B	C	D	E	F	G	H	I	J	K	L
Increase of dune area from 1938 until 2003 (sq. m)	0	82,196	70,590	56,959	50,773	51,386	63,746	41,805	54,307	65,585	76,572	50,456

Figure 3.3. Area of dune movement from 1938 until 2003 (total 664 375 m^2).

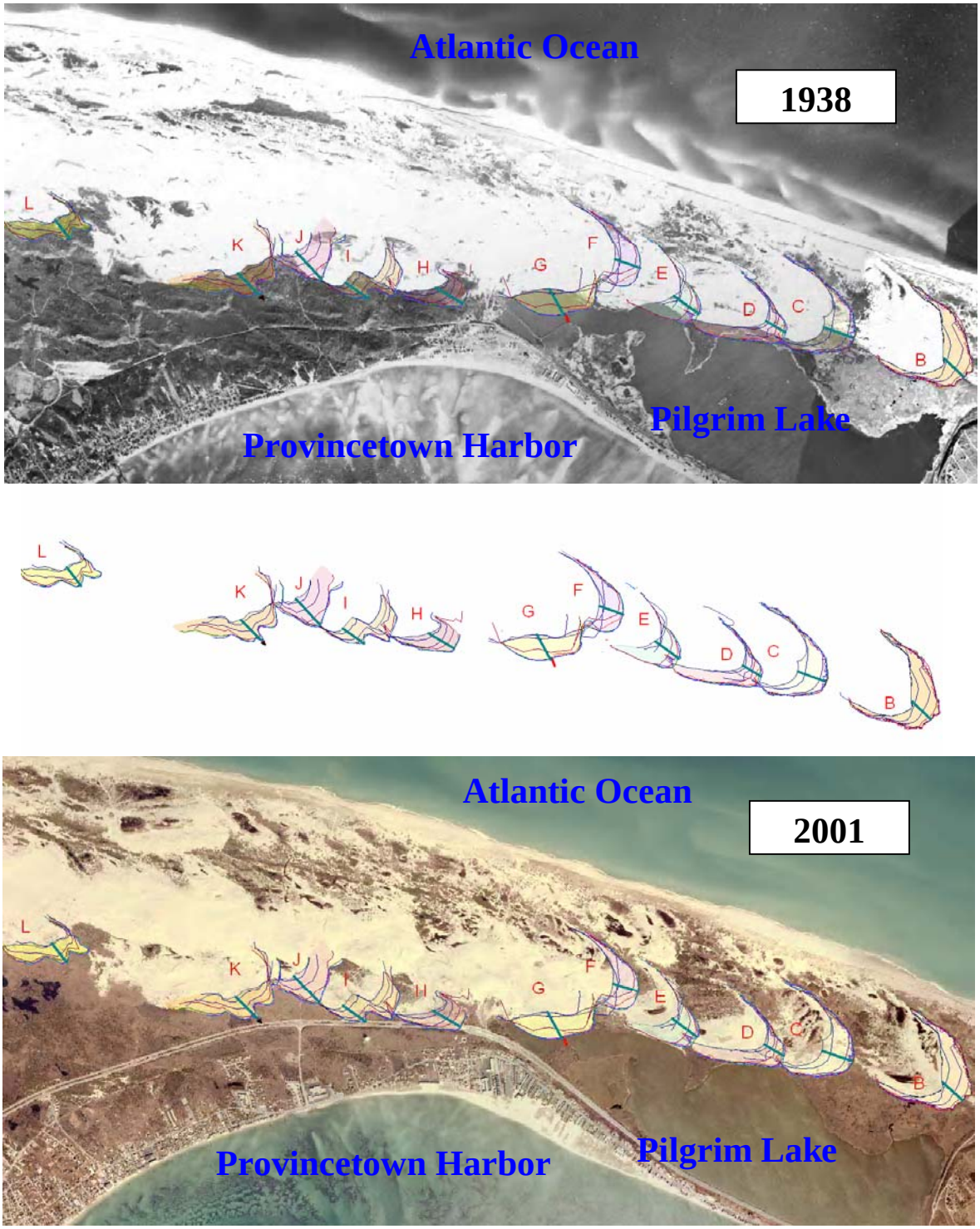

Figure 3.4. 1938 and 2001 aerial photograph composite showing dune fronts.

3.2. Climatic context, Palmer Drought Severity Index

Cape Cod's maritime climate is highly variable from day to night and from day to day. Because it is a peninsula, it is more temperate than surrounding areas (i.e. cooler in summer, warmer in winter). The Cape's weather changes significantly with the seasons. Spring can often be cool and damp with temperatures ranging in the mid-40s Fahrenheit. Summer usually provides warm days, ranging between 70 and 80^{o}F, and cool nights. Winter on Cape Cod is milder than inland, but dampness and wind chill can make winter days bitter cold. Temperatures range between 30 and 40^{o}F in mid-winter, but intervals below zero as well as milder temperatures can also occur (Tables 3.4 and 3.5) (NCDC, 2006).

A variety of studies in the US show possible relationships between episodes of past eolian activity and drought intervals (Woodhouse and Overpeck, 1998; Forman et al., 2001; Wolfe et al., 2001; Forman and Pierson, 2003).

Month	Avg. daily max	Avg. daily min	Avg. daily
January	38.1	21.1	29.6
February	39.2	21.9	30.6
March	44.9	28.6	36.8
April	54.7	36.3	45.5
May	64.7	45.3	55.0
June	74.0	55.3	64.7
July	79.4	61.4	70.4
August	78.5	53.4	62.7
September	71.9	53.4	62.7
October	63.0	43.6	53.3
November	52.3	35.2	43.7
December	42.5	34.0	34.4

Table 3.4. Temperature data for Cape Cod (NCDC, 2006).

Month	Precipitation inches	Snowfall inches
January	3.72	5.40
February	3.74	11.20
March	3.69	3.50
April	3.94	0.20
May	3.77	0.00
June	2.82	0.00
July	2.79	0.00
August	4.15	0.00
September	3.54	0.00
October	3.66	0.00
November	4.37	0.10
December	4.52	3.60

Table 3.5. Monthly precipitation data for Cape Cod (NCDC, 2006).

Aridity in the U.S. is associated with deficits in growing season moisture; this lack of moisture reflects a reduction in rainfall and an increase in evapotransporation (Lancaster, 1997; Muhs and Been, 1997); however, sustained drought is also associated with complex surficial processes that promote the heterogeneous distribution of soil nutrients leading to degradation of grasslands (Shulka and Mintz, 1982; Schlesinger et al., 1990; Huenneke et al., 2002). Other surface disturbances such as activity by grazers and off-road vehicles increase soil heterogeneity and erosion (Smith, 2004), enhancing the availability of sediments for eolian entrainment (Schlesinger et al., 1990). Questions remain regarding the sensitivity of dune systems in landscapes, like those in the CCNS system, to drought variability in the 20th Century.

CCNS contains mostly parabolic dune types. Fronting the dune mass to the south, south-west, and south-east is a sand sheet that harbors mostly vegetated and stabilized parabolic dunes (Fig. 3.1). The Cape Cod climate, with a mean of normal annual precipitation of 50 in/year (NCDC, 2006) or 127 cm/year, is sensitive to droughts, which could transform vegetated areas into active dune complexes.

The parabolic dunes indicate dominant winds from the west-north, north, and north-east. The clear morphology of these dunes, well-defined wind formational processes, and readily identifiable forms in remotely sensed images provide straightforward interpretations to assess changes in dune position.

Drought has occurred periodically in the Cape Cod region during the 20th Century. The Palmer Drought Severity Index (PDSI) (Palmer, 1965; Wells, 2003) provides an approach to the dune mobility index (Lancaster, 1997) for assessing environmental conditions conducive for enhanced dune migration.

The Palmer Drought Index (PDI) and Palmer Hydrological Drought Index (PHDI) were created by Wayne Palmer in the 1960s as a way of integrating water supply (precipitation) with water demand (evapotranspiration as computed from temperature) in a soil moisture model (Palmer, 1965). They are standardized indices where values of zero represent near-normal conditions, negative values indicate drought, and positive values indicate wet conditions (Heim, 2002)

The PDSI includes data for precipitation and temperature, and also includes a supply and demand model for soil moisture. The PDSI reflects deviations in soil moisture from normal conditions for past and present PDSI values. Thus, the PDSI is not solely representative of current conditions, but includes soil moisture status in the recent past (<6 months) (Wells, 2003). In the current study the lowest quartile annual PDSI value was regressed against dune migration because it reflects the maximum moisture deficit per year (Table 3.6 and Figs. 3.5-3.7) that would impact above-ground net primary productivity (Schlesinger et al., 1990) and subsequent eolian activity (Forman et al., 2001). The lower quartile PDSI also mirrors annual variations, but with greater amplitude, providing a consistent and sensitive metric for relating parabolic dune migration to potential climate variations (Table 3.6 and Figs. 3.5-3.7).

Drought and corresponding PDSI values in the Cape Cod region during the 20th Century include 1965 (PDSI 3.611); 1949 (PDSI 2.794); 1957 (PDSI 2.728); and 1941(PDSI 2.56). A lesser drought extent occurred in 1966 (PDSI 2.497); and 1964 (PDSI 2.016) (Table 3.6 and Figs. 3.5-3.7). Wetter conditions occurred in 1984 (PDSI 3.365); 1973 (PDSI 3.254); 1998(PDSI 3.328), and 2003 (PDSI 2.263).

Year	PDSI	Year	PDSI	Year	PDSI
1929	-0.016	1954	2.523	1979	0.681
1930	-1.471	1955	0.250	1980	-0.902
1931	0.321	1956	-0.093	1981	-0.132
1932	-1.459	1957	-2.728	1982	1.569
1933	-0.386	1958	1.366	1983	1.108
1934	-0.917	1959	0.075	1984	3.675
1935	-0.073	1960	0.822	1985	-1.296
1936	0.161	1961	0.511	1986	0.868
1937	0.564	1962	-0.841	1987	-0.994
1938	2.060	1963	-1.049	1988	-1.238
1939	-0.225	1964	-2.016	1989	1.038
1940	0.793	1965	-3.611	1990	1.462
1941	-2.560	1966	-2.497	1991	-1.026
1942	-0.884	1967	0.756	1992	0.642
1943	1.150	1968	-0.463	1993	-1.615
1944	-2.058	1969	0.189	1994	-0.387
1945	1.584	1970	0.192	1995	-1.388
1946	-0.254	1971	-0.477	1996	0.864
1947	1.587	1972	2.280	1997	-0.644
1948	0.209	1973	3.254	1998	3.328
1949	-2.794	1974	1.897	1999	-1.737
1950	-1.600	1975	-0.379	2000	1.395
1951	0.929	1976	1.606	2001	0.692
1952	0.661	1977	0.448	2002	-1.264
1953	0.064	1978	-0.333	2003	2.263

Table 3.6. PDSI for the Cape Cod region, 1929-2003 (NCDC, 2006).

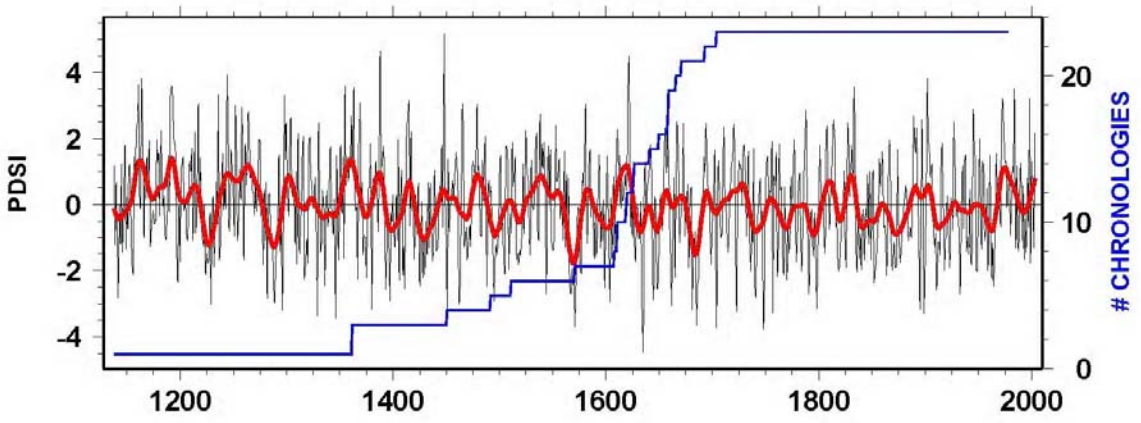

Figure 3.5. Climatic data for Cape Cod. Tree-ring reconstructed droughts (NCDC, 2006).

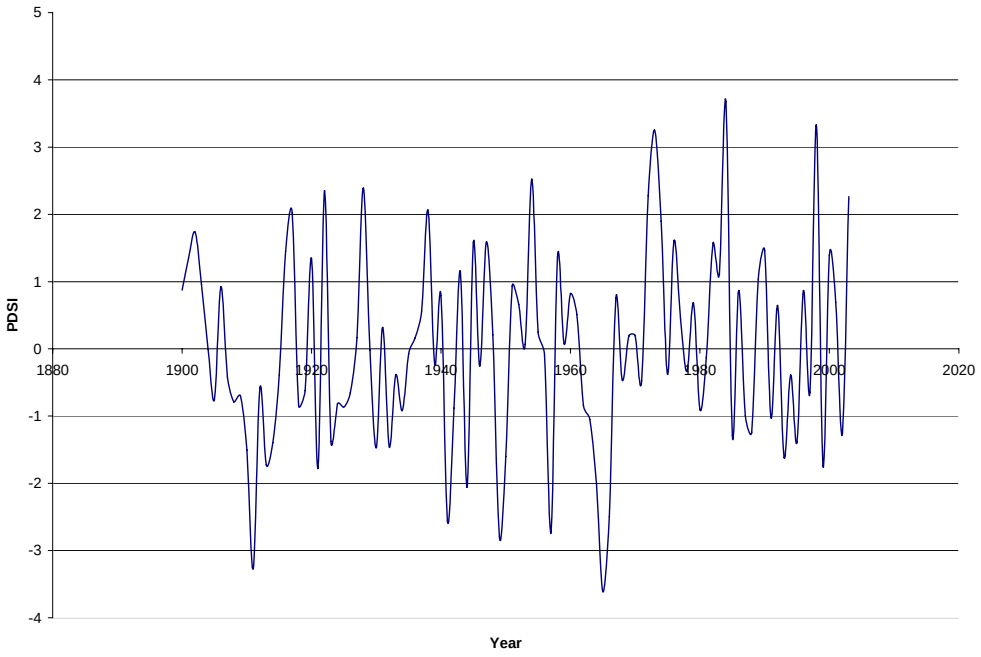

Figure 3.6. Climatic data for Cape Cod using the PDSI. Adapted based on data from NCDC (2006).

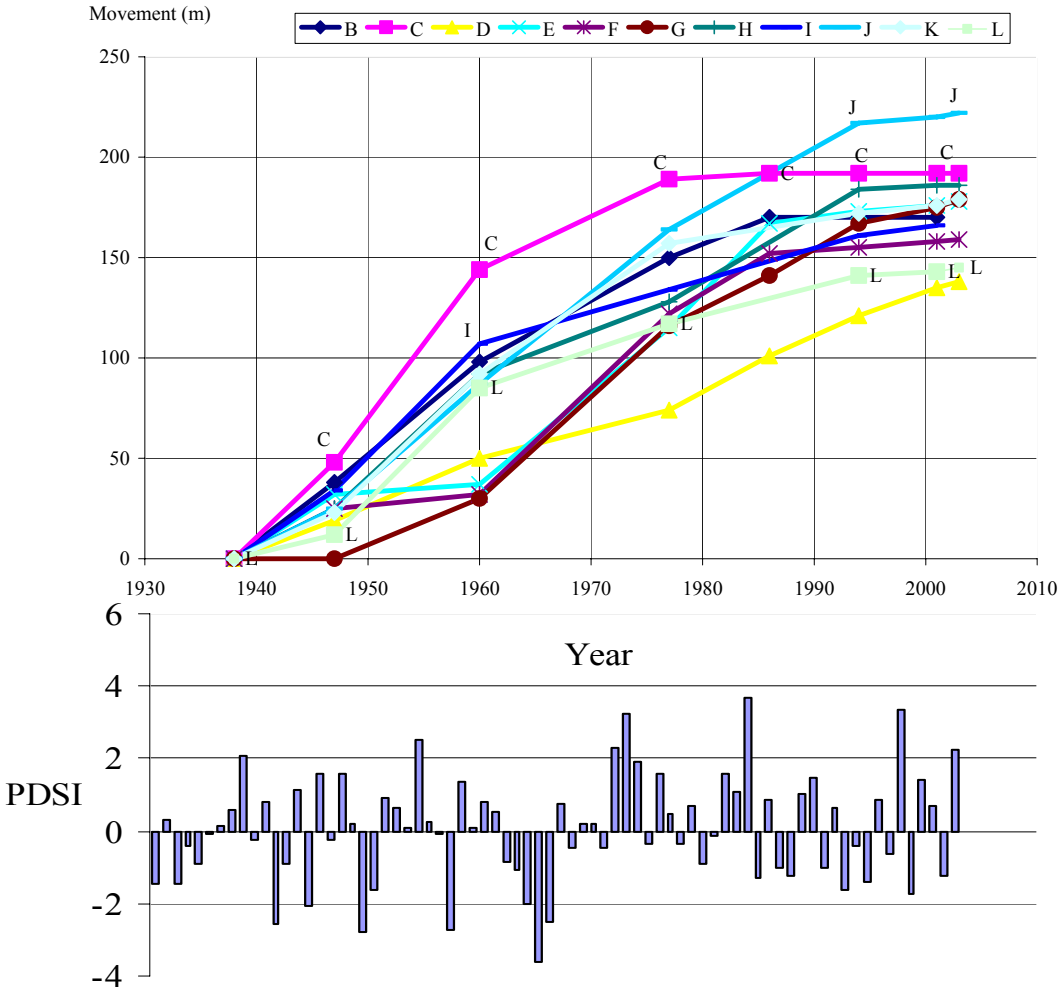

Figure 3.7. Dune movement with PDSI in the Cape Cod region.

Dune drift rates for the Cape Cod region increased during droughts and decreased with ensuing wetter intervals indicating the predominance of vegetation cover changes in controlling dune migration. A hallmark of 20th Century droughts at Cape Cod is the multiseason deficit in precipitation, which leads to a decrease in grassland primary productivity (Sala et al., 1988). Large areas, combined with grazing pressure, wind, and associated surface water erosion, are effectively denuded (Schlesinger et al., 1990).

The relation between absolute parabolic dune migration and corresponding average lower quartile PDSI is approximately logarithmic. Maximum dune migration is associated with PDSI values lower than –2 (Fig. 3.7) and reflects moderate drought conditions (Palmer, 1965; Lawrimore et al., 2003). Maximum average dune migrations occurred from 1939 until 1970 (Fig. 3.7) and may be associated with PDSI values which are mostly negative during this period. The majority of the strongly negative drought PDSI values were detected during this time, such as in 1965 (-3.611); 1949 (-2.794); 1957 (-2.728); and 1941(-2.56) (Table 3.6).

The dunes stabilized, i.e., there was less movement during wetter periods, for example after 1970 until 2003. Cape Cod received the greatest annual precipitation in 1984 (PDSI 3.365); 1973 (3.254); 1998 (3.328); and 2003 (2.263) (Fig. 3.7 and Table 3.6).

The current study shows that during the past 70 years rates of parabolic dune migration vary with regional moisture status (e.g., drought versus moisture) at CCNS. Dune drift rate increased during pronounced droughts in the 1940s, 1950s, and late 1960s compared to the intervening wet years (Fig. 3.7). Accelerated dune migration is associated

with lower quartile PDSI values (< -2) and with decreasing precipitation, resulting in reduced grass coverage and the expansion of shrubs. The late 20th Century increase in dune drift at Cape Cod was similar to that of other regions of the US, for example in southwestern Colorado and much of the western US (Piechota et al., 2004).

Aerial photographs by Wiegand (1977) and Martin (2005) show dune migration in the Great Sand Dunes National Park (GSDNPP) in Colorado, where dunes advanced up to 9 m/year toward the northeast and east from 1966 to 1975. Parabolic dunes advanced between 2 and 16 m/year from 1936 to 1975. Dune migration rates 3–10 m/year between 1966 and 1975.

Hammond (1998) determined the extent, number, size, and the spatial distribution of wetlands for an area adjacent to Sand Creek (CO) using 12 sets of aerial photographs from 1936 to 1995. This analysis indicates that the number and area of the wetlands is greatest in the 1930s, decreasing in number from 114 in 1937 to 22 in 1979. In 1995, the number of wetlands increased to 51 in response to sub irrigation of meadows and to groundwater discharge (Hammond, 1998).

In the current study remote sensing is demonstrated as an efficient and accurate tool for detecting dune migration. It would be a very time-consuming and complicated process to carry out similar measurements on land.

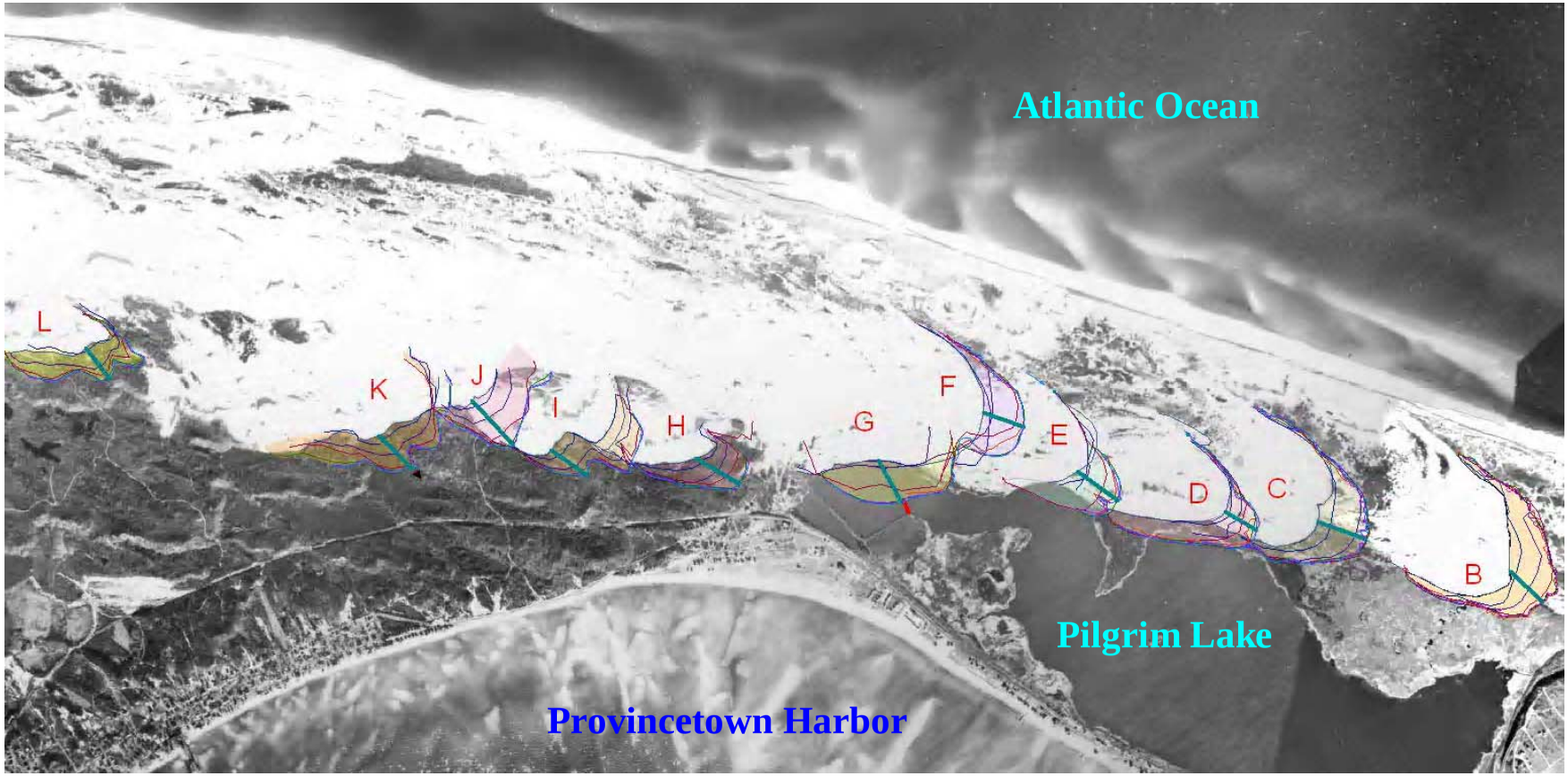

Figure 3.8. 1938 aerial photograph composite showing dune movement and areas covered until 2003.

3.3. Dune movement and effects on humans

Land use in the 17th through mid-19th centuries dramatically altered the uplands of the Cape Cod region; forests were cut for wood products and fuel, broad areas were cleared and plowed for crops, and pastures and woodlands were grazed (Altpeter, 1937; Ruberstone,1985; Friedman, 1992; Dunwiddie and Adams, 1995). Regional economic decline, widespread emigration, and farm abandonment characterized the mid- to late 19th century, and further agricultural decline combined with increased tourism and development occurred throughout the 20th century (Holmes et al., 1998; Stone, 1999).

A major concern to the NPS is the constant change in vegetation cover and land use in and around park units. Similarly, the CCNS does not exist in a vacuum; it is affected by what occurs in the communities in which it exists.

Historical maps and documents, aerial photographs, and field sampling of vegetation and soils to determine patterns of land-cover and land-use change, species composition and abundance, site conditions, and fire history of the Cape Cod area were studied by Eberhardt (2002). In 1848–1856 eastern Cape Cod was extensively settled and deforested, with approximately 20% of Truro (the current dune study region) remaining wooded. Only 44% of current woodlands in CCNS were wooded between 1848 and 1856. Buildings and fences occurred throughout open areas, and roads crossed open and wooded areas. Field evidence and historical sources confirm the accuracy of these mid-19th century land-cover depictions. All but one of 38 plots (Eberhardt et al., 2002) with an Ap horizon are mapped as open on 1848–1856 maps, and woodland on the 1848–1856 maps coincides with historical descriptions of pine–oak woodland (Dwight, 1969;

Thoreau, 1989). Forty-four percent of plots were plowed historically and open in the mid-19th century, 42% were wooded in 1848–1856, and 14% were open and subject to other uses. Minimum stand ages in plowed (Fig. 3.9) or open plots range from 26 to 113 yr. Aerial photos indicate that 80% of plots supported woodlands or shrublands in the 1938 figure, with the remainder in heathland or grassland (14%) and agriculture (6%). All woodlot plots were woodland or shrubland in 1938 with stands ranging from 51 to 180 yr old with a mean of 85 ± 28 yr (Eberhardt et al., 2002).

The changes in Cape Cod land use and corresponding changes in vegetation cover, focusing on the period from1951 to 1990 (Table. 3.7) were studied by Stone (1998). Stone (1998) measured the area of land use units from aerial photographs from 1951 to 1990 and calculated the change in land use categories with Arcview. This study was a good example as to how to apply landscape analysis by using remote sensing technologies and GIS.

Land Cover	1951		1990	
	Percent	Sq. Miles	Percent	Sq. Miles
Forested, Woody, and Open Land	70.6	293.1	50.3	207.9
Commercial and Residential	10.5	43.4	31	127.9
Gravel mining and Transportation	0.9	3.8	2.2	9.3
Agriculture, Pasture, and Cranberry Bogs	4.8	20.1	1.5	6.3
New Ocean	0.2	1	0.4	1.8
Waste Disposal	0.1	0.3	0.4	1.7
Total	100%	416	100%	413

Table 3.7. Cape Cod land cover changes from 1951 until 1990 (Stone, 1998).

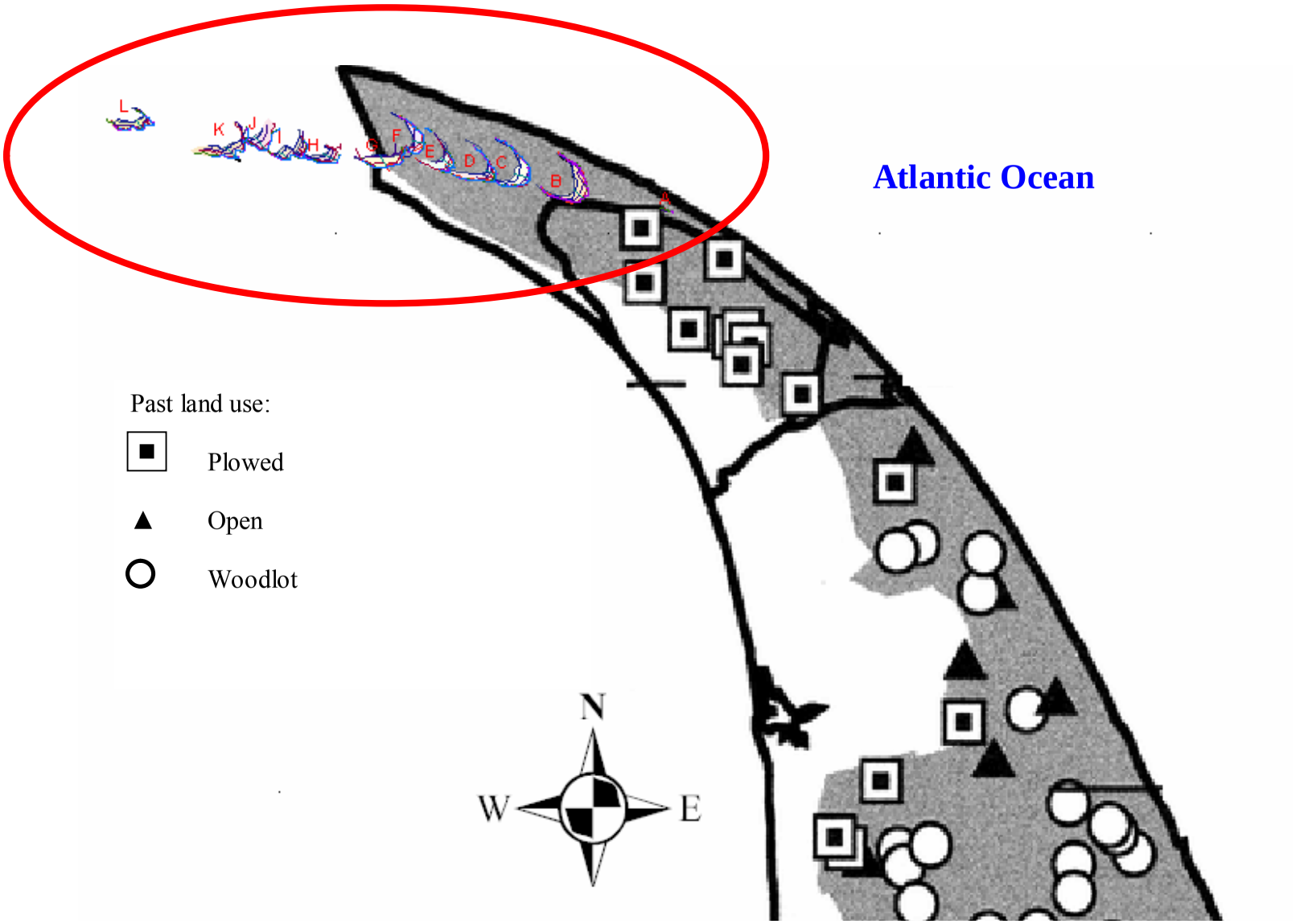

Figure 3.9.Distribution of categories of past land use of woodlands, adopted from Eberhardt (2002). Dune study region in oval.

Comparison of 1990 figures with those for 1951 provides evidence that dramatic changes in vegetation types have occurred during these 40 years. The percentage of commercial and residential land cover has tripled, the amount of forest cover has declined by almost 100 sq. miles (about 25% of the Cape) and the amount of agricultural land has declined by 75% from 20 sq. miles to only 6 sq. miles. It seems clear that population pressure, and residential and commercial construction are the dominant forces driving the current alterations in the land cover and land use of Cape Cod (Stone, 1998).

Human disruption of the local environment may stimulate dune movement. Dune migration may concurrently affect human activities.

Dunes H, I, J, and K are close to the Cape Cod highway; dunes H and I are already covering the highway (Fig. 3.10). Dune H is closest to the highway (Fig. 3.11). Such encroachment will cause public safety hazards. Dune G is moving toward Pilgrim Lake (Figs. 3.12 and 3.13); in some cases Dune G has already encroached upon Pilgrim Lake (Fig. 3.14).

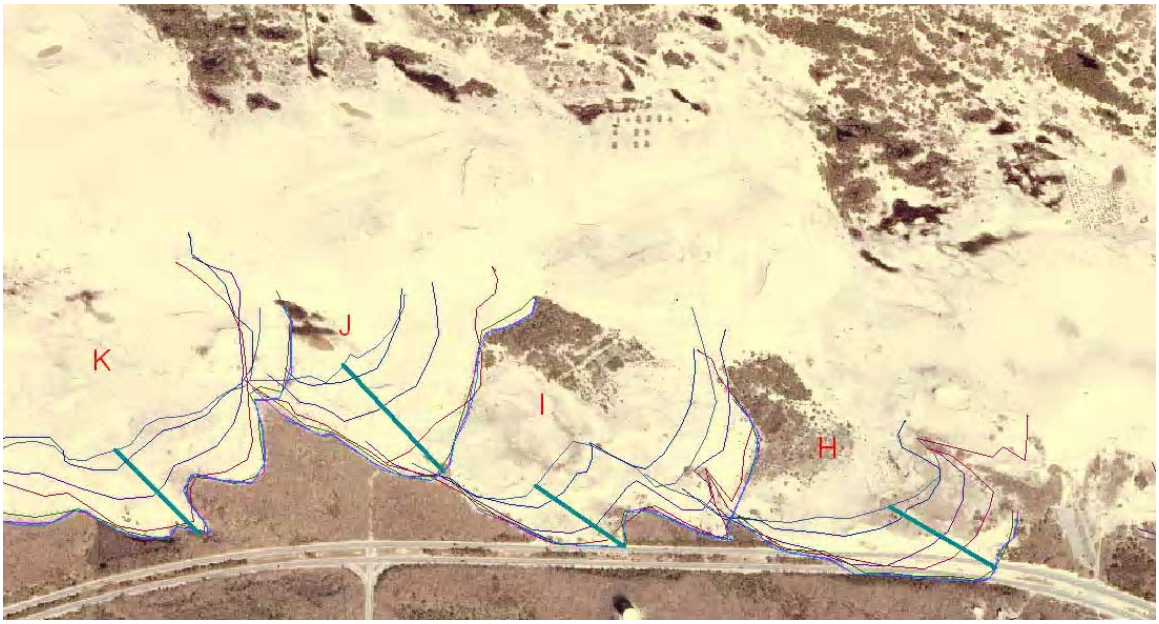

Figure 3.10. Dunes H, I, J, and K showing movement from 1938 until 2003.

Figure 3.11. Dune H, 2005.

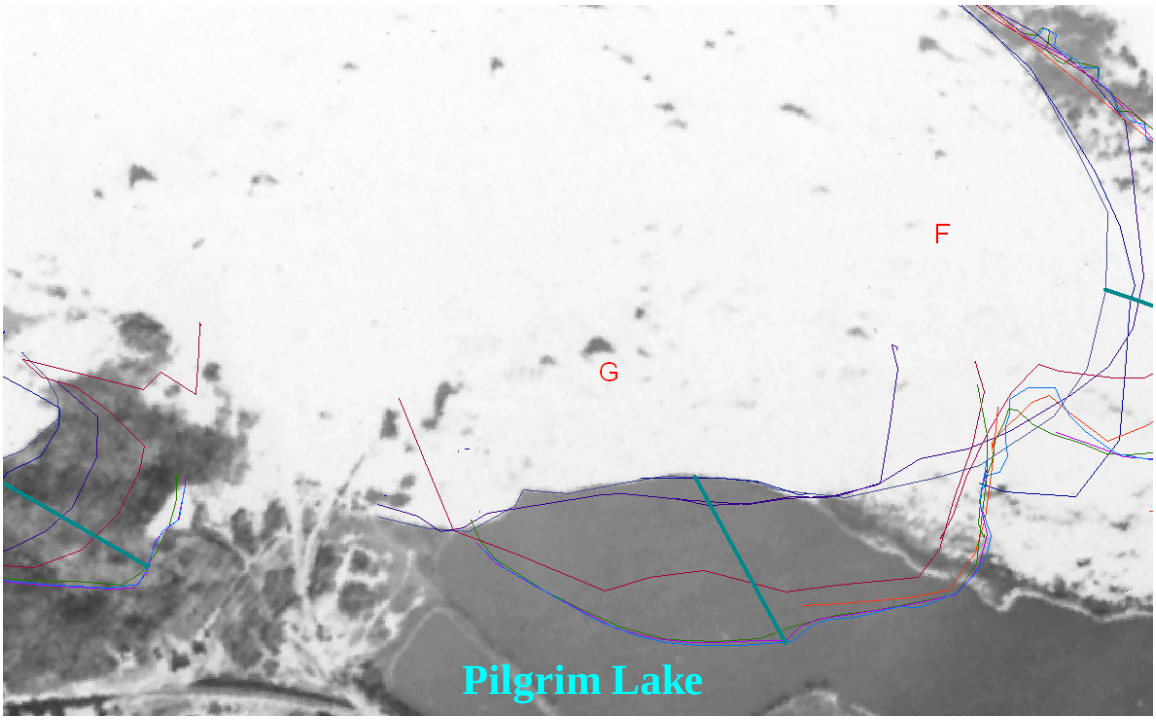

Figure 3.12. 1938 Cape Cod aerial photograph showing location of dune G.

Figure 3.13. 2001 Cape Cod aerial photograph showing dune G movement.

Figure 3.14. Dune G region, 2005.

Dune G net migration was 179 meters from 1938 until 2003 (Table 3.1) with a migration rate of 2.8 meters per year (Table 3.2). Approximately 6 ha of Pilgrim Lake are covered by dune G (Fig. 3.8 and Table 3.7). At this same migration rate dune G may reach the opposite side of Pilgrim Lake by 2015 (Fig. 3.15) and may cover about 10 ha of lake surface.

Dune K may reach the Cape Cod highway by 2015 if this dune continues the same migration rate of 2.8 meters per year (Table 3.16). A small forest is currently blocking dune K movement toward the Cape Cod highway.

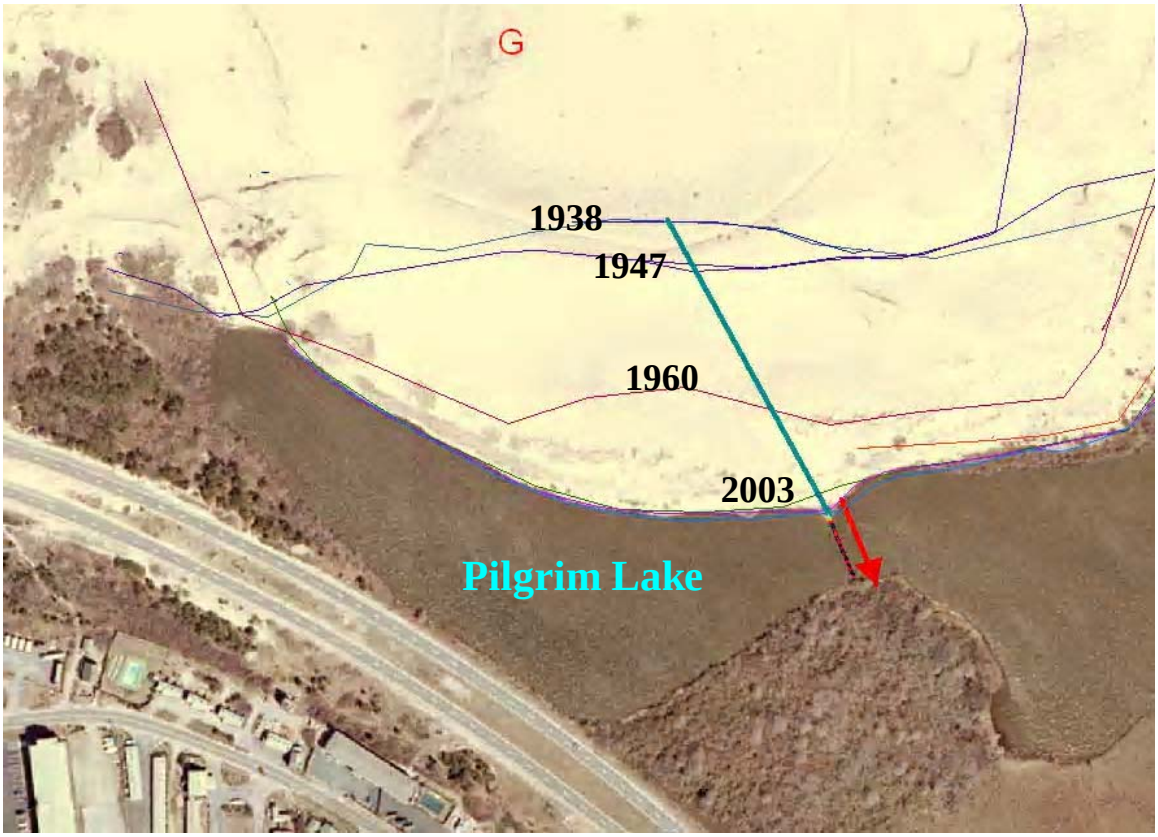

Figure 3.15. Dune G may reach the opposite side of Pilgrim Lake by 2015.

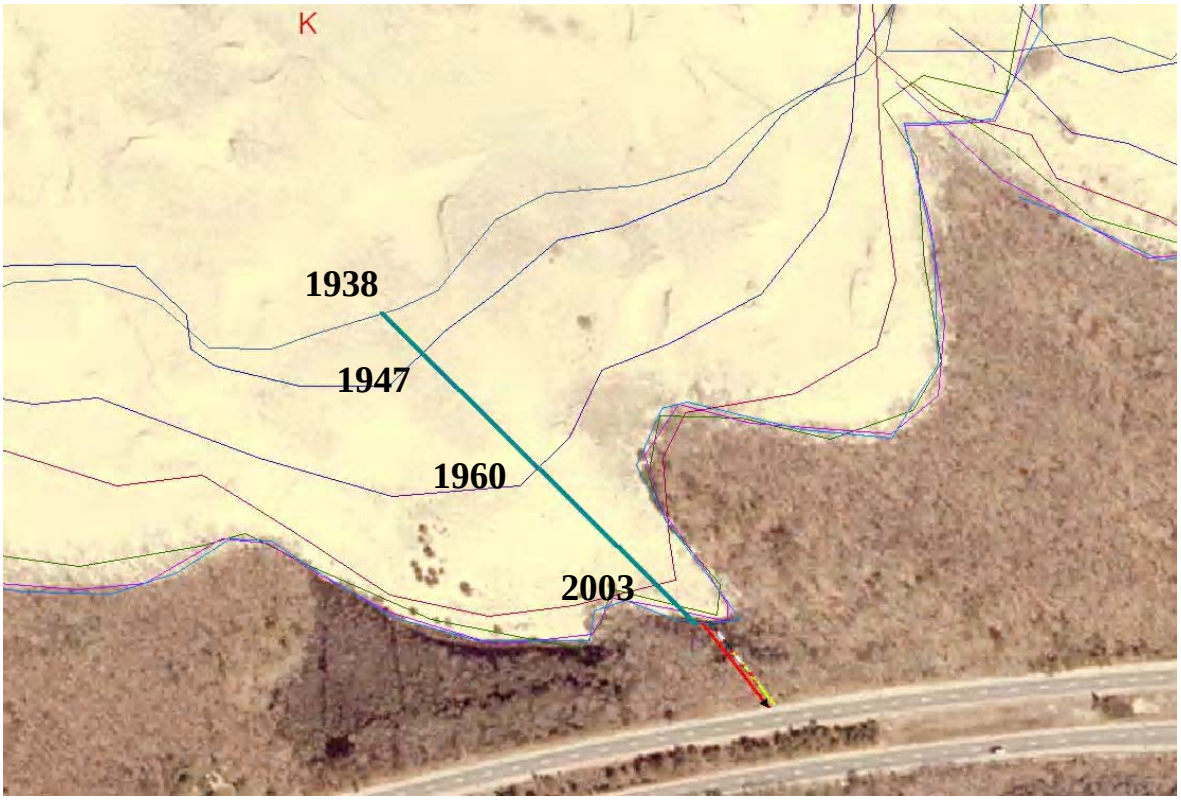

Figure 3.16. Dune K movement from 1938.

A large area of parabolic, migrating dunes with sparse vegetation within Cape Cod is termed Province Lands. The National Park Service is working to restore the natural vegetation of this dune system that was disturbed by historical deforestation and past, unregulated off-road vehicle use (Smith, 2004). The Park Service is attempting to influence dune migration by establishing vegetation in some regions (Figs. 3.17 and 3.18). One of the main management goals is to keep the park zone untouched by human activities, i.e. to keep this region in a pristine state. The dune system of Cape Cod is highly appealing to both locals and tourists; with dune movement human settlements and other structures may be covered by sand from dunes. Monitoring of dune movement should help the CCNS Park Service better understand both the history and current dune situation in order to formulate the proper strategies for the management of dunes.

Figure 3.17. Vegetation established (oval) by NPS.

Figure 3.18. Newly-established vegetation (inside oval) near dune G region, 2005.

3.4. Wetland migration

One of the sub-problems in this research activity was to quantify "white" areas of active moving sand from 1938 until the present time. In order to analyze the "dark" areas of vegetation, including vegetation movement and correlation of dune and wetlands movement, it was necessary to delineate the watersheds and define the stream networks, i.e., the drainage area.

A DEM was used for the watershed and stream network delineation (Fig. 3.19). DEM is generated using 2000 LIDAR aerial photographs; however, such technologies did not exist until the 1980s. This is why the DEM was created starting from 1947 using stereo pairs of aerial photographs. Brief instructions to conduct these procedures were prepared and are presented in Appendices A and B. These instructions could be useful for specialists who are conducting similar projects.

Wetland areas changes from 1947 until 2001 are presented in Figs. 3.20-3.22. Wetlands followed dune movement direction, with a distance moved reaching about 200 meters in some areas. The wetland area changes are correlated to dune changes; i.e., dunes and wetlands are moving in the same direction. With increase of the dune movement distance, the corresponding distance of wetland movement also increased.

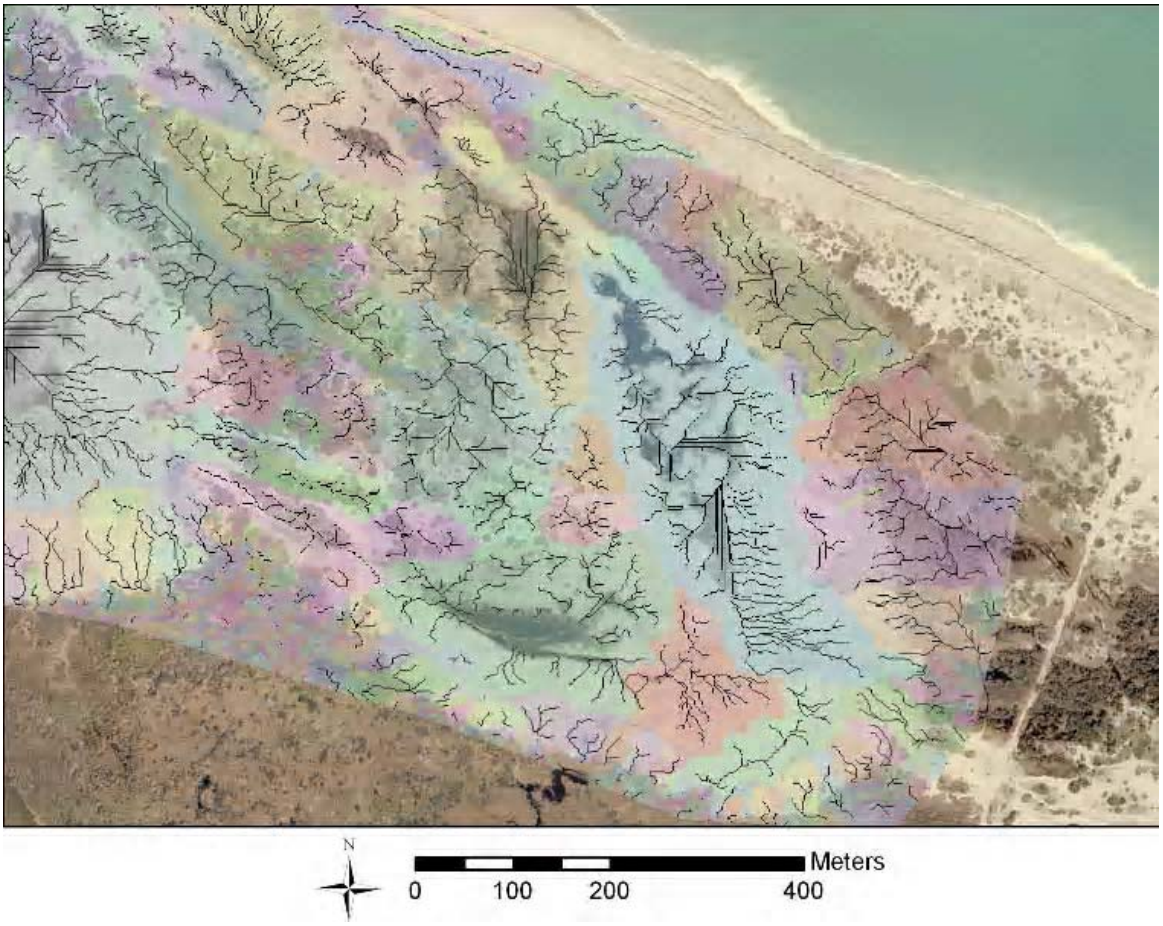

Figure 3.19. 2000 image showing wetland region on CCNS, dune B.

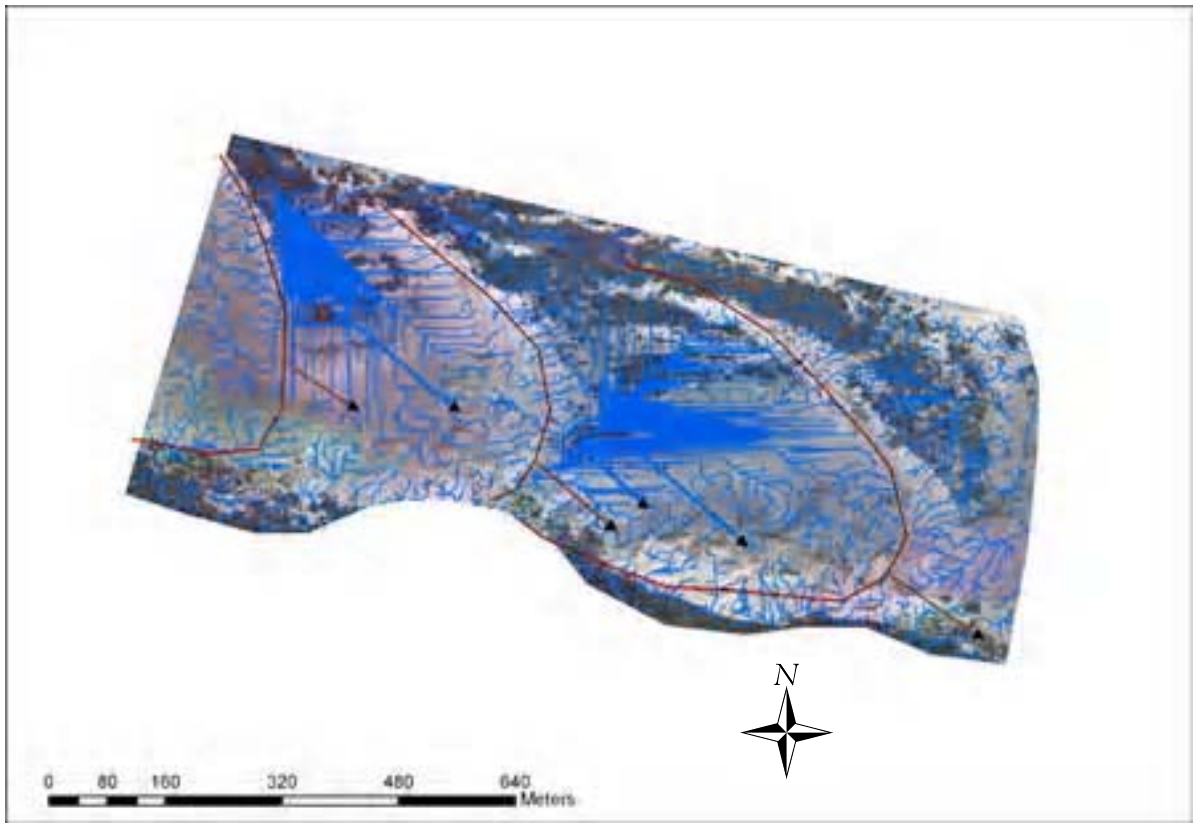

Figure 3.20. 1947 orthoimage showing stream network, catchment areas and dune fronts with direction of movement: blue arrows for wetlands and red arrows for dunes.

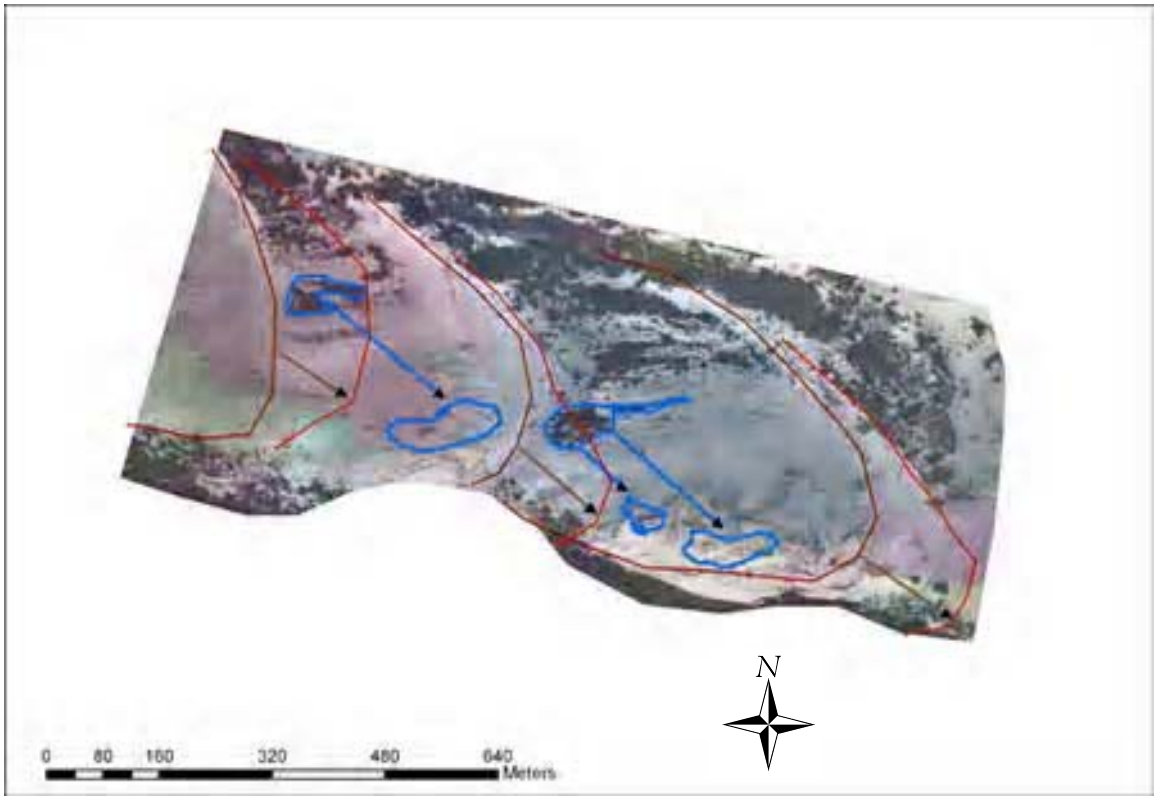

Figure 3.21. 1947 orthoimage showing wetland movement in blue arrows: beginning of arrows are wetland areas in 1947 and arrow endings show wetland position in 2001; red arrows show dune movement from 1947 until 2001.

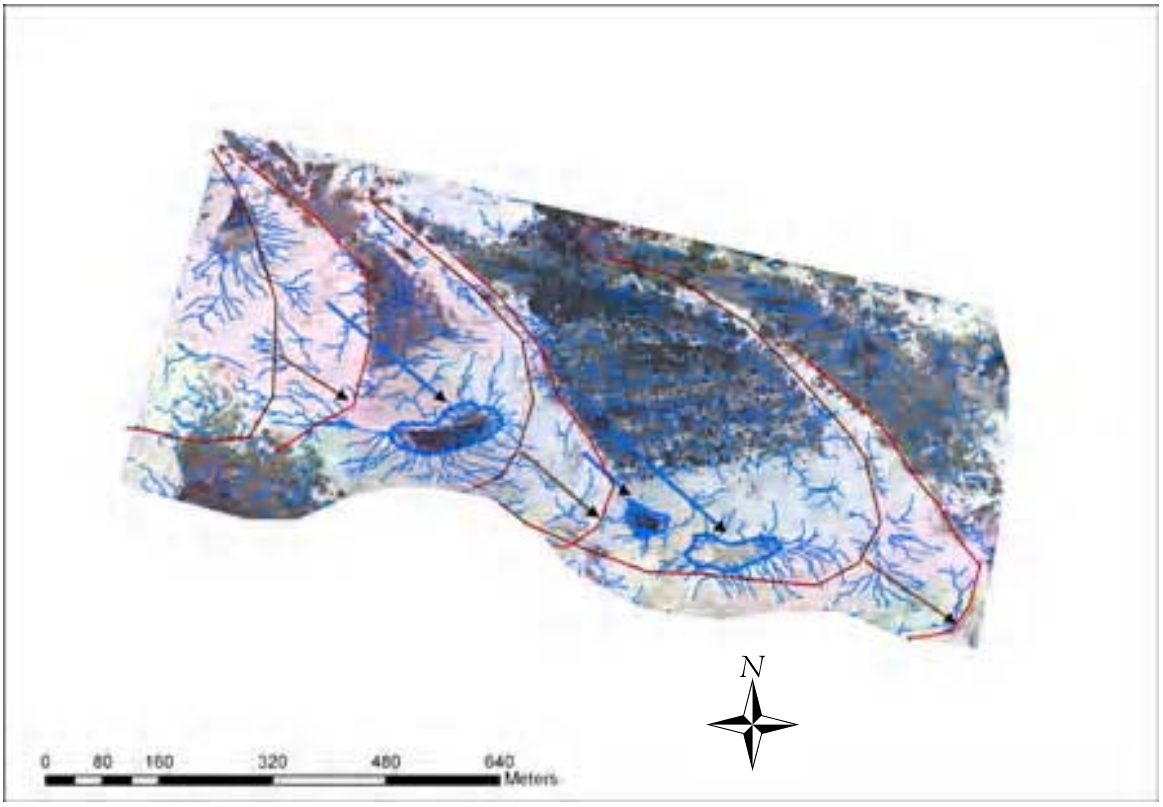

Figure 3.22. 2001 orthoimage showing stream networks, catchment areas and dune fronts: blue arrow endings show new wetland locations in 2001.

Dune movement rates are approximately 3 m/y and wetland migration rate is also approximately 3 m/y in some areas. However, it is necessary to collect more samples to compare dune and wetland migration from other parts of Cape Cod to allow for more comprehensive conclusions. Some wetlands may simply have subsided and new wetlands developed; i.e., dune movement may not always cause wetland movement. The hydrologic system of Cape Cod should be thoroughly studied for enhancing such a research endeavor.

The Great Sand Dunes and associated wetlands migration were studied at Colorado State University (NPS, 2004). Researchers used aerial photos from different time periods to examine changes in wetland area. The need for aerial photography limited the study to the years after photos became available. At least one set of photographs was collected for each decade from the 1930s to the 1990s. The photos were scanned into a digital format so the researchers could remove lens distortions and then geo reference all photos. This task was difficult due to the lack of stable landforms in the dune area; however, the researchers were eventually able to print and analyze the digital images using various computer-aided and visual techniques. Once the source of the water was identified, 120 shallow groundwater monitoring wells were installed near Sand Creek and the Elk Springs wetland complex to observe groundwater input and flow. Finally, the Palmer Drought Severity Index, a formula that combines data about temperature and dryness, was correlated with changes in the size and number of the wetlands as documented in the photo record (NPS, 2004).

Aerial photo analysis showed that both the number of interdunal ponds and the total acreage of wetlands decreased between 1935 and 1995. Examination of the digitized images revealed that the greatest loss of wetland area occurred between 1935 and 1953,

when the number of ponds decreased from 114 to 38, and the total wetland area from about 70 acres to about 21 acres. The 1980s and 1990s saw a reverse in the trend; several new ponds developed in the southern portion of the study area, accounting for a thirty percent increase in total wetland acreage between 1975 and 1995. These changes, first a decline and then a modest increase, correlated well with changes in the PDSI during corresponding time periods (NPS, 2004).

Janke (2002) evaluated changes in the dune mass extent and in land cover for the GSDNPP. This study concluded that semidesert scrub was the only class that increased by 5% (1457.3 ha) during this interval, at the expense of dune grass. The most dramatic changes occurred on the western side of the main mass, where dune grass was replaced by scrub and on the eastern side where dune grass and scrub expanded on the dunes. Janke (2002) concluded that the main dune mass is stable, although studies by Schlesinger et al. (1990) indicate that eolian transport may be enhanced on semiarid landscapes with the dominance of shrubs.

3.5. Uncertainties and errors

The quality of 1938 aerial photographs was not good; however, it was possible to identify general dune edges. It was difficult to create a DEM using stereo pairs of interconnected images and problematic to find reasonable GCPs in interdunal areas; thus, many uncertainties arose for the identification of wetland regions in 1938.

The quality of the 1947 aerial photographs was much better compared to those of 1938. This is why 1947 photographs were used to create the DEM, catchments, and stream network and wetland areas. The qualities of the 2000 aerial photographs are very good and suitable for creating DEM images. Qualities of the photographs between 1947 and 2005 were reasonable to create DEM; however, it was problematic to obtain aerial photograph details of the cameras, located on platforms of aircraft for the 1977, 1986, and 1987 photographs. Different types of cameras were used from 1977 to 1987, and which type of camera used to take the photographs of the Cape Cod region is unknown. Detailed information about camera type can improve the quality of geographic references and assist in preparing DEMs for digital aerial photographs. Only one type of camera was used on the airplanes in 1947; these details helped to create a reasonable DEM with fewer uncertainties.

CHAPTER 4: SUMMARY AND CONCLUSIONS

The objective of the reported research activity was to assess, using remote sensing and GIS technologies, the general movement of selected dunes at CCNS, and to determine the effect of dune movement on the distribution of associated wetlands. Absolute dune movement rates were computed for several intervals from 1938 through 2003, with a plot of dune movement as a cumulative function. Aerial photographs in 1938, 1947, 1960, 1977, 1986, 1994, 2001 and 2003 were analyzed to track individual dune movements and subsequent wetland propagation and expansion. The extent of dune migration was evaluated with respect to climate parameters including PDSI to better understand landscape response to varying drought conditions during the 20th Century.

The dynamic and coupled CCNS wetland and dune system may primarily reflect landscape non-equilibrium response to human disturbance. Based on review of aerial photographs, parabolic dunes have migrated 150 to 250 m since 1938, with 60% of the movement occurring between 1938 and 1977. Based on review of georeferenced aerial photographs, it is concluded that noticeable stabilization of dunes occurred in the 1980s and 1990s, with renewed movement in the 21st Century. Wetlands expanded following dune movement, particularly from the 1950s to the 1980s.

Dune drift rates for the CCNS increased during droughts and decreased with ensuing wetter intervals indicating the predominance of vegetation cover changes in controlling dune migration. The relation between absolute parabolic dune migration and corresponding average lower quartile PDSI is approximately logarithmic. Maximum dune

migration is associated with PDSI values lower than –2 and reflects moderate drought conditions and reduction in grass coverage. Maximum average dune migrations occurred during the period from 1939 until 1970 and may be associated with PDSI values which are mostly negative during this period; the majority of the strongly negative drought PDSI values were detected during this time. The dunes stabilized, i.e., there was less movement during wetter periods from 1970 until 2003. Cape Cod received the greatest annual precipitation in 1984 (PDSI 3.365); 1973 (3.254); 1998 (3.328); and 2003 (2.263).

The current study shows that during the past 70 years rates of parabolic dune migration varied with regional moisture status (e.g. drought versus moisture) at Cape Cod. Dune drift rate increased during pronounced droughts in the 1940s, 1950s, and late 1960s compared to the intervening wet years. The late 20th Century increase in dune drift at Cape Cod is similar to that of other regions of the US, for example in southwestern Colorado and much of the western U.S.

The total area at Cape Cod that the 12 dunes newly covered as a result of migration from 1938 until present was 664,375 m^2. All these 65 hectares of land were covered by vegetation until 1938 except dune G, which covered the Pilgrim Lake with an area of about 6 ha. An aerial photograph mosaic for 1938 shows these 65 hectares as a dark vegetated region. This information can be used for the prediction for future changes of this region. The base information such as movement rate per year (3 m/y) and covered area (about one ha/y) can be used for prediction analyses.

This study provides a practical application for assessment of dune migration and vegetative transformations over time using remote sensing and GIS technologies. The data

also provides insight into how landscapes respond to drought and quantifies thresholds and rates for dune migrations at CCNS.

The reported study has employed a variety of tools to study regional patterns of dune movement and wetland areas in CCNS. The combination of new technologies and techniques, such as aerial photography, GIS, remote sensing, and visualization provide great practical value to environmental researchers. These types of analyses can be helpful for the monitoring of, and predicting dune movement to improve land use practices in CCNS and to prepare a sound dune management strategy.

CHAPTER 5: SUGGESTIONS FOR FUTURE RESEARCH

Further studies are appropriate for use of GIS and remote sensing for the CCNS ecosystem; for example, it is suggested to retrieve the earliest sequence of aerial photographs for CCNS from 1920 until 1930, geo reference these photographs and review dune changes from these earliest times. The next task is to investigate the impact of dune migration on the hydrologic system. For this purpose it is necessary to create DEM for several dune areas in different years from 1920 until the present. This work, using aerial photographs, is proposed by the Earth Science and Remote Sensing Lab at the Geosciences Department of Western Michigan University. Such studies were conducted for the Great Sand Dunes and associated wetlands migration at Colorado State University (NPS, 2004).

Vegetation study connected to the dune migrations from the 1920 until the present could be another practical study. Such a study is necessary to obtain a better assessment of plant types as a function of soil moisture status, climate, time, and other relevant variables.

Correlation of dune and wetland characteristics with stratigraphy at CCNS can be a valuable tool for interpretation of its changing landscape. Sequence stratigraphy, i.e., evaluating the strata of past thousands of years using optically stimulating luminescence (OSL) dating is one avenue to pursue. Stratigraphy is a branch of geology specifically concerned with the arrangement of layered rocks (dunes in the present case). Stratigraphy is based on the law of superposition, which states that in a normal sequence of dune layers the youngest is on top and the oldest on the bottom. Local sequences are studied, and

after considering such factors as the average rate of deposition of the different dunes, their composition, the width and extent of the strata, the fossils contained, and the periods of uplift and erosion, the geological history of the sequence is reconstructed. These sequences are then correlated to those of similar age in other regions with the ultimate aim of establishing a consistent geochronology for the entire earth. The OSL for the dune study is well developed by S. Forman, the Department of Earth and Environment Sciences, University of Illinois at Chicago.

OSL has emerged in the past decade as valuable Quaternary (geological time which covers the last two million years up to the present day) dating method for a variety of eolian, fluvial, marine and colluvial sediments. The OSL clock, like in thermo luminescence (TL) dating is reset by exposure to sediment to sunlight prior to deposition. A key advantage of OSL dating is that the luminescence of quartz and feldspar grains is reduced to a low definable level after a few minutes of sunlight exposure versus hours for the corresponding TM response. This level, called the residual level, is the point from which the geological luminescence accumulated after burial. OSL dating uses light of a particular wavelength or range of wavelengths, usually blue, green or infrared light, releasing rapidly the lightest sensitive trapped electrons from the crystal lattice. The decrease in the OSL after a 20 second exposure to sunlight is equivalent to the reduction in TL after a 20 hour light exposure. There are currently two major analytical approaches that translate the time-stored luminescence to an equivalent dose, and thus to an age.

The multiple aliquot additive dose method (MAAD) is used principally on the fine-grained polymineral or the quartz fraction. This method applies additional doses (beta or gamma) to the natural luminescence on separate aliquots of the sample effectively

building a dose response curve, simulating future dose and interpolating an equivalent dose to the solar reset level. MAAD is a method that was originally developed for TL dating and in largely unaltered form is currently used in OSL analysis. Numerous studies indicate the robustness of this procedure because it has yielded ages in agreement with other chronologic controls for at least the past one hundred thousand years.

The other relevant OSL method is the single aliquot regeneration method (SAR), which determines an age for each aliquot by matching a regenerated signal from the light reset level to the original natural level, while compensating for apparent sensitivity changes. This technique is used on both fine (4 - 11 μm) - and coarse (100 - 300 μm)-grained fractions containing mono- or poly-mineral separates. The SAR method is particularly useful for sediments less than fifty thousand years and provides decadal scale resolution for dating sediments, particularly of eolian origin, that are less than one million years old.

REFERENCES

Allen M., Raper S., and Mitchell K. 2001. Uncertainty in the IPCC's Third Assessment Report. Climate Change. Science. 293 (5529): 430-433.

ASPRS. 2006. American Society for Photogrammetry and Remote Sensing. http://www.asprs.org/.

Anderson, J.R., Hardy, E., Roach, J. and Witmer R. 1976. A Land-Use and Land-Cover Classification System for Use with Remote Sensor Data. Washington: U.S. Geological Survey, Professional Paper 964, 28 p.

Atkinson, P.M. and Lewis, S. 2000. Geostatistical Classification System for Remote Sensing: An Introduction. Computers & Geosciences. 26: 361-371.

Arens, S.M., Slings, Q., and de Vries, C.N. 2004. Mobility of a Remobilized Parabolic Dune in Kennemerland. The Netherlands. Geomorphology. 59 (1–4):175–188.

Bailey, S.D., and Bristow, C.S. 2004. Migration of Parabolic Dunes at Aberffraw, Anglesey, North Wales. Geomorphology 59 (1–4): 165–174.

Barbosa, L.M., and Dominguez, J.M.L. 2004. Coastal Dune Fields at the Sao Francisco River Strandplain, Northeastern Brazil: Morphology and Environmental Controls. Earth Surface Processes and Landforms. 29 (4): 443– 456.

CCNS. 2005 – 2006. Cape Cod National Seashore. http://www.nps.gov/caco/.

Carson, M.A., and MacLean, P.A., 1986. Development of Hybrid Dunes: The William River Dunefield, Northwest Saskatchewan, Canada. Canadian Journal of Earth Sciences. 23 (13): 1974– 1990.

Chamberlain, B. B., 1964. These Fragile Outposts, Doubleday. Reprinted, Parnassus Imprints (1981), Yarmouth Port, MA, 327 p.

Clark, A. G. 1992. Lighthouses of Cape Cod, Martha's Vineyard and Nantucket – Their History and Lore. East Orleans, Massachusetts: Parnassus Imprints, pp.50-53.

Clifford, C. 1994. Inventory of Historic Light Stations. Washington, D.C.: National Maritime Initiative; National Park Service History Division.

Cook, E.R., Meko, D.M., Stahle, D.W., and Cleaveland, M.K. 1998. Drought Reconstructions for the Continental United States. Journal of Climate 12 (4): 1145– 1162.

Cook, E.R., Meko, D.M., Stahle, D.W., and Cleaveland, M.K. 1999. Reconstruction Of Past Drought Across The Conterminous United States From A Network Of Climatically Sensitive Tree-Ring Data. http://www.ngdc.noaa.gov/paleo.

Cook, E.R., Krusic, P.J., and Woodhouse, C.A. 2003. North American Drought Atlas. IPCC Workshop on Droughts November, Tucson, AZ, pp. 1 –3.

Curran, P.J. and Williamson, H.D. 1986. Sample Size for Ground and Remote Sensed Data. Remote Sensing of Environment. 20: 31 –41.

Dunwiddie, P. W. 1997. Long-term effects of sheep grazing on coastal sandplain vegetation. Natural Areas Journal. 17: 261–264.

Dunwiddie, P. W., and M. B. Adams. 1995. Fire suppression and landscape change on Outer Cape Cod 1600–1994. U.S. Department of Interior Technical Report NPS/NESO-RNR/NRTR/96-08, Washington, D.C., USA.

Dunwiddie, P. W., R. E. Zaremba, and K. A. Harper. 1996. A classification of coastal heathlands and sand plain grasslands in Massachusetts. Rhodora 98: 117–145.

Eberhardt R.W., Foster D.R., Motzkin G., and Hall B. 2002. Conservation of Changing Landscapes: Vegetation and Land use history of Cape Cod National Seashore. Ecological Applications. 13 (1): 68–84.

Environmental Systems Research Institute, Inc. 2005. ArcGIS 9.0, Geographic Information System, Use's Guide. Redlands, California.

Finch, R. 2003. Cape Cod, its Natural and Cultural History: U.S. National Park. Service Handbook 148, 111 p.

Foody, G., and Atkinson, P. 2002. Uncertainty in Remote Sensing. C.E. Woodcock, Uncertainty in Remote Sensing and GIS. England: Wiley Press, pp. 19-24

Forman, S.L., and Maat, P. 1990. Stratigraphic Evidence for Late Quaternary Dune Activity near Hudson on the Piedmont of Northern Colorado. Geology 18: 745-748.

Forman, S.L., and Pierson, J. 2003. Formation of Linear and Parabolic Dunes on the Eastern Snake River plain, Idaho In The Nineteenth Century. Geomorphology 56 (1–2): 189– 200.

Forman, S.L., Goetz, A.F.H., and Yuhas, R.H. 1992. Large-Scale Stabilized Dunes on the High Plains of Colorado: Understanding the Landscape Response to Holocene Climates with the Aid of Images from Space. Geology. 20: 145-148.

Forman, S.L., Oglesby, R., and Webb, R.S. 2001. Temporal and Spatial Pattern of Holocene Dune Activity on the Great Plain of North America: Megadroughts and Climate Links. Global and Planetary Change 29: 1– 29.

Forman, S.L., Pierson, J., Go.mez, J., Marı.n, L., Miller, G.H., and Webb, R.S. 2006 in review. Eolian Sand Depositional Records from Western Nebraska: Potential Landscape Response to Droughts in the Past 1500 Years. Holocene.

Forman, S.L., Spaeth, M., Marı.n, L., Pierson J., Go.mez J. Bunch, F., and Valdez, A. 2006. in review. Episodic Late Holocene Dune Movements on the Sand Sheet Area, Great Sand Dunes National Park and Preserve, San Luis Valley. Colorado, USA. Quaternary Research.

Foster, D. R., Motzkin, G. and Slater, B. 1998. Land-use history as long-term broad-scale disturbance: regional forest dynamics in central New England. Ecosystems 1: 96–119.

Fryberger, S.G. 1979. Dune Forms and Wind Regime. In: McKee, E.D. (Ed.), A Study of Global Sand Seas, United States Geological Survey Professional Paper. 1052. U.S. Government Printing Office, Washington, D.C., pp. 137– 169.

Fryberger, S.G. 1999. Overview of the Eolian Depositional System, Great Sand Dunes National Monument and Vicinity. In: Schenk, C.J. (Ed.), Hydrologic, Geologic and Biologic Research at Great Sand Dunes National Monument, Colorado: Proceedings of the National Park Service Research Symposium, No. 1, USGS, Denver, CO, pp. 195–214.

Gleason, S. C. 1991. Kindly Lights: A History of the Lighthouses of Southern New England. Boston, Beacon Press.

Greeley, R., and Iversen, J.D. 1987. Wind as a Geological Process on Earth, Mars, Venus and Titan. Cambridge University Press, New York. 333 pp.

Holmes, R. D., Hertz, C.D., and Mulholland, M. T. 1998. Historical cultural land use study of lower Cape Cod. Cultural Resource Center, Northeast Region, National Park Service, U.S. Department of the Interior, Lowell, MA.

Huenneke, L., Anderson, J., Remmenga, M., and Schlesinger, W. 2002. Desertification Alters Patterns of Aboveground Net Primary Production in Chihuahuan Ecosystems. Global Change Biology. 8: 247–264.

Huete, A.R. 1988. A Soil-adjusted Vegetation (SAVI). Remote Sensing of Environment 25: 295 –309.

Jacobberger, P.A. 1988. Drought-Related Changes to Geomorphic Processes in Central Mali. Geological Society of America Bulletin 100 (3): 351– 361.

Janke, J.R. 2002. An Analysis of the Current Stability of the Dune Field at Great San Dunes National Monument (1984–1998). Remote Sensing of Environment 83: 488– 497.

Jensen, J. R. 2000. Remote Sensing of the Environment: An Earth Resource Perspective. Upper Saddle River, NJ: Prentice Hall, pp. 1-106.

Johnson, R.B. 1967. The Great Sand Dunes of Southern Colorado. U.S. Geological Survey Professional Paper, 575 C. U.S. Government Printing Office, Washington, D.C., pp. 177–183.

Keller E. 2004. Natural Hazards. Environmental Geology. Prentice Hall, 3 edition, pp.340-350.

Lancaster, N., 1988. Development of Linear Dunes in the Southwestern Kalahari, Southern Africa. Journal of Arid Environments. 14: 233– 244.

Lancaster, N. 1997. Response of Eolian Geomorphic Systems to Minor Climate Change: Example from the Southern California Deserts. Geomorphology 19: 333– 347.

Lawrimore, J.H., Karl, T.R., Levinson, D.H., Heim, R.R., Vose, R.S., and Groisman, P.Y. 2003. Cotemporary Trends in Drought on the North American Continent. IPCC Workshop on Droughts November, Tucson, AZ, pp. 1 – 10.

Leica Ceosystems. 2005. ERDAS. http://gis.leica-geosystems.com

Lillesand, T.M., Kiefer, R.W. 1994. Remote Sensing and Image Interpretation. John Wiley and Sons, Inc., New York, pp. 527– 530.

MacConnell, W. P., N. A. Pywell, D. Robertson, and W. Niedzwiedz. 1974. Remote sensing 20 years of change in Barnstable, Dukes, and Nantucket Counties, Massachusetts, 1951–1971. Massachusetts Agricultural Experiment Station Bulletin Number 623, Amherst, MA, USA.

Mangimeli, J. 1999. Dendroclimatological Research at Great Sand Dunes National Monument, Colorado. In: Schenk, C.J. (Ed.), Hydrologic, Geologic and Biologic Research at Great Sand Dunes National Monument, Colorado: Proceedings of the National Park Service Research Symposium, No. 1, USGS, Denver, CO, pp. 243–248.

Mapmart. 2004. www.mapmart.com.

Marin, L., S. Forman, A. Valdez and F. Bunch. 2005. 20th Century Dune Migration at the Great Sand Dunes National Park and Preserve, Colorado and Relation to Drought Variability. Geomorphology. 70: 163-183.

Mason, J.A., Swinehart, J.B., Globe, R.J., Loope, D.B., 2004. Late- Holocene Dune Activity Linked To Hydrological Drought, Nebraska Sand Hills, USA. The Holocene 14 (2), pp. 209– 217.

MassGIS. 2006. MassGIS Datalayer Descriptions and a Guide to User Services. Executive Office of Environmental Affairs, Environmental Data Center, Boston, MA, USA.

McKee, E.D. 1979. A Study of Global Sand Seas. United States Geological Survey Professional Paper, 1052. U.S. Government Printing Office, Washington D.C., pp. 146–148.

Muhs, D.R., and Been, J.M. 1997. Reactivation of Stabilized Sand Dunes n the Colorado Plateau: Impact of Climate Change and Land Use in the Southwestern United States. USGS. http://geochange.er.usgs.gov/sw/impacts/geology/sand/.

Muhs, D.R., and Wolfe, S.A. 1999. Sand Dunes of the Northern Great Plains of Canada and the United States. In: Lemmen, D.S., Vance, R.E. (Eds.), Holocene Climate and Environmental Change in the Palliser Triangle, Bulletin, 534. Geological Survey of Canada, pp. 183– 197.

NCDC. 2006. National Climatic Data Center. www.ncdc.noaa.gov/oa/ncdc.html.

NMAH. 2006. National Museum of American History. http://americanhistory.si.edu/

NOAA. 2006. National Ocean and Atmospheric Administration. http://www.noaa.gov/

NPS. 2004. National Park Service. Great Sand Dunes National Monument and Preserve. http://www.nps.gov/grsa/.

NASA. 2006. National Aeronautic and Space Administration. http://www.nasa.gov/

National Park Service. Parabolic Dunes. 2006. http://www.nps.gov/grsa/resources/parabolic.htm

O'Brien, Greg, ed. 1990. A Guide to Nature on Cape Cod and the Islands. Viking Penquin, New York, 240 p.

Oldale, R. N. 1981. Geologic History of Cape Cod, MA. U.S. Geological Survey Popular Publication, 23 p.

Oldale, R. N. 1992. Cape Cod and the Islands, the Geologic Story. Parnassus Imprints, East Orleans, MA, 208 p.

Oldale, R. N., and Barlow, R. A. 1986. Geologic Map of Cape Cod and the Islands, MA. Reprinted 1995, U.S. Geological Survey Miscellaneous Investigation Map I-763, scale 1/100,000.

Overpeck, J.T. 1996. Warm Climate Surprises. Science. 271: 1820–1821.

Paisley, E.C.I., Lancaster, N., Gaddis, L.R., and Greeley, R. 1991. Discrimination of Active and Inactive Sand From Remote Sensing: Kelso Dunes, Mojave Desert, California. Remote Sensing and the Environment. 37: 153–166.

Palmer, W.C. 1965. Meteorological Drought. Res. Paper 45. Department of Commerce, Washington, D.C. 58 pp.

PCI Geomatics. 2005. PCI, Ortho Engine Air photo Models, User's Guide. Toronto, Canada: PCI Geomatics.

Pinet, P.R. 1992. Oceanography: An Introduction to the Planet Oceanus. St. Paul, Minn.: West Publ.

Piechota, T., Timilsena, J., Tootle, G., and Hidalgo, H. 2004. The Western U.S. Drought: How Bad Is It? EOS. 85 (32): 301–304.

Pye, K. 1982. Morphological Development of Coastal Dunes in a Humid Tropical Environment, Cape Bedford and Cape Flattery, North Queensland. Geografiska Annaler. Series A. Physical Geography. 64: 213–227.

RSI. 2000. Research Systems Incorporated. ENVI, The Environment for Visualizing Images, User's Guide. Boulder, Colorado: Research Systems.

Rockmore, M. 1979. Documentary Review of the Historical Archeology of the Cape Cod National Seashore. Division of Cultural Resources, North Atlantic Regional Office, National Park Service, Lowell, MA, USA.

RSI. 2005. Solutions for Data Visualization and Image Analysis, ENVI. http://www.rsinc.com/

Sadler, P.M. 2004. Quantitative Biostratigraphy - Achieving Finer Resolution In Global Correlation. Annual Review of Earth and Planetary Sciences. 32: 187– 213.

Sadler, P.M., and Strauss, D.J. 1990. Estimation of Completeness of Stratigraphical Sections Using Empirical Data and Theoretical Models. Journal of the Geological Society. 147: 471–485.

Schlesinger, W.H., Reynolds, J.F., Cunningham, G.L., Huenneke, L.F., Jarrel, W.M., Virginia, A., and Whitford, W.G., 1990. Biological Feedbacks in Global Desertification. Science. 247: 1043–1048.

Schott, J. R. 1997. Remote Sensing: The Image Chain Approach. New York, Oxford University Press.

Shulka, J., and Mintz, Y. 1982. Influence of Land-Surface Evapotranspiration on the Earth's Climate. Science. 215: 1498–1501.

Smith, S.M., R. Abed M.M., and Garcia-Piche F. 2004. Biological Soil Crusts of Sand Dunes in Cape Cod National Seashore, MA. Microbial Ecology 48: 200-208.

Snow, E. R. 1973. The Lighthouses of New England. New York: Dodd, Mead & Company.

Stone, T. A. 1998. Land Cover and Land Use of Cape Cod. Environment Cape Cod. 1 (4): 35-49.

Strahler, A. N. 1988. A Geologist's View of Cape Cod: Doubleday. Reprinted Parnassus Imprints, Orleans, Massachusetts, 115 p.

Strahler, A. N. 1966. A Geologist's View of Cape Cod: Doubleday. American Museum of Natural History, Garden City, New York.

Terraserver. 2004. http://terraserver.microsoft.com.

Thornthwaite, C.W. 1931. The Climate of North America According to a New Classification. Geographical Review. 21: 633– 655.

Thoreau, H. D. 1989. Cape Cod. Penguin Books, New York, New York, USA.

Thornthwaite, C.W. 1948. An Approach toward a Rationale Classification of Climate. Geographical Review. 38: 55–94.

Tsoar, H. 1989. Linear Dunes Forms and Formation. Progress in Physical Geography. 13: 507–528.

Tsoar, H., and Blumberg, D.G. 2002. Formation of Parabolic Dunes from Barchans and Transverse Dunes along Israel's Mediterranean Coast. Earth Surface Processes and Landforms. 27 (11): 1147–1161.

Tsoar, H., and Karnieli, A. 1996. What determines the Spectral Reflectance of the Negev–Sinai sand dunes. International Journal of Remote Sensing 17 (3): 513–525.

Uchupi, E., Driscoll, N., Ballard, R.D., and Bolmer, S.T. 2001. Drainage of Late Wisconsin Glacial Lakes and the Morphology and Late Quaternary Stratigraphy of the New Jersey–Southern New England Continental Shelf And Slope: Marine Geology. 172: 117–145.

USDA. 2006. United States Department of Agriculture. www.usda.gov.

USGS. 2006. United States Geological Society. www.usgs.gov.

Wells, N. 2003. PDSI User Manual. National Agricultural Decision Support System. http://nadss.unl.edu.

Wells, S.G., McFadden, L.D., and Schulz, J.D. 1990. Eolian Landscape Evolution and Soil Formation in the Chaco Dune Field, Southern Colorado Plateau. New Mexico. Geomorphology. 3: 517–546.

Winkler, M.G. 1992. Development of Parabolic Dunes and Interdunal Wetlands in the Provincelands. Cape Cod National Seashore, SEPM Special Publication. 48: 57-64.

Winkler, M. G. 1985. A 12,000-year Old History of Vegetation and Climate for Cape Cod, Massachusetts. Quaternary Research. 23: 301–312.

Wolfe, S.A., Huntley, D.J., David, P.P., Ollerhead, J., Sauchyn, D.J., and MacDonald, G.M., 2001. Late 18th Century Drought-Induced Sand Dune Activity, Great Sand Hills, Saskatchewan. Canadian Journal of Earth Sciences. 38: 105– 117.

Woodhouse, C.A., and Overpeck, J.T. 1998. 2000 Years of Drought Variability in the Central United States. Bulletin of the American Meteorological Society. 79 (12): 2693–26271.

APPENDIX A

Extracting DEM from aerial photographs used for the Cape Cod project

OrthoEngine tools of PCI Geomatics software (PCI, 2005) can be used for extracting DEM from the stereo pairs of aerial photographs. OrthoEngine is a powerful orthorectification and mosaic constructing package containing a triangulation method for generating orthophotos and mosaics from scanned or digital camera aerial photographs.

The illustration below shows the workflows for airphoto projects in this tutorial (Fig. A.2).

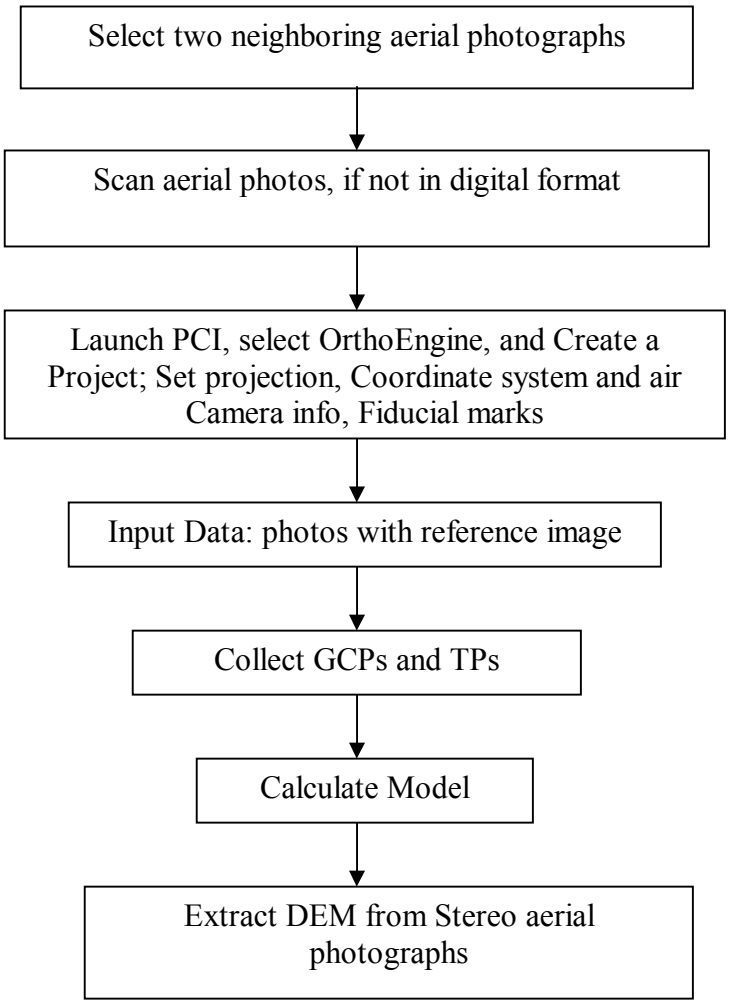

Figure A.1. Flowchart showing DEM extraction aerial photographs.

Below is explanation of each step from the previous workflow.

Step 1: Select two neighboring aerial photographs (Fig. A.2)

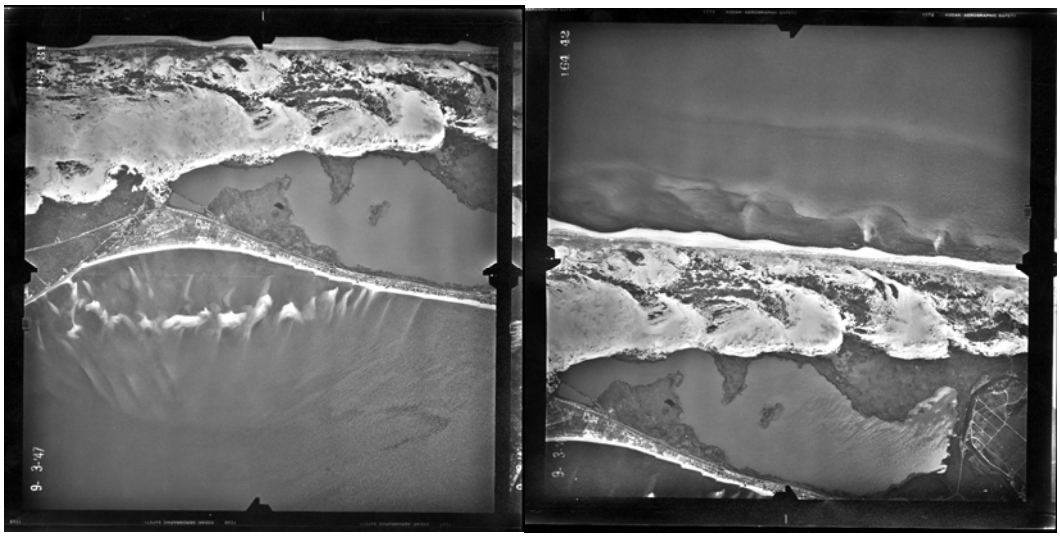

Figure A.2. Two neighboring aerial photographs.

Step 2: Scan aerial photos, if they are not in digital formats.

It is notably important to use a sophisticated scanner with specialized software for scanning; otherwise it may be complicated to make useful georeferenced images for the DEM.

Step 3: Launch PCI, select OrthoEngine, and Create a Project; Set projection, Coordinate system and air Camera info, Fiducial marks

To start OrthoEngine:

1. Double click the **PCI Geomatica** icon. The Geomatica Toolbar opens and the Focus starts automatically.
2. **Close** the Focus application.
3. Click the **OrthoEngine** button on the Geomatica Toolbar. The main OrthoEngine panel opens (Fig.A.3).

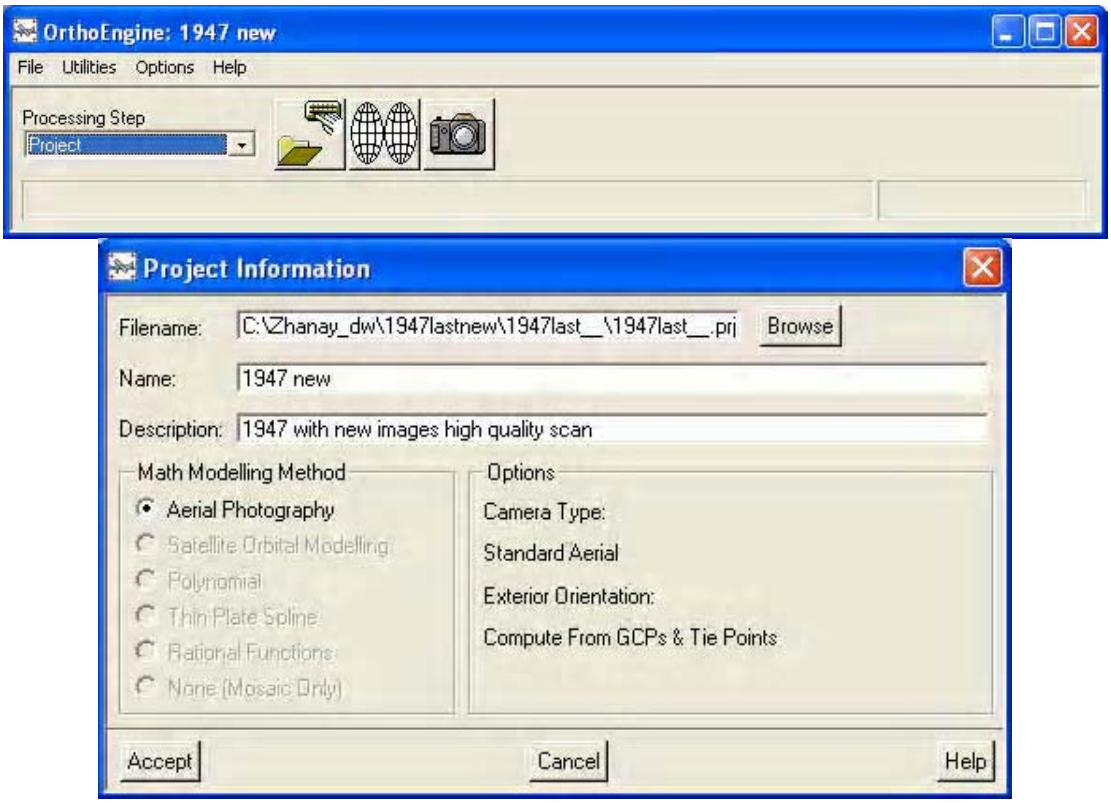

Figure A.3. Project in OrthoEngine.

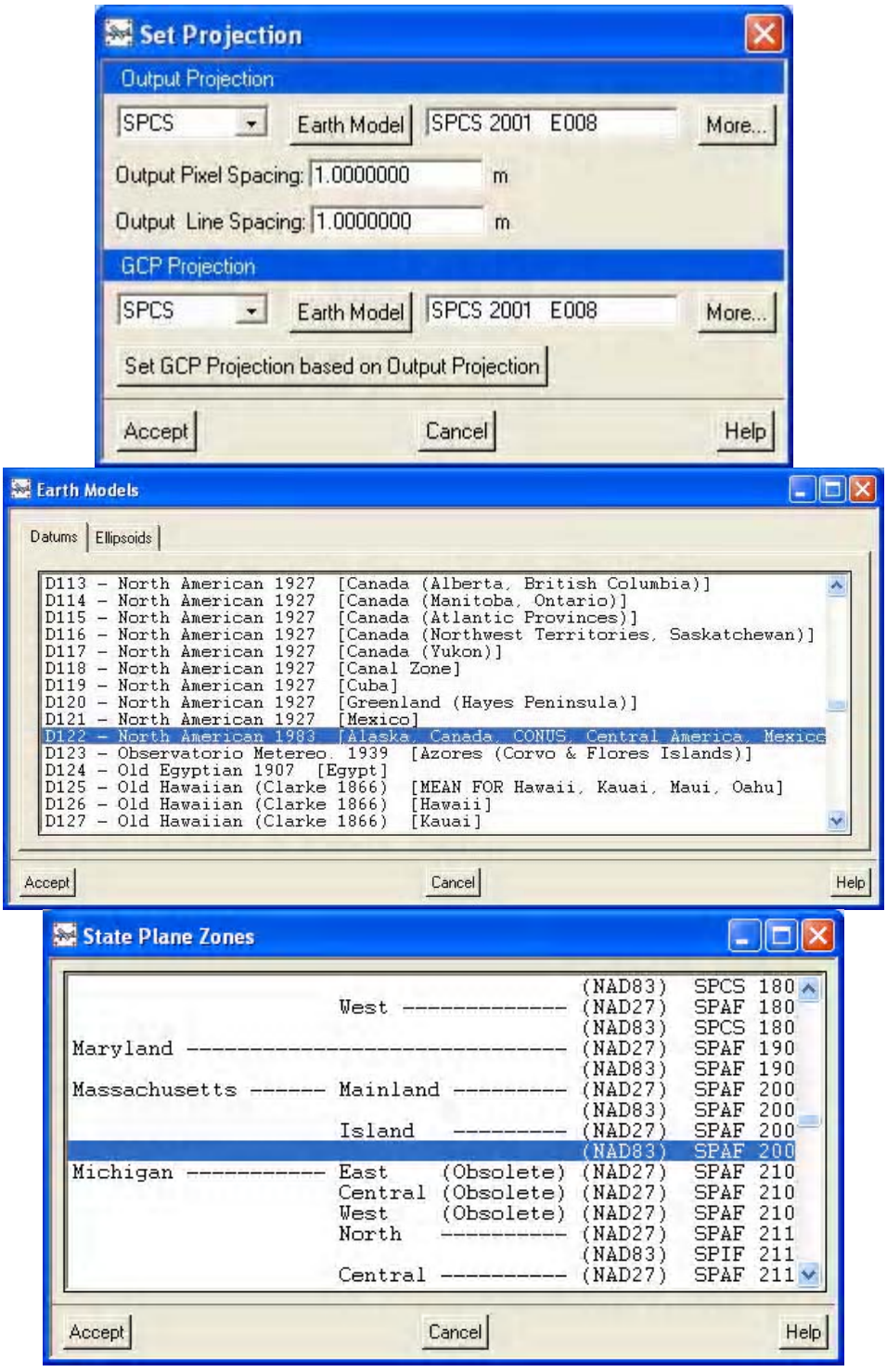

Figure A.4. Projection and coordinate system.

Camera information is as follow (Fig.A.5.):

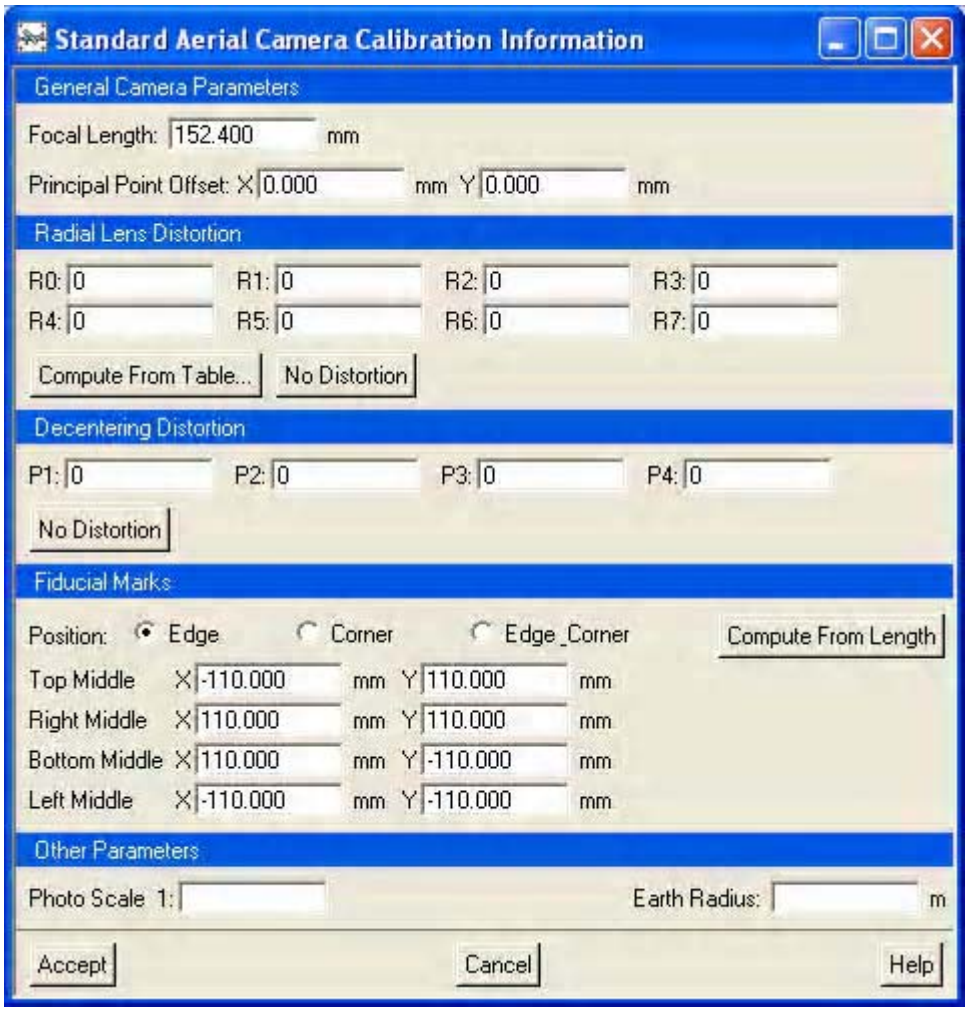

Figure A.5. Aerial Camera Calibration.

Fiducial marks

Four fixed points in each aerial photographs to which other ground control points can be related were selected; these four fixed points are called fiducial marks (Fig. A.6).

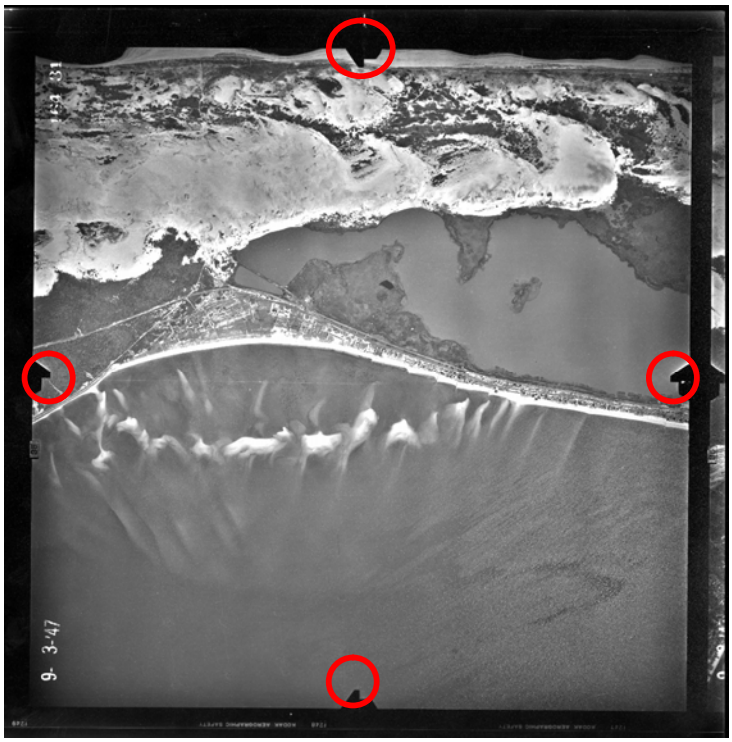

Figure A.6. Fiducial marks.

Step 4: Input Data: photos with reference image

Select the **Data Input** processing step (Fig. A.7).

The reference image is a geo coded image that has already been georeferenced which enables the user to apply its x, y, and z coordinates.

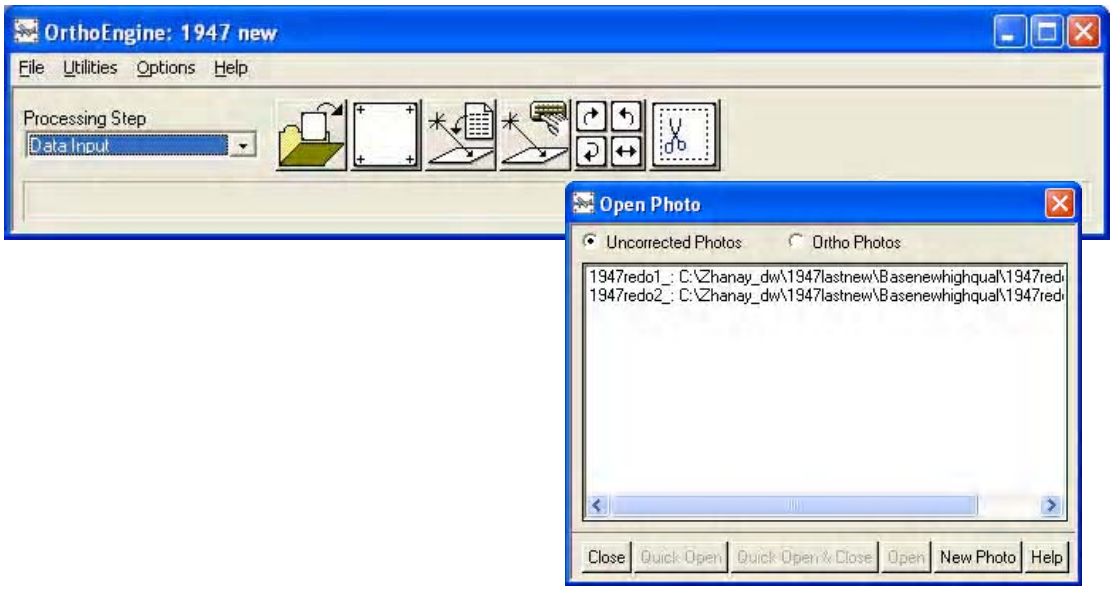

Figure A.7. Data Input.

Step 5: Collect GCPs, TPs

Select the **GCP/TP Collection** processing step (Fig. A.8).

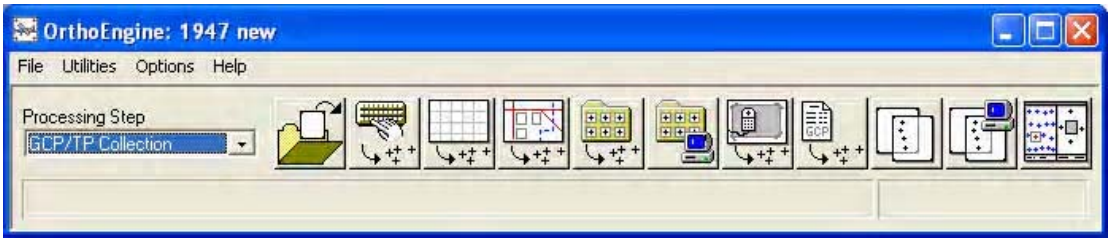

Figure A.8. GCP/TP Collection.

GCP: A Ground Control Points (GCP) is a feature that can be clearly identified in a raw image for which the coordinate is known. GCPs are used to determine the relationship between the raw image and the ground by associating the pixels (P) and lines (L) in the image to the x, y, and z coordinates on the ground.

Choosing Good Ground Control Points:

The quality of GCPs directly affects the accuracy of the model, and that, in turn, determines the outcome of the project. When the GCPs are collected it is necessary to (Fig. A.9):

1) Choose features that can be identified accurately at the resolution of the raw image. Image edges are effective sites to collect such points;
2) Avoid using shadows as GCPs; although shadows may be easy to see in the image, they are not permanent and can move from one image to another;
3) Collect GCPs from a variety of elevations in a wide distribution over the image;
4) Collect GCPs in an area of overlap between two or more images when possible; the same ground coordinate collected in multiple images helps to produce a more accurate model.

The Number of GCPs to Collect:

A reasonable number of GCPs are about 20 points.

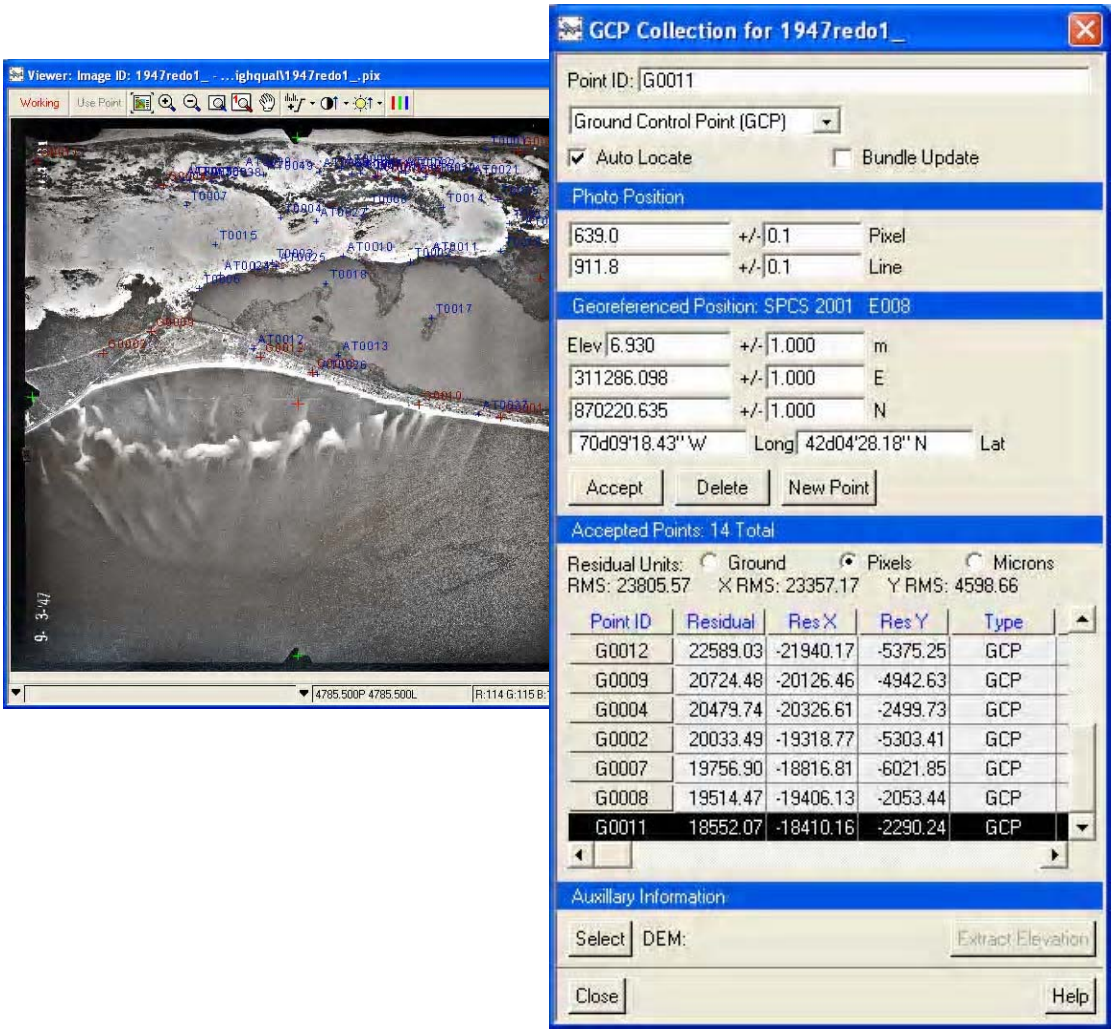

Figure A.9. GCP/TP Collection.

Note: When selecting and accepting GCPs, GCP collection only applies to the working image, not the reference image. Select “Reference” to switch between images.

Error adjustments with respect to elevations and positions can be made with each individual GCP by adjusting the tolerance values to the desired limits.

Tie points collections

Tie points are points that are co-located on two images that have an overlapping geographic extent.

Select the number of tie points per area, approximate elevation, and matching threshold. The tie point distribution pattern should be placed uniformly throughout the image or per overlapping area. The auxiliary information is used if the elevations of these locations is computed (Fig. A.10).

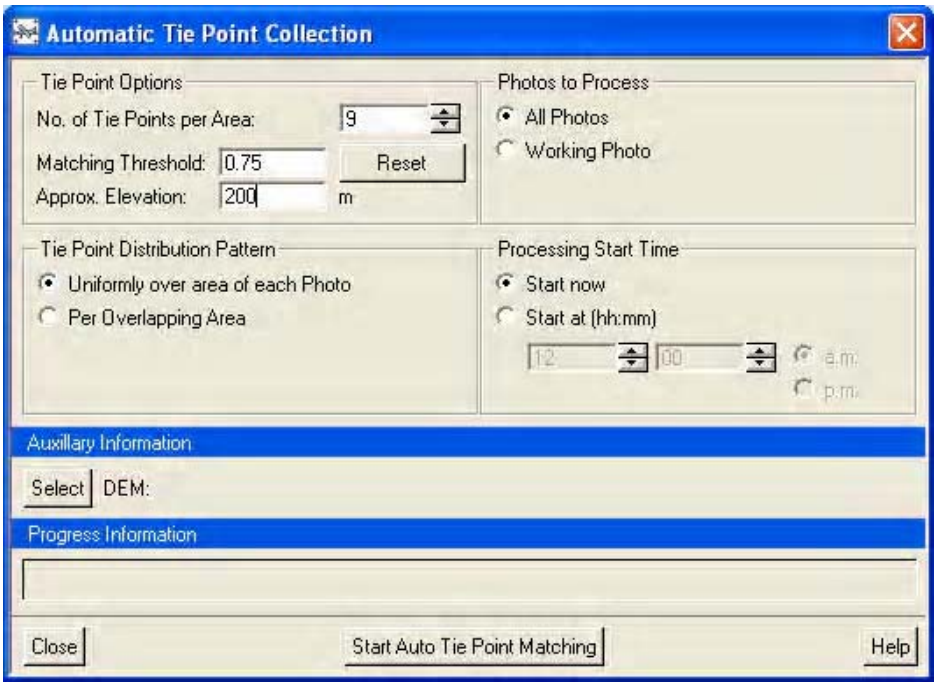

Figure A.10. GCP/TP Collection.

Step 6: Calculate Model

Select the **Model Calculations** processing step (Fig. A.11).

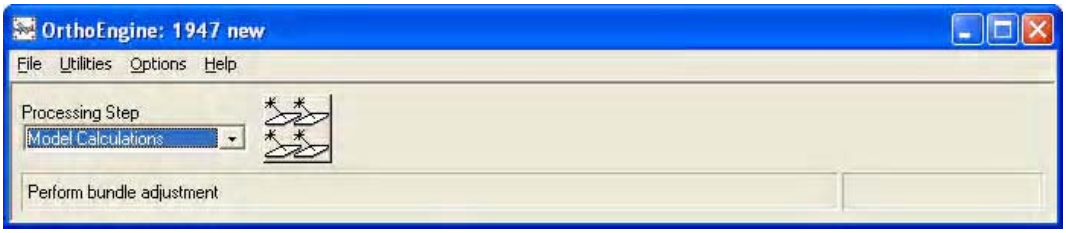

Figure A.11. Model Calculations.

Step 7: Extract DEM from stereo aerial photographs

Select the **DEM from Stereo** processing step. **Create Epipolar Image** (Fig. A.12).

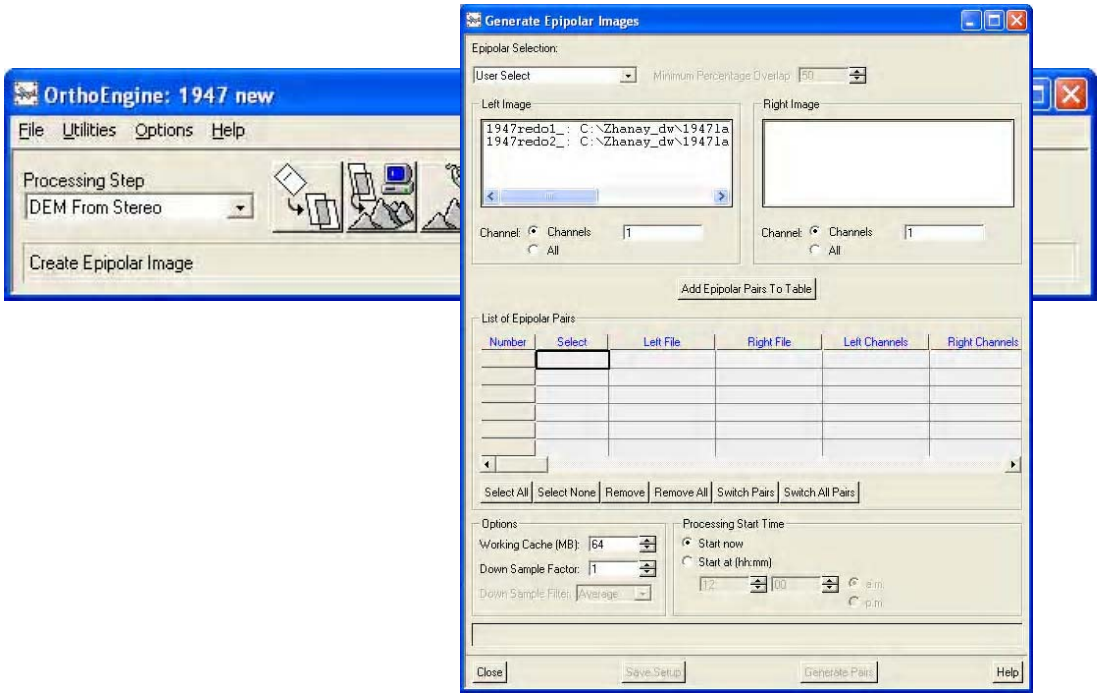

Figure A.12. Epipolar Image creation.

Select the **Generate Epipolar Images** processing step (Fig. A.12).

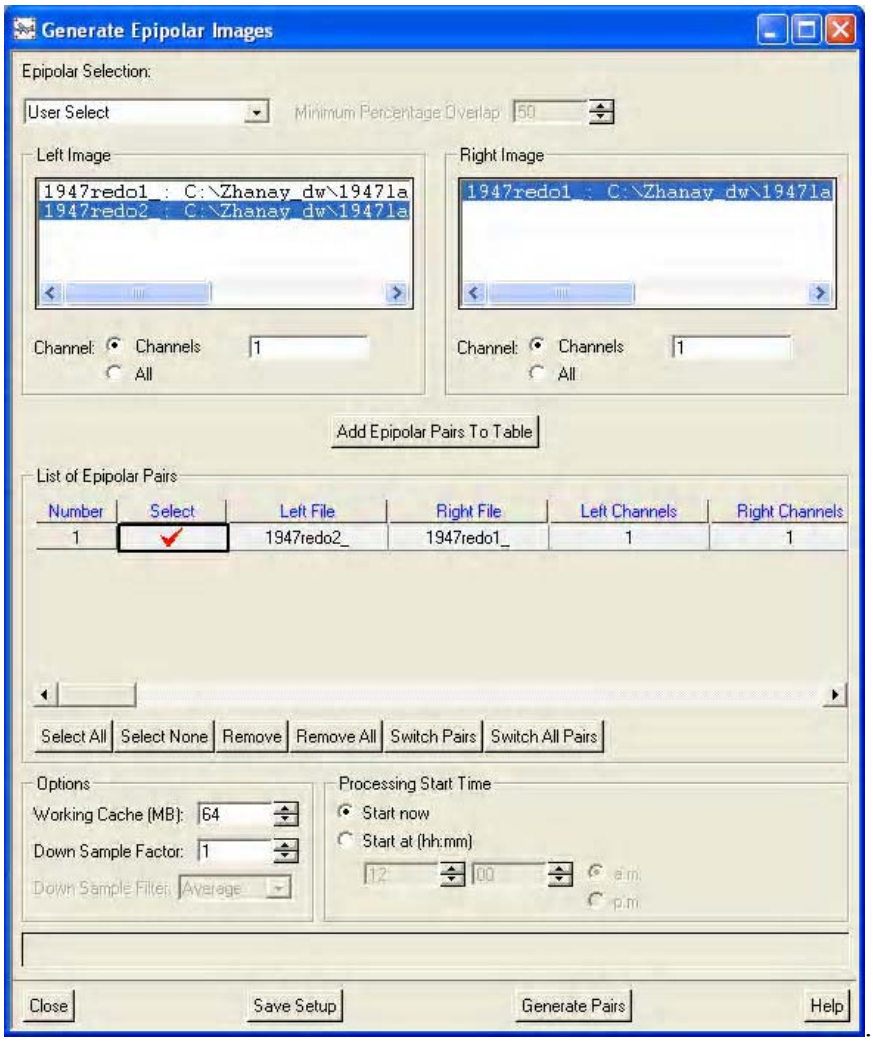

Figure A.12. Epipolar Image creation.

Epipolar images are stereo pairs that are re-projected so that the left and right images have a common orientation, and matching features between the images appear along a common x-axis.

In the “Left Image” window, select one of the aerial photographs; this will automatically move another one to the “Right Image” window. Select the right aerial

photograph in the “Right Image” window. The output filenames will be assigned automatically.

Set “Working Cache” to a value that the computer can support and then click **Create**.

Select the **Extract DEM automatically** processing step (Fig. A.13).

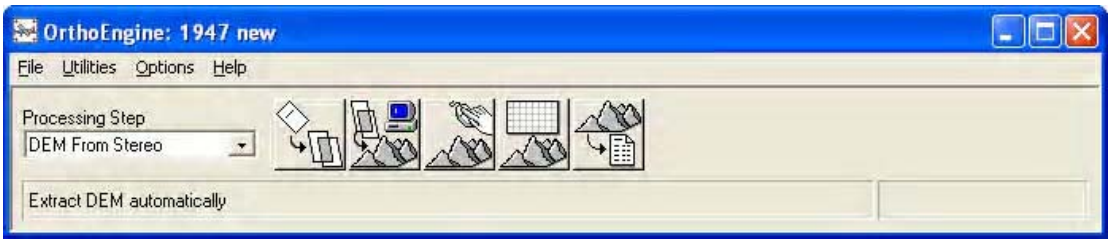

Figure A.13. Epipolar Image creation.

A DEM is a Digital Elevation Model which allows extracting the elevation of an area. Select the epipolar pair from the “Stereo Pair Selection” table.

Enter a minimum and maximum elevation, as well as failure and background values.

Select the desired pixel spacing and “DEM Detail.”

Enter output DEM and Report filenames and click **Start DEM Extraction** (Fig. A.14)**.**

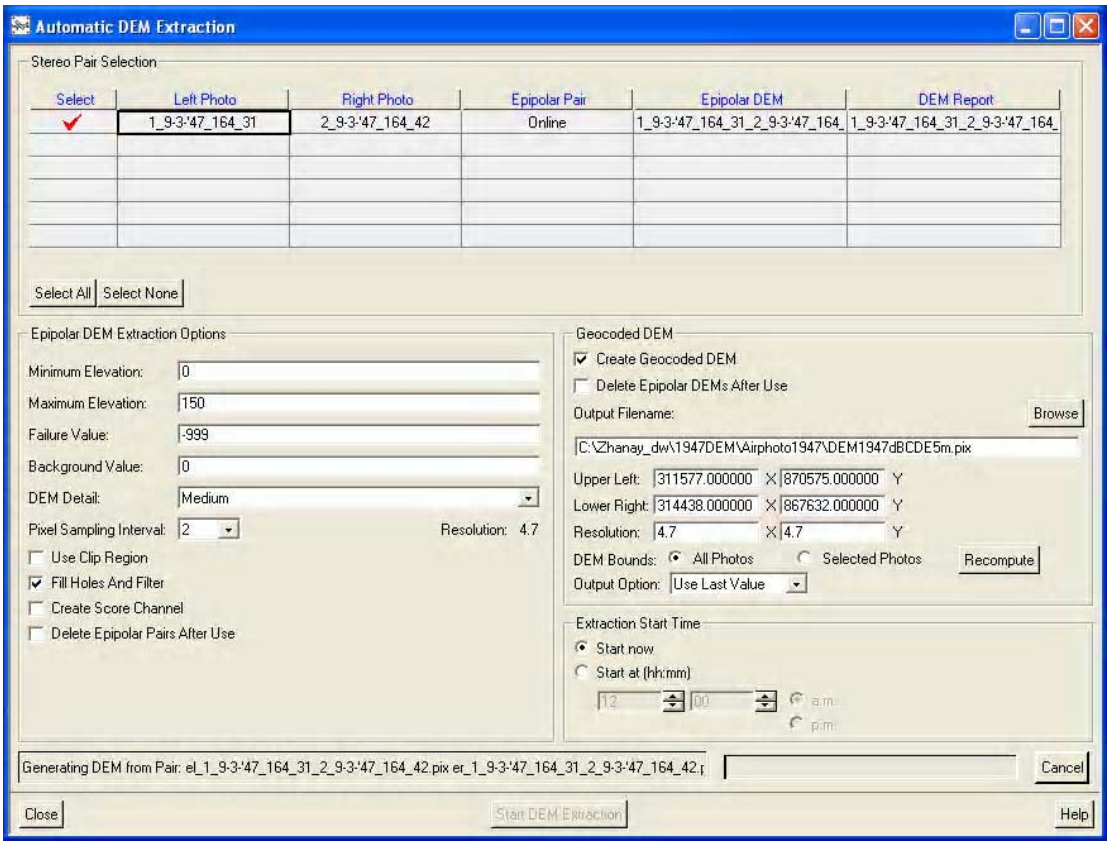

Figure A.14. Epipolar Image creation.

The topographic map, watersheds and streams can be delineated from the extracted DEM by using GIS software (ESRI, 2005).

APPENDIX B

Watershed and Stream Delineation from DEM

ArcGIS was used for watershed and stream network delineation using a DEM. This short tutorial was used to work with drainage basins of Cape Cod region for the D, E, and F dunes area. The working steps are shown in the following flowchart (Fig. B.1).

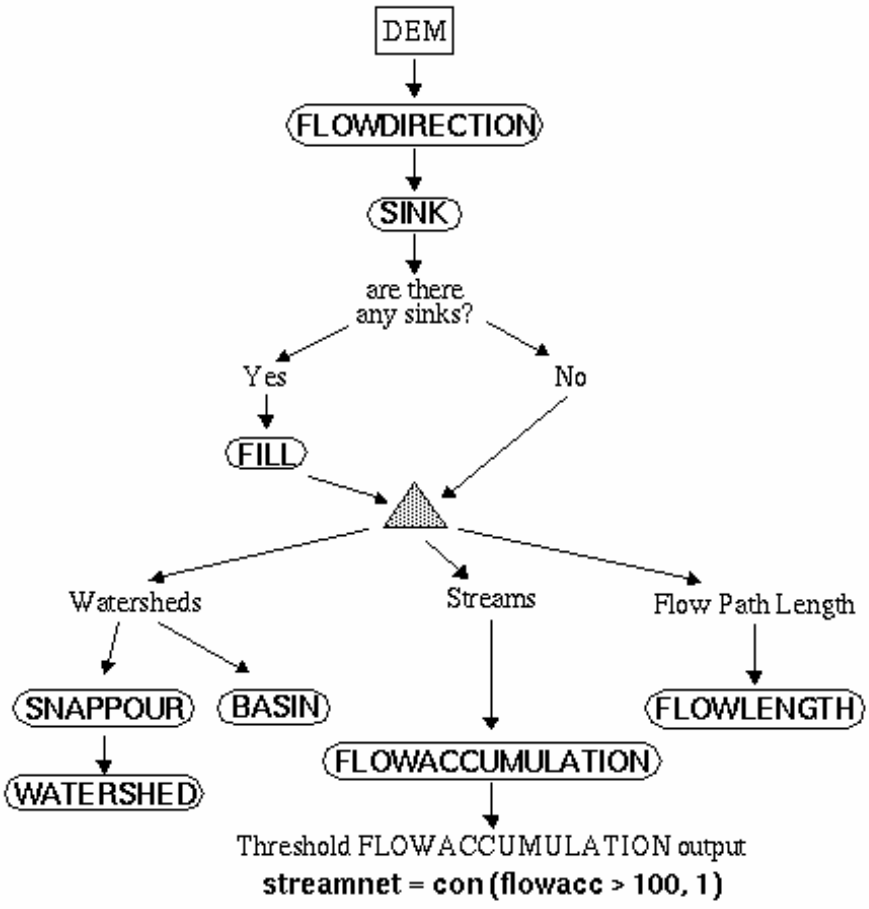

Figure B.1. Outline of steps to derive surface characteristics from a DEM.

Start Arc Catalog, ArcMap connect to the data folder with DEM file (Fig. B.2).

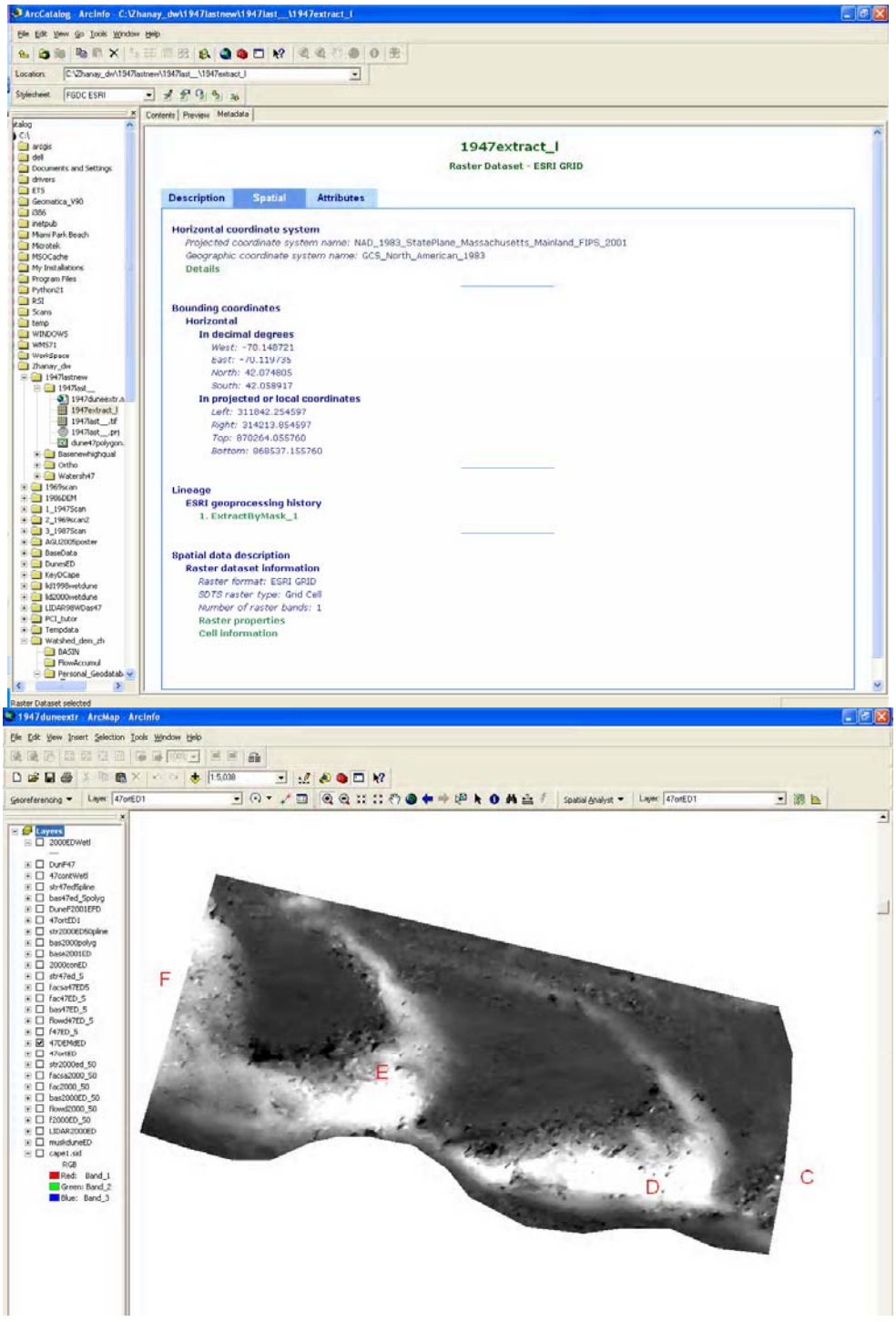

Figure B.2. ArcMap with a DEM file.

Activate **Command Line** on the Arc map (Fig. B.3).

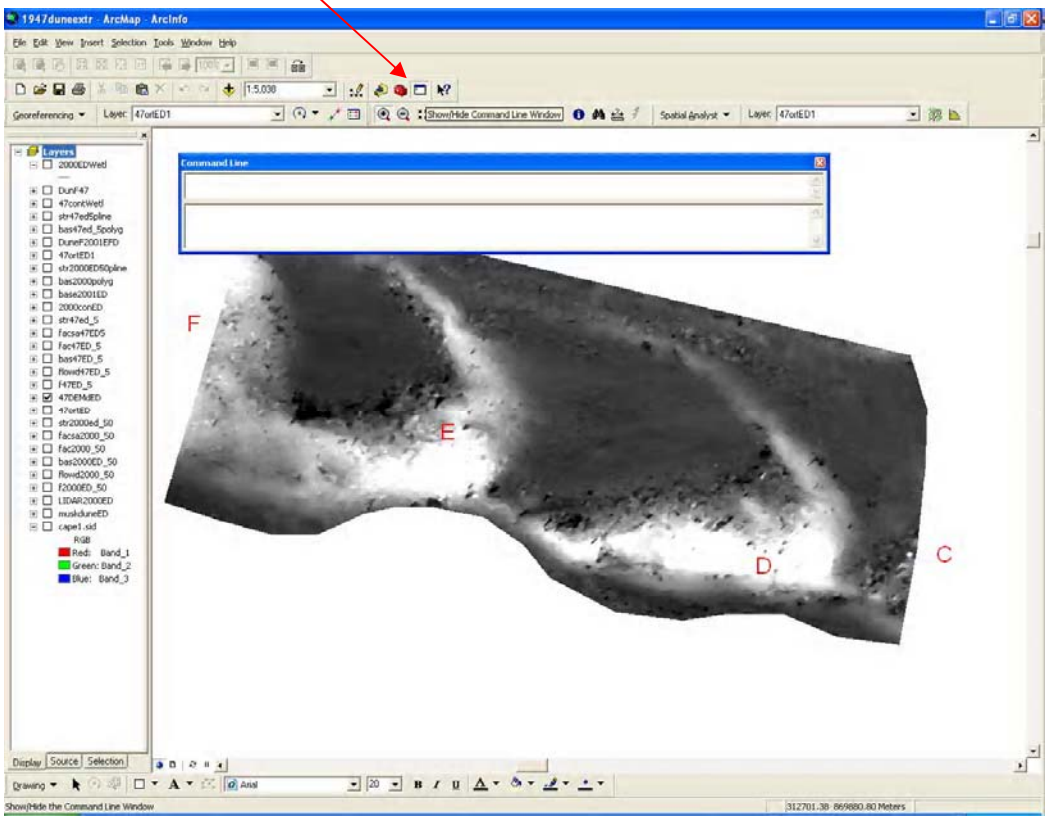

Figure B.3. Command Line activation.

Fill Sinks

The data may have “dead ends” – channels smaller than the grid space, or errors in the DEM can cause this. To eliminate such “ dead ends” use the **Fill command** (Fig. B.4).

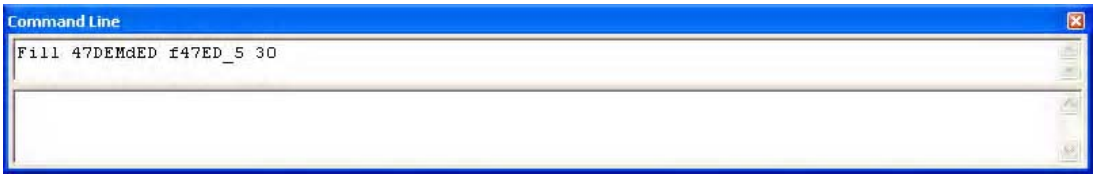

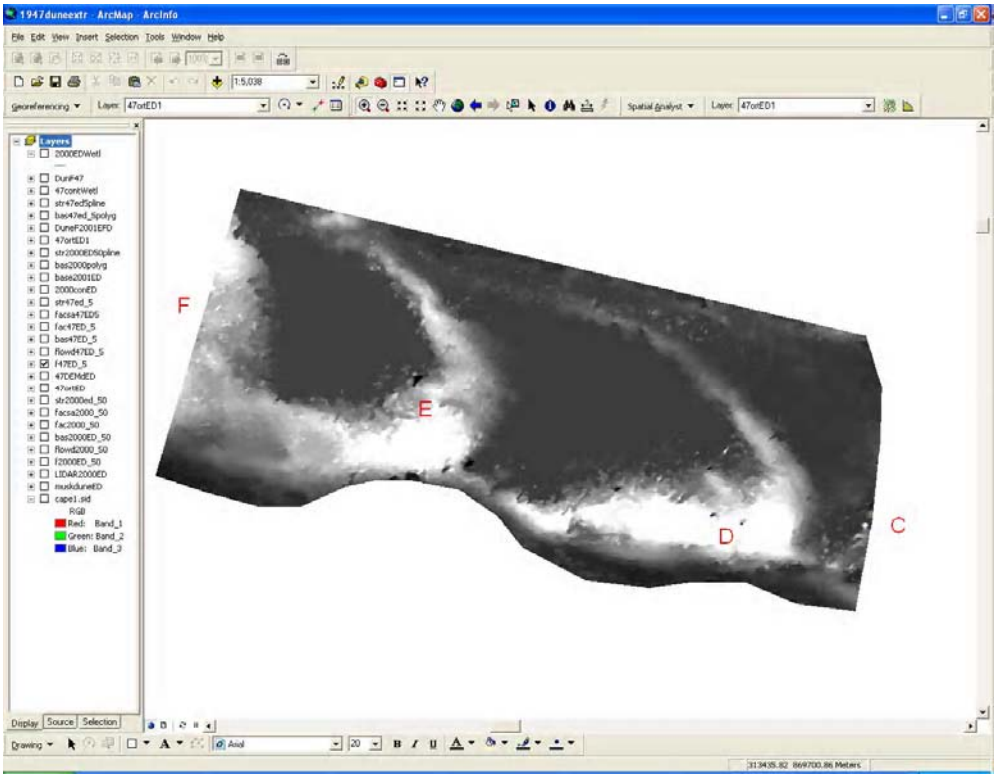

Figure B.4. Fill Sinks.

After the filling step the next step is **Flow direction** procedure (Fig. B.5).

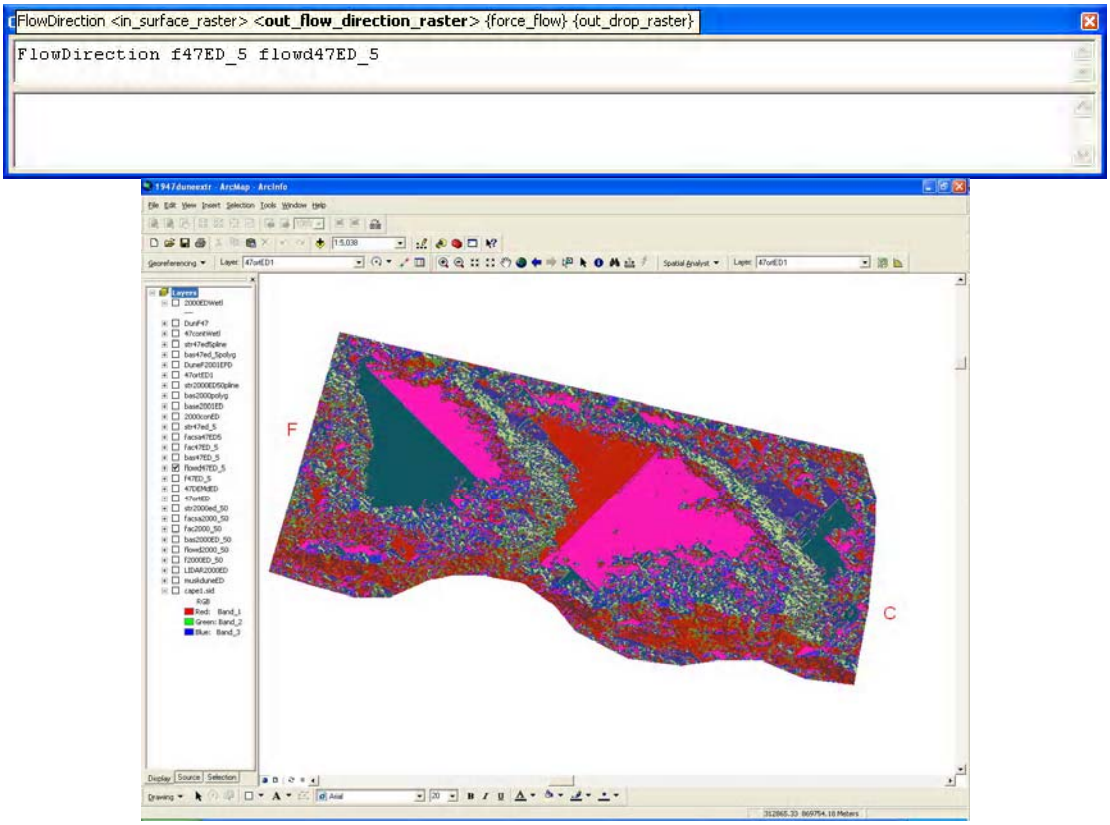

Figure B.5. Flow direction procedure.

The next step is to compute **Basin** Extents (Fig. B.6). This will compute the area of each drainage basin.

The GIS Symbology tab of properties can help in identification of each basin by presenting a unique color. Some issues related to the edge of data can be seen. This info should help to identify the acceptable sink value, if Basins are acceptable

Too many basins – Increase sink z-value

Too few basins – Decrease sink z-value)

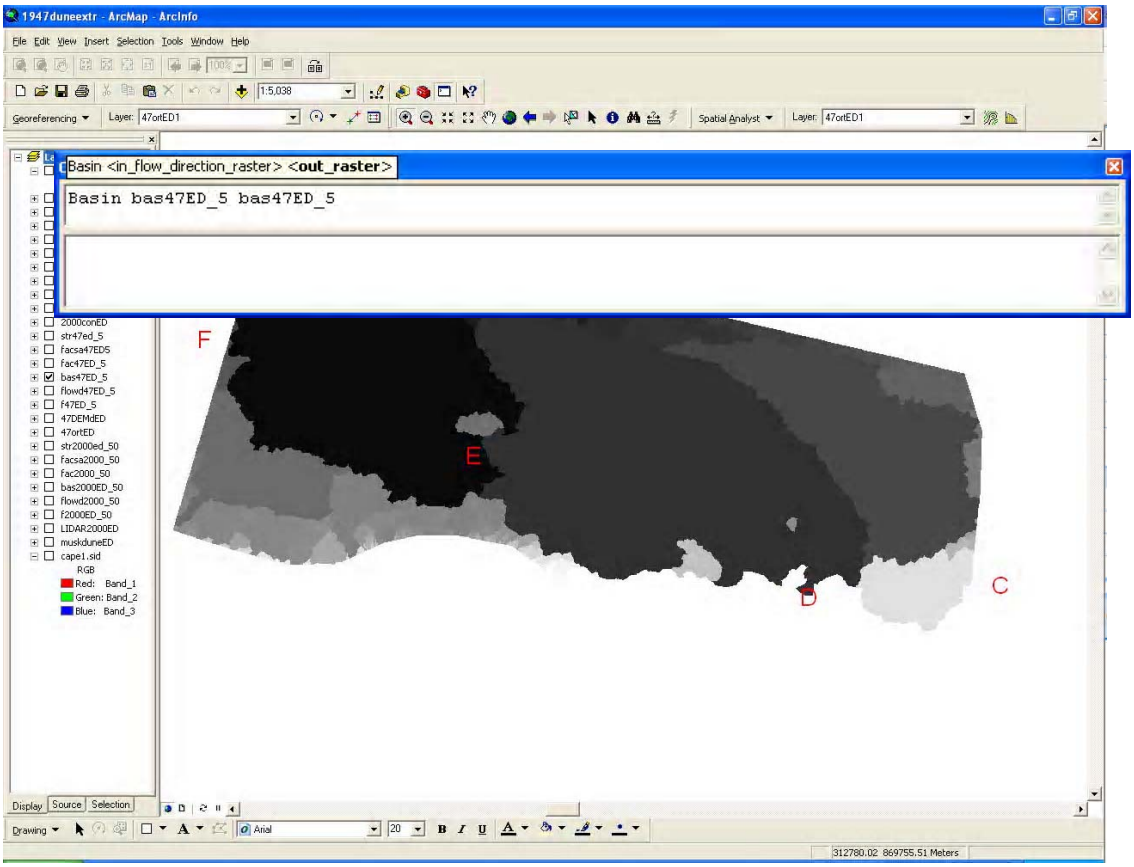

Figure B.6. Basin Extents procedure.

At this point, it is better for displaying to the outlines these basins, and not just a raster image.

Under **ArcToolbox,** choose **Conversion Tools**, then **Raster to Polygon**; select the basins grid as the input, the output type as polygon, and assign the file an appropriate filename (Fig. B.7).

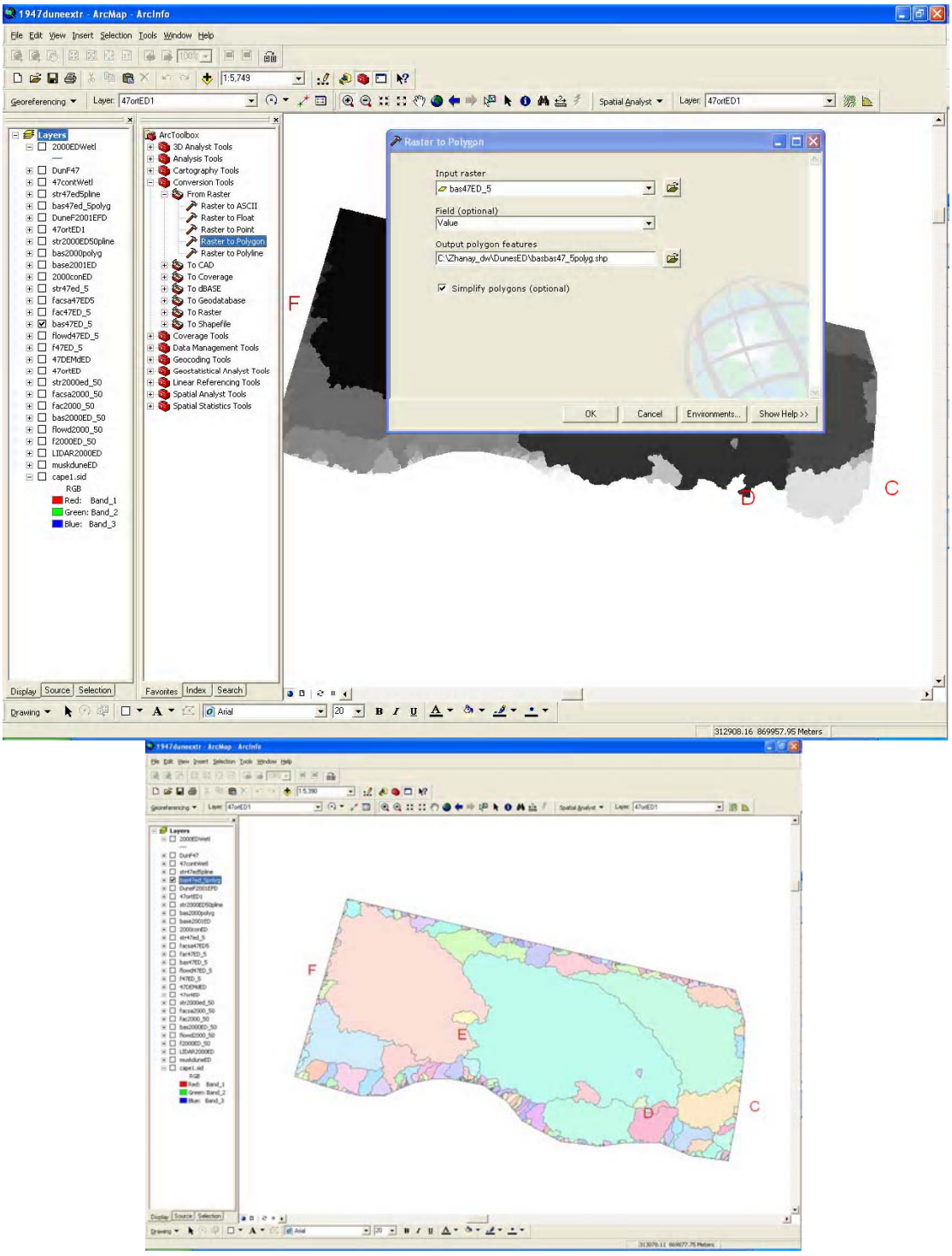

Figure B.7. Conversion from Raster to Polygon.

The next step is to calculate **Flow accumulation,** that calculates which cells accumulate water from surrounding cells (Fig. B.8).

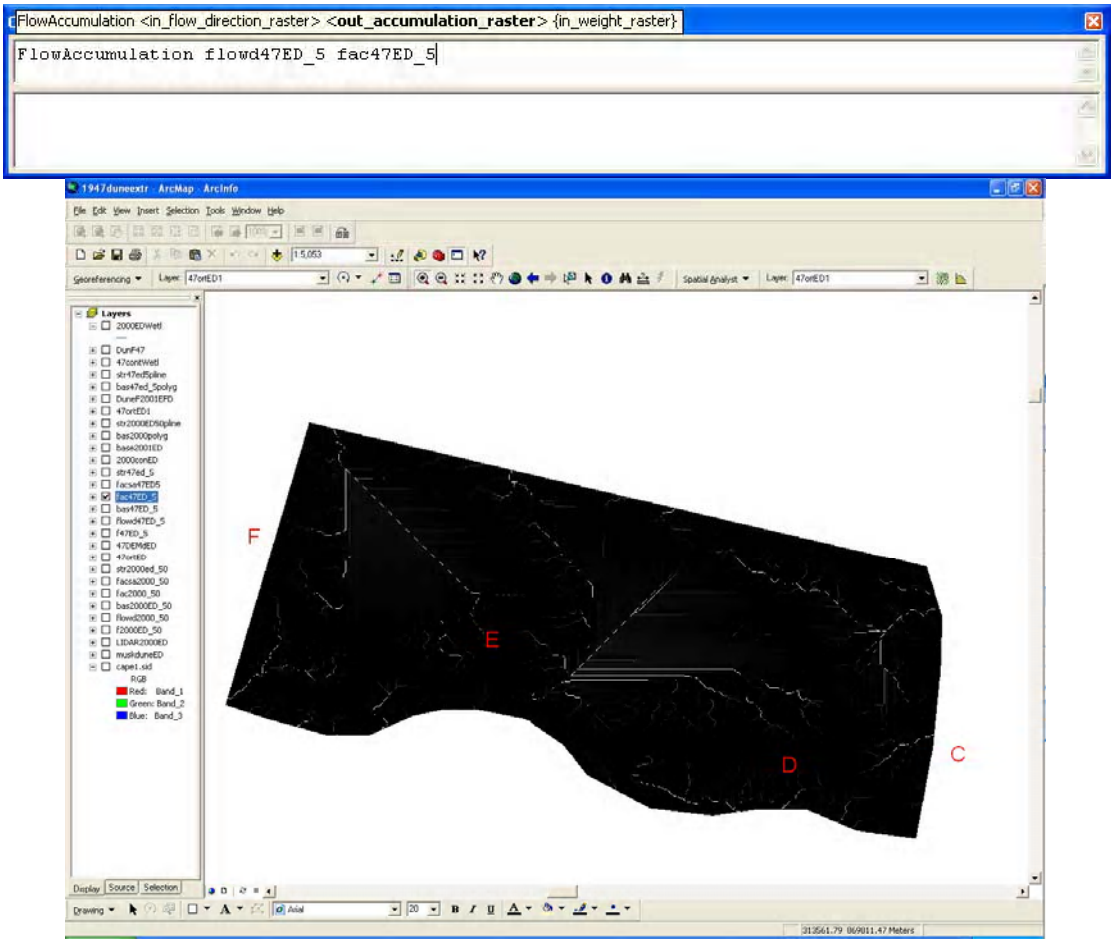

Figure B.8. Flow accumulation procedure.

Conversion to **Integer** from floating point is the next step (Fig. B.9).

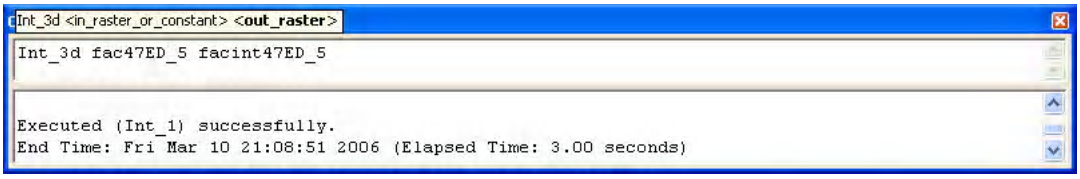

Figure B.9. Conversion to Integer.

The streams are still raster data, so the next step is to create vector data (Fig. B.10).

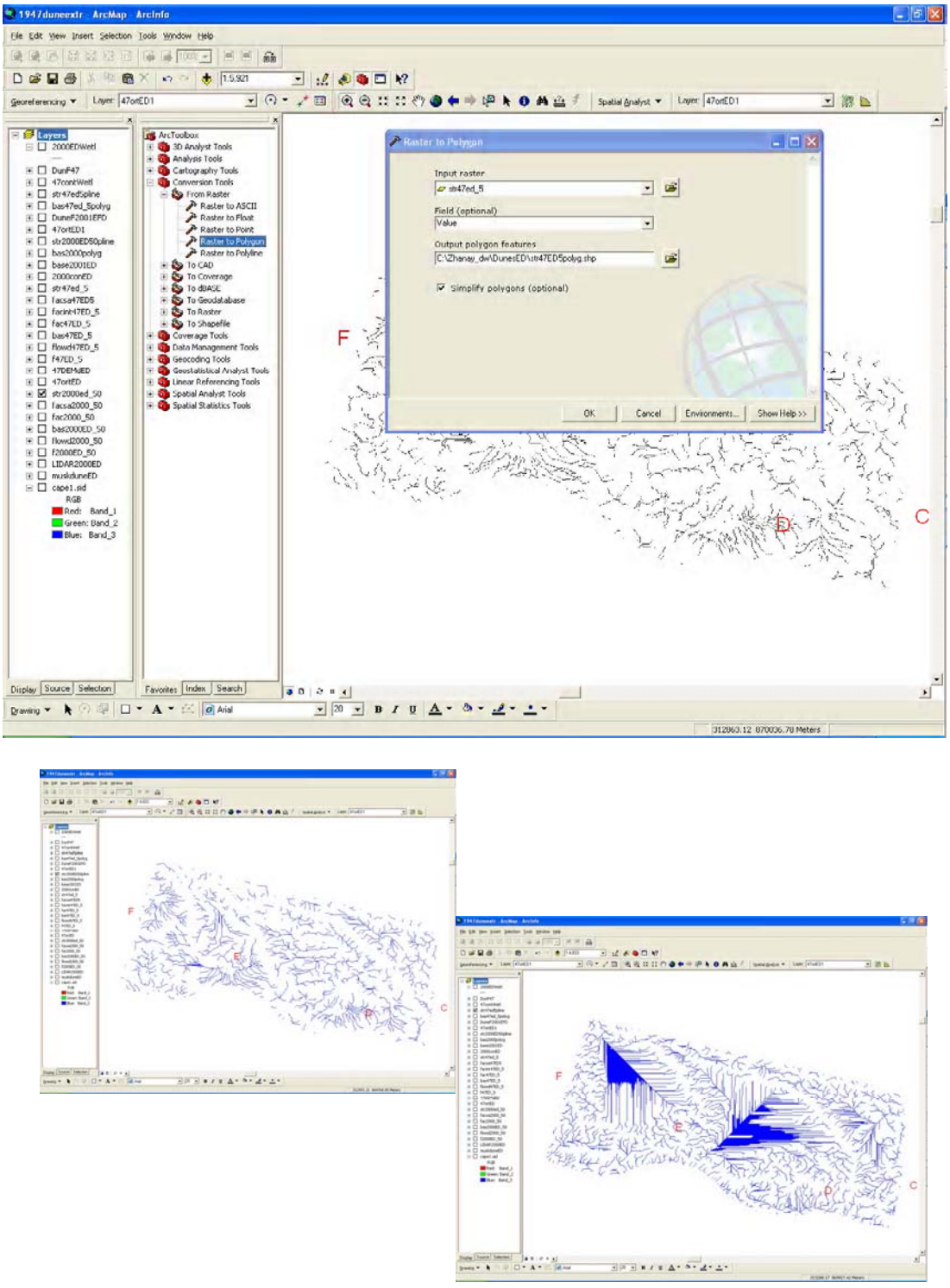

Figure B.10. Conversion from raster to polygon.

The final coverage of stream networks, watershed boundaries, catchment areas and drainage networks is presented below (Fig. B.11).

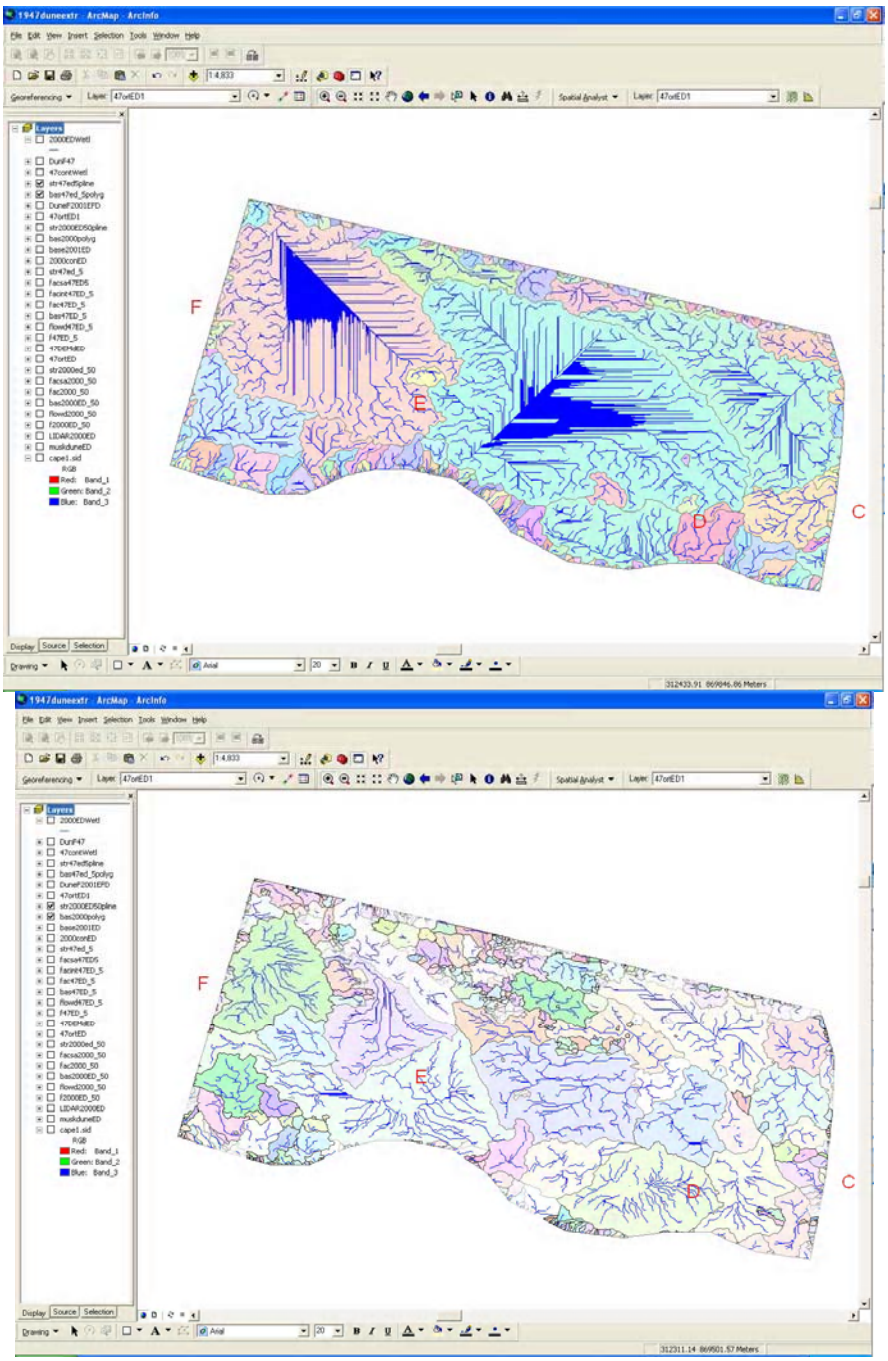

Figure B.11. Final polygon image of stream networks.